

**Thermodynamic and Kinetic Studies
of Redox Reactions within
Polyelectrolyte Coatings on Electrodes**

**Thesis by
Yu-Min Tsou**

**In Partial Fulfillment of the Requirements
for the Degree of
Doctor of Philosophy**

**California Institute of Technology
Pasadena, California**

1985

(Submitted January 18, 1985)

To my wife, Yah-Lih

and my daughter, Amy

To my parents

Acknowledgements

I express my deepest gratitude to past and present Anson group members for creating a scientifically stimulating environment in which I developed as a scientist.

I would like to thank my advisor, Fred Anson, for his guidance, encouragement, and scientific insight. The innumerable discussions with him have been the most important source of inspiration. His intense desire to make every concept clear strongly impressed me. Many colleagues have contributed to my research effort. Dr Kiyotaka Shigehara, Dr. Hans Zumbrennen, and Dr. Takeo Ohsaka deserve special credit for their guidance in electrochemical principles and techniques during my earlier scientific ventures. I owe special thanks to Dr. Mark Bowers who was the source of computational assistance and cheerfulness, Dr. Hsue-Yang Liu who offered helpful suggestions and useful computational techniques, Dr. Thomas Guarr, Dr. Rich Durand and Dr. Dan Buttry who provided some useful discussions.

I am indebted to many people outside the Anson group. Special thanks go to Professor Terrence Collins for helpful discussions in inorganic chemistry, Professor Robert Grubbs for guidance in organometallic synthesis, Professor Sunney Chan for general advice, and Professor J.-M. Saveant for helpful discussions in electrochemistry.

I would like to thank Dr. Chi-Ming Che for his friendship and for his introducing me into ruthenium and osmium chemistry. I learned a lot from his amazing synthetic techniques and broad scientific knowledge.

Special thanks are due to Huey-Jenn Chiang for his assistance in variable temperature experiments and his warm friendship. The many enjoyable conversations we have had have enlightened me on both chemistry and life. I also thank Ching-Long Ni for sharing happy times and providing information about word processing

I owe a special debt of gratitude to Maribelle Denslow for her inexhaustible love and support during my stay in California. The great deal of help from her to my family will always be appreciated. The countless happy times we shared with her and her family will always be remembered. I would also like to thank Sylvia Jacoby for her friendship and generous help in many ways.

My parents are always a great source of support. Finally, the radiant love, appreciable understanding and tireless patience of my wife, Yah-Lih, have been the sources of my strength, especially in those most frustrating days. For these and for typing the whole thesis she deserves much of the credit for this work.

Abstract

The formal potentials of several redox couples incorporated in coatings of a perfluorocarboxylate on graphite electrodes are measured and compared with the formal potentials of the same couples in homogeneous solution. For every redox couple investigated, the difference observed agrees with that calculated from the Nernst equation with the independently measured ratio of incorporation coefficients of the two halves of the couple. The dependences of the shifts in formal potentials on the nature of the incorporated complex ion, the ionic strength, and the temperature are also determined. They indicate that the incorporation equilibrium is governed by electrostatic and hydrophobic interactions that act in opposite directions. The incorporation of most cations examined is driven by large increases in entropy which overcome the usually unfavorable enthalpy changes.

The mediated oxidation of ascorbate by $\text{Os}(\text{bpy})_3^{3+}$ incorporated in Nafion coatings on graphite electrodes is examined. Attempts to account for the magnitude of the mediated ascorbate oxidation currents in terms of current models and theories are only partially successful. As the ascorbate concentration is increased, the limiting oxidation currents at coated rotating disk electrodes do not increase as rapidly as expected on the basis of the models. Some possible reasons for this deviant behavior are suggested. The implications of the results on the general utility of Nafion-coated electrodes in electrocatalysis are presented.

The heterobinuclear complex $(\text{NH}_3)_5\text{-RuN} \text{---} \text{C}_6\text{H}_4 \text{---} \text{CH}_2\text{-NH-C(=O)-CpFeCp} \rightleftharpoons \text{RuLFe}$
 (Cp=cyclopentadienide) is synthesized and used as a probe to gain the insight

into the diffusional behavior of redox reactants within polymeric coatings. Its diffusion coefficient within Nafion coatings is measured chronocoulometrically in all three of its possible redox states ($\text{Ru}^{\text{III}}\text{LFe}^{\text{III}}$, $\text{Ru}^{\text{III}}\text{LFe}^{\text{II}}$, $\text{Ru}^{\text{II}}\text{LFe}^{\text{II}}$). The three oxidation states exhibit large differences in their diffusional rates. Possible origins of the differences and their concentration dependences that are considered include intermolecular electron self-exchange, single-file diffusion and electrostatic cross-linking. Both enhancement and depression of charge transport rates produced by electron transfer cross-reactions between the fully oxidized and fully reduced complex are observed and compared with those calculated on the basis of a simple model. Reasonable agreement is obtained. The important effect that intermolecular cross-exchange reactions can exert on the diffusive flux of reactants is demonstrated.

Table of Contents

	Page
CHAPTER I	
Introduction	1
CHAPTER II	
Shifts in Redox Formal Potentials Accompanying the Incorporation of Cationic Complexes in Perfluoro Polycarboxylate and Polysulfonate Coatings on Graphite Electrodes	9
CHAPTER III	
Outer-Sphere Oxidation of Ascorbate with $\text{Os}(\text{bpy})_3^{3+}$ Incorporated in Nafion Coatings on Graphite Electrodes	46
CHAPTER IV	
Charge-Transport Rates in Nafion Coatings on Electrodes Disparate Diffusion Coefficients for a Single Molecule Containing Two Electroactive Centers	86
Appendix	
Synthesis and Characterization of $\text{Ru}(\text{bpy})_2 \text{MoS}_4$	123

LIST OF FIGURES

Figure	Description	Page
2.1	Cyclic voltammogram (CV) for $\text{Ru}(\text{NH}_3)_6^{3+}$ solution at polyelectrolyte II-coated electrodes.	14
2.2	CV for $\text{Ru}(\text{NH}_3)_6^{3+}$ in homogeneous solution and coatings of polyelectrolyte II.	17
2.3	Chronopotentiograms for the $\text{Ru}(\text{NH}_3)_6^{3+/2+}$ and $\text{Os}(\text{bpy})_3^{3+/2+}$ couples in coatings of polyelectrolyte II.	21
2.4	Temperature dependences of formal potentials of the $\text{Ru}(\text{NH}_3)_6^{3+/2+}$ and $\text{Os}(\text{bpy})_3^{3+/2+}$ couples in various media.	28
2.5	Incorporation of $\text{Ru}(\text{NH}_3)_6^{3+}$ by polyelectrolyte II as a function of pH.	33
3.1	CV for the oxidation of ascorbate at a bare electrode, a Nafion-coated electrode, and a (Nafion- $\text{Os}(\text{bpy})_3^{3+}$)-coated electrode.	50
3.2	Current potential curves for the oxidation of ascorbate at a rotating (Nafion- $\text{Os}(\text{bpy})_3^{3+}$)-coated electrode.	57
3.3	Levich plots for the oxidation of ascorbate at a rotating (Nafion- $\text{Os}(\text{bpy})_3^{3+}$)-coated electrode.	60

Figure	Description	Page
3.4	Koutecky-Levich plots of some of the data from Figure 3.3.	62
3.5	Current-potential curve and Koutecky-Levich plot for the reduction of $\text{Fe}(\text{edta})^-$ at a $(\text{Nafion-Os}(\text{bpy})_3^{2+})$ -coated electrode.	67
3.6	Levich plots for the oxidation of ascorbate at higher concentrations of ascorbate.	73
3.7	Comparison of experimental data for the oxidation of ascorbate at a $(\text{Nafion-Os}(\text{bpy})_3^{3+})$ -coated electrode with the calculated values.	76
3.8	A plot of all the experimental data according to eqn. (3.6).	79
4.1	CV and normal pulse voltammograms for the binuclear complex, RuLFe , at a bare electrode.	93
4.2	CV for RuLFe in a Nafion coating.	95
4.3	Concentration dependences of the four diffusion coefficients evaluated for RuLFe .	101
4.4	Concentration dependences of diffusion coefficients for mono-nuclear ruthenium and ferrocene complexes.	106
5.1	Electronic absorption spectrum of $\text{Ru}(\text{bpy})_2\text{MoS}_4$ in DMSO.	126

Figure	Description	Page
5.2	Enlargement and second derivative of Figure 5.1.	128
5.3	CV of $\text{Ru}(\text{bpy})_2\text{MoS}_4$ in DMSO.	131
5.4	CV of the reduction of $\text{Ru}(\text{bpy})_2\text{MoS}_4$ at various scan rates and reversal switching potentials.	134

LIST OF TABLES

Table	Description	Page
2.1	Calculated and observed shifts in formal potentials of redox couples in coatings of polyelectrolyte II.	23
2.2	Ionic strength dependences of the formal potential shifts.	26
2.3	Differences in half-reaction entropies and enthalpies for the $\text{Ru}(\text{NH}_3)_6^{3+/2+}$ and $\text{Os}(\text{bpy})_3^{3+/2+}$ couples in coatings of Nafion and polyelectrolyte II.	31
2.4	Thermodynamic parameters for several ion exchange reactions.	40
3.1	Rate constant for the reaction of ascorbate with $\text{Os}(\text{bpy})_3^{3+}$ on the surface of Nafion coating on a graphite electrode.	71
4.1	Diffusion coefficients for the RuLFe complex in a Nafion coating.	99
4.2	Chronocoulometric slopes for the reduction of $\text{Ru}^{\text{III}}\text{LFe}^{\text{III}}$ in Nafion coatings by one- or two-electron steps.	109
4.3	Chronocoulometric slopes for the oxidation of $\text{Ru}^{\text{II}}\text{LFe}^{\text{II}}$ in Nafion coatings by one- or two-electron steps.	111

CHAPTER I

Introduction

Intense research on the modification of electrode surfaces have been conducted recently.¹⁻³ Attentions were attracted into this new field because fruitful opportunities were provided to investigate novel redox processes by attaching the redox groups to the electrode surfaces. Chemists are interested in the thermodynamics, charge transport mechanism, and electron exchange reactions associated with the surface-confined electroactive groups. Promising applications in various fields make this field even more attractive. These include electrocatalysis,⁴ inhibition of the photocorrosion of semiconductor electrodes⁵ and electrochromic devices⁶ as well as other applications.⁷ Many different electrodes have been combined with different surface modifying reagents to yield a variety of modified electrodes to achieve desired properties for these applications.¹ Three methods have been used to attach redox groups to the electrode surfaces: they are irreversible (strong) adsorption, chemical binding or coating by a polymer.¹ This discussion will be concerned only with polymer modified electrodes.

Polymers have been attached to electrodes by coating from solution⁸, organosilane bonding,⁹ electrochemical polymerization¹⁰ and discharge polymerization.¹¹ Coating from solution is the simplest way to prepare the polymer modified electrode. In this method an aliquot of the polymer solution is transferred to the electrode surface, and the solvent is allowed to evaporate slowly. The polymer adheres to the electrode surface due to interactions between the polymer and the electrode and/or from the insolubility of the

polymer in the supporting electrolyte solution used.

Redox groups can be covalently bonded to the polymers¹² or incorporated into coatings of polymers bearing charged ionic groups¹³. The latter case is based on the principle of ion-exchange and is commonly known as electrostatic binding although other interaction(s) such as hydrophobic interaction have been discovered to play an important role¹⁴. Oyama and Anson¹³ first demonstrated that polyelectrolyte films (such as protonated polyvinylpyridine) deposited on graphite electrodes can incorporate ions of opposite charge (such as $\text{Fe}(\text{CN})_6^{3-}$) from aqueous solutions. The incorporations of the redox complexes were easily detectable by their redox reactions with the use of electrochemical techniques, such as cyclic voltammetry.

It was also shown that the electrochemical responses of these incorporated complexes persist for some time even after the coated electrode has been transferred to a solution which does not contain the redox complexes. These attractive features have initiated a lot of physical studies on the ionic redox complexes in the polyelectrolyte films¹⁵. Although stable cationic polyelectrolyte films on electrodes could be easily obtained, stable anionic films could not be found presumably due to the dissolution of the anionic polymers from the electrode surface¹⁵. However, in 1980, Rubinstein and Bard¹⁶ reported that Nafion, a perfluorinated, sulfonate-based polyelectrolyte could be used to prepare films on electrodes which exhibit exceedingly good stability in aqueous media. The stability is even better than those of the cationic polyelectrolyte films. Thus, with the availability of stable films of polymers having either anionic or cationic charged groups, the electrostatic binding method began to show promise of general applicability for the incorporation of a wide variety of

charged redox complexes.

Although the phenomenon of incorporation of multiply-charged redox complexes into polyelectrolyte films of the opposite charge was known for years, the shifts in redox formal potentials accompanying the incorporation and their thermodynamic significances have not been studied. In Chapter II,¹¹ experiments are performed to demonstrate that the formal potential of a redox couple in a polyelectrolyte, measured by common electrochemical methods, agrees with that calculated from the Nernst equation with the independently measured ratio of incorporation coefficients of the two halves of the couple. The dependences of the shifts in formal potentials on the nature of incorporated redox couple, the ionic strength, and the temperature are also determined. The results are analyzed to identify the factors which are responsible for these potential shifts and the associated thermodynamic parameters.

One of the most important applications of electrodes coated with polymers or polyelectrolytes is the catalysis of electrochemical reactions. In order to know how to design the desired electrocatalytic systems based on polymer (or polyelectrolyte) modified electrodes, it is important to understand how to extract information from the properly designed experiments. Thus, in Chapter III,¹⁸ $\text{Os}(\text{bpy})_3^{3+}$ (bpy=2,2'-bipyridine) is incorporated into Nafion film as a catalyst for the oxidation of ascorbate dissolved in the supporting electrolyte solution that permeates the Nafion film. The magnitude of the mediated ascorbate oxidation currents are analyzed in terms of the model and theory presented by Andrieux, Saveant and co-workers.¹⁹ Some implications of the results on the general utility of Nafion-coated electrodes in electrocatalytic applications are presented.

The mechanism by which charge propagates through polymeric films containing redox species has attracted considerable attention recently¹⁹. Understanding this subject is of interest in its own right and is also important to numerous applications⁴⁻⁷. The commonly accepted concept²¹ for polymeric films with redox sites anchored to the polymer chains is that charge is carried by electrons that hop between adjacent oxidized and reduced sites. The same type of mechanism may also contribute to the charge propagation when ionic redox species are incorporated into polyelectrolyte films^{14,22}. However, for the latter case, molecular diffusion of the redox species also makes contributions to the charge propagations. Buttry^{14b,c} in this group has done several studies on a number of inorganic redox couples. One of the goals is to identify and analyze contributions from the two mechanisms, molecular motion and/or electron exchange.

The result^{14c} on $\text{Co}(\text{bpy})_3^{2+}$ in Nafion coatings was particularly interesting. It exhibits a much larger diffusion coefficient when its concentration gradient was established at the electrode surface by reducing it to $\text{Co}(\text{bpy})_3^+$ than when the gradient arose from its oxidation to $\text{Co}(\text{bpy})_3^{3+}$. The difference was attributed to the much larger self-exchange rate constant for $\text{Co}(\text{bpy})_3^{2+}/^+$ couple than the $\text{Co}(\text{bpy})_3^{3+}/^{2+}$ couple, and the result was shown to be consistent with that expected from theory. This interesting observation provoked the study presented in Chapter IV. A molecule bearing two separate reversible redox groups is synthesized and the similar experiments as in the case of $\text{Co}(\text{bpy})_3^{2+}$ are performed. One of the goals of this study is to enlarge the scope of the research concerning the influence of self-exchange reactions on the rates of charge propagation in a polyelectrolyte film by covalently linking two redox groups. In addition, the enhancement or depression of the diffusion

currents by means of intermolecular electron cross-exchange reactions is detected and the results are compared with that calculated from a derived equation.

Finally, a preliminary report on the synthesis and characterization of $\text{Ru}(\text{bpy})_2\text{MoS}_4$ is presented in the Appendix.

References

- 1 R.W.Murray, *ACC. Chem. Res.*, 13(1980)135.
- 2 W. J. Albery and A. R. Hillman, *Annual Reports C, R. Soc. Chem. Lond.*, (1981)377.
- 3 K. D. Snell and A. G. Keenan, *Chem. Soc. Rev.*, 8(1979)259.
- 4 F. C. Anson, T. Ohsaka and J. M. Saveant, *J. Am. Chem. Soc.*, 105(1983)4883.
- 5 M. S. Wrighton, *ACS Sym. Ser.*, No.192(1982) 99.
- 6 (a)F. B. Kaufman, A. H. Shroeder, E. M. Engler and V. Patel, *Appl. Phys. Lett.*, 36(1980)422; (b) K. Itaya, H. Akahoshi, S. Toshima, *J. Electrochem. Chem. Soc.*, 129(1982)762.
- 7 (a) R. W. Murray, in " *Electroanalytical Chemistry* ", A. J. Bard, ed.; Marcel Dekker, Inc., New York, 1984; vol.13; (b) L. R. Faulkner, *Chem. Eng. News*, 62(1984)29.
- 8 (a) L. L. Miller and M. R. Van De Mark, *J. Am. Chem. Soc.*, 100(1978)639; (b) H. Tachikawa and L. R. Faulkner, *J. Am. Chem. Soc.*, 100(1978)4379; (c) F. B. Kaufman and E. M. Engler, *J. Am. Chem. Soc.*, 101(1979)547.
- 9 (a) J. R. Lenhard and R. W. Murray, *J. Am. Chem. Soc.*, 100(1978)7870; (b) M. S. Wrighton, R. C. Austin, A. B. Bocarsly, J. M. Bolts, O. Hass, K. D. Legg, L. Nadjo and M. C. Palazzotto, *J. Electroanal. Chem.*, 87(1978)429.
- 10 M.-C. Pham P.C. Lacaze and J.-E. Dubois, *J. Electroanal. Chem.*, 86(1978)147; (b) *ibid*, 99(1979)331.

- 11 R. Nowak, F. A. Schultz, M. Umana, H. Abruna and R. W. Murray, *J. Electroanal. Chem.*, 94(1978)219.
- 12 See, for example, R. D. Rocklin and R. W. Murray, *J. Phy. Chem.*, 85(1981)2104.
- 13 N. Oyama and F. C. Anson, *J. Electrochem. Soc.*, 127(1980)247.
- 14 (a) C. R. Martin and K. A. Dollard, *J. Electroanal. chem.*, 159(1983)127; (b) D. A. Buttry and F. C. Anson, *J. Am. Chem. Soc.*, 105(1983)685.
- 15 N. Oyama, T. Shimomura, K. Shigehara and F. C. Anson, *J. Electroanal. Chem.*, 112(1980)271.
- 16 I. Rubinstein and A. J. Bard, *J. Am. Chem. Soc.*, 102(1980)6641.
- 17 Y.-M. Tsou and F. C. Anson, *J. Electrochem. Soc.*, 131(1984)595.
- 18 F. C. Anson, Y.-M. Tsou and J.-M. Saveant, *J. Electroanal. Chem.*, 178(1984)113.
- 19 (a) C. P. Andrieux, J.-M. Dumas-Bouchiat and J.-M. Saveant, *J. Electroanal. Chem.*, 131(1982)1; (b) C. P. Andrieux and J.-M. Saveant, *J. Electroanal. Chem.*, 134(1982)163; (c) C. P. Andrieux and J.-M. Saveant, *J. Electroanal. Chem.*, 142(1982)1.
- 20 Ref 14(b) and references therein.
- 21 F. B. Kaufman and E. M. Engler, *J. Am. Chem. Soc.*, 101(1979)547.
- 22 (a) H. S. White, J. Leddy and A. J. Bard, *J. Am. Chem. Soc.*, 104(1982)4811; (b) C. R. Martin, I. Rubinstein and A. J. Bard, *ibid*, 104(1982)4817; (c) J.

Facci and R. W. Murray, *J. Phys. Chem.*, 85(1981)2870.

CHAPTER II

Shifts in Redox Formal Potentials Accompanying the Incorporation of Cationic Complexes in Perfluoro Polycarboxylate and Polysulfonate Coatings on Graphite Electrodes

Introduction

The formal potential of a redox couple depends on the medium. It may shift with the solvent, the ionic strength (for charged redox couples) etc. Studies on these potential shifts should provide some important information about the interactions of the redox couples with their environments. Oyama and Anson¹ first demonstrated that polyelectrolyte films on electrodes could incorporate redox couples of the opposite charge. The redox processes could be easily detected by electrochemical methods. Since then numerous studies² have been carried out in this area. In several cases³, the formal potentials of the redox reactants in the polyelectrolyte coatings were noted to be significantly different from those corresponding values in homogeneous solutions. In a recent study⁴ this aspect of the electrochemistry of redox polymer coatings was examined in more detail.

Some studies in Anson's group have been made on the electrochemical responses from redox reactants at electrodes coated with Nafion, I, and the related polyelectrolyte, II.

Unusually large shifts in the formal potentials of certain redox couples were noted upon incorporation into these coatings. Both the magnitude of the shift in formal potential and its sign were influenced strongly by the nature of

the ligands coordinated to the metal center of the redox couples. In this chapter, it is demonstrated that the difference in formal potential of a redox couple in solution and incorporated within the polyelectrolyte coating, as evaluated by cyclic voltammetry, reliably reflects the difference between the free energy changes associated with the incorporation of the two halves of the couple by the polyelectrolyte. The behavioral differences observed with several redox couples and attempts to understand their origins are also documented. The results point out that both electrostatic and hydrophobic interactions of incorporated electroactive ions with the polyelectrolyte combine to determine the direction of shifts in formal potentials. The temperature dependences of the shifts in formal potentials were also measured. They pointed to large entropic contributions to the differences in the equilibrium incorporation of the oxidized and reduced halves of the redox couples. The changes in the solvation structures of the redox reactants and the ionic groups on the polyelectrolytes are proposed to account for the large entropy contributions.

Experimental

Material

Nafion coatings were prepared as previously described⁵ by evaporation of aliquots of a solution of the polymer supplied by E. I. du Pont de Nemours & Co. several years ago. Polymer II was supplied in the form of a fine suspension of the methyl ester by Asahi Glass Company, Tokyo. To prepare coatings, aliquots of the suspension were evaporated on freshly cleaved electrodes. The resulting deposit was exposed to 1M NaOH for 5 min to convert the ester to the carboxylate, and the electrode was then washed thoroughly with water. The

extent and uniformity of the de-esterification were not examined in detail, but it was established that increasing the time that the coatings were exposed to the 1M NaOH produced no changes in their behavior. Electrodes were prepared from pyrolytic graphite (Union Carbide Company, Chicago) and mounted according to previously described procedures⁶. $\text{Ru}(\text{NH}_3)_6\text{Cl}_3$ (Matthey Bishop Company) was recrystallized before use.

$[\text{CpFeCp-CH}_2\text{-N}^+(\text{CH}_3)_3]\text{Br}^-$ (Cp=cyclopentadienide) (Research Organic/Inorganic Company) was used as received. $[\text{Ru}(\text{NH}_3)_5 \text{isonicotinamide}](\text{ClO}_4)_2$ ⁷ and $\text{Os}(\text{bpy})_3(\text{ClO}_4)_2$ ⁷ were synthesized according to the cited references. Solutions were prepared with distilled water which was further treated by passage through a purification train (Barnstead Nanopure).

Procedures

Conventional two-compartment cells and apparatus were employed to obtain cyclic voltammograms. To evaluate formal potentials for reactants incorporated in electrode coatings, the cyclic voltammograms were recorded at scan rates low enough (e.g., a few mV s^{-1}) to obtain symmetrical waves with almost equal peak potentials. The quantities of the oxidized and reduced halves of redox couples incorporated by coatings were measured chronopotentiometrically⁸ to avoid possible alterations in the equilibrium ratio of oxidant to reductant by insufficiently precise potentiostatic control of the electrode potential. Potentials were measured and are quoted with respect to a calomel reference electrode saturated with sodium chloride, SSCE.

Temperature dependences of formal potentials were evaluated from cyclic voltammograms recorded in a nonisothermal cell having a thermally jacketed

compartment for the working and auxiliary electrodes and a separate compartment for the reference electrode. The reference electrode was maintained at a fixed temperature. The principles and assumptions involved in the use of such cells have been examined in detail¹⁰ and several recent experimental examples of their successful applications are available¹¹. Exposure of the polyelectrolyte coatings to solutions at 50°C caused the measured formal potentials of incorporated redox couples to drift slightly before new stable potentials resulted. We believe this behavior is the result of reproducible structural changes in the coatings. For this reason, the temperature dependences of formal potentials were measured with coatings that had been exposed to a solution at 50°C long enough for the cyclic voltammetric response to stabilize (ca. 30 min). Thereafter, reproducible peak potentials were obtained at all temperatures.

Results

When a graphite electrode coated with a thin film of the carboxylate polyelectrolyte, II, is immersed in a $\text{Ru}(\text{NH}_3)_6^{3+}$ solution and the potential of the electrode is cycled between +0.5V and -1.0V, a steady-state response soon develops. The response depends on the film thickness and the scan rate. The effects are illustrated in Figure 2.1. Figure 2.1A shows the effects of changes in scan rate, while 2.1B demonstrates the effects of changes in the coating thickness at a fixed scan rate. With thinner coatings or lower scan rates, the voltammograms exhibit two waves. These are clearly separated in the anodic half of the voltammograms. The anodic peak at -0.15V is quite close to the corresponding peak obtained at an uncoated electrode, and it is this peak (and the cathodic counterpart which appears as a shoulder) that disappears when

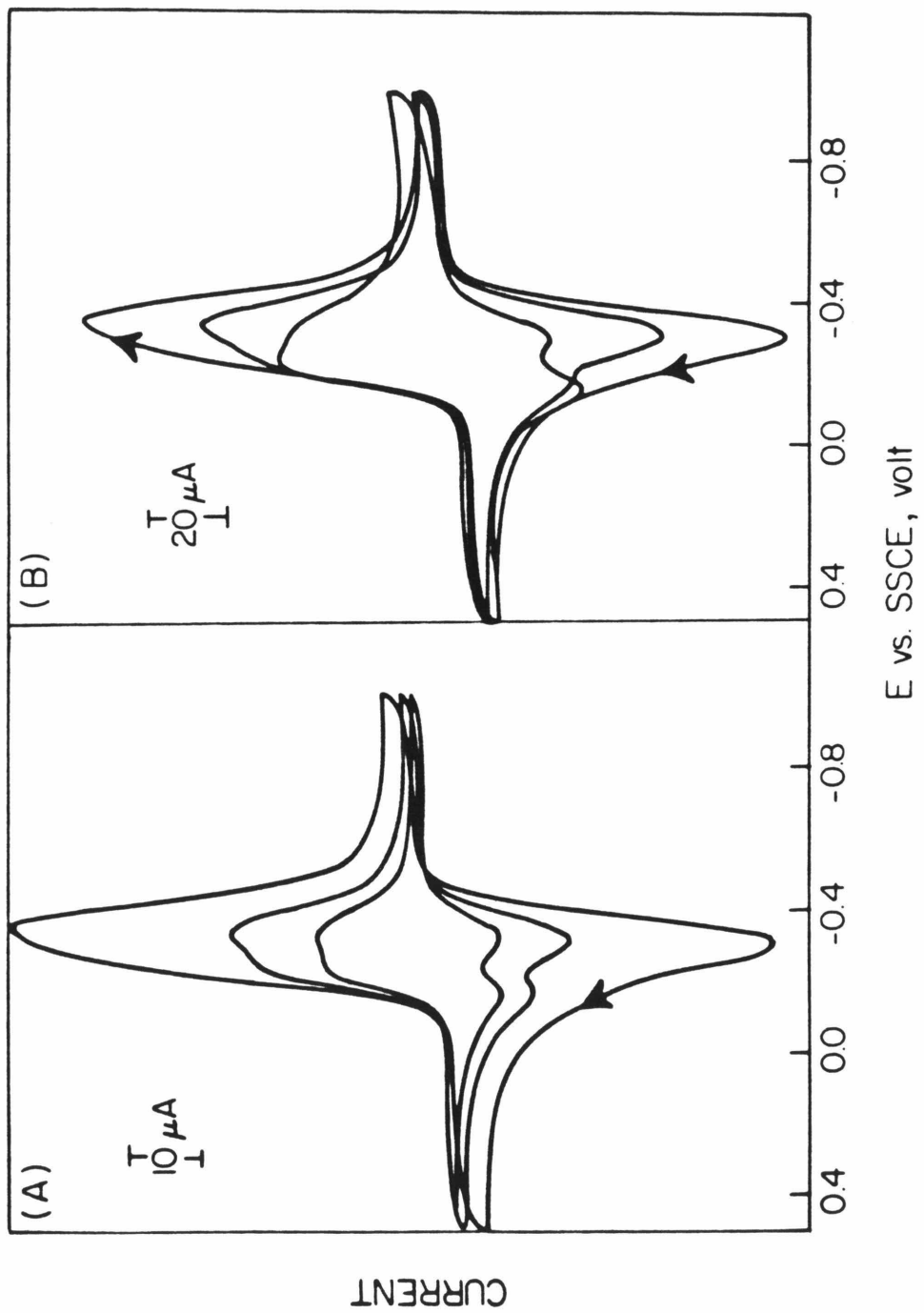
Figure 2.1

Steady state cyclic voltammograms for 1.0 mM $\text{Ru}(\text{NH}_3)_6^{3+}$ solution at a graphite electrode coated with polyelectrolyte

II. Supporting electrolyte: 0.2 M KCl at pH 5.5.

A. Coating contained 2.1×10^{-7} mole cm^{-2} of carboxylate groups; scan rate: 10, 20, 50 mV s^{-1} .

B. Scan rate: 100 mV s^{-1} . Coatings contained 4.2, 8.4 and 21×10^{-8} mole cm^{-2} of carboxylate groups.



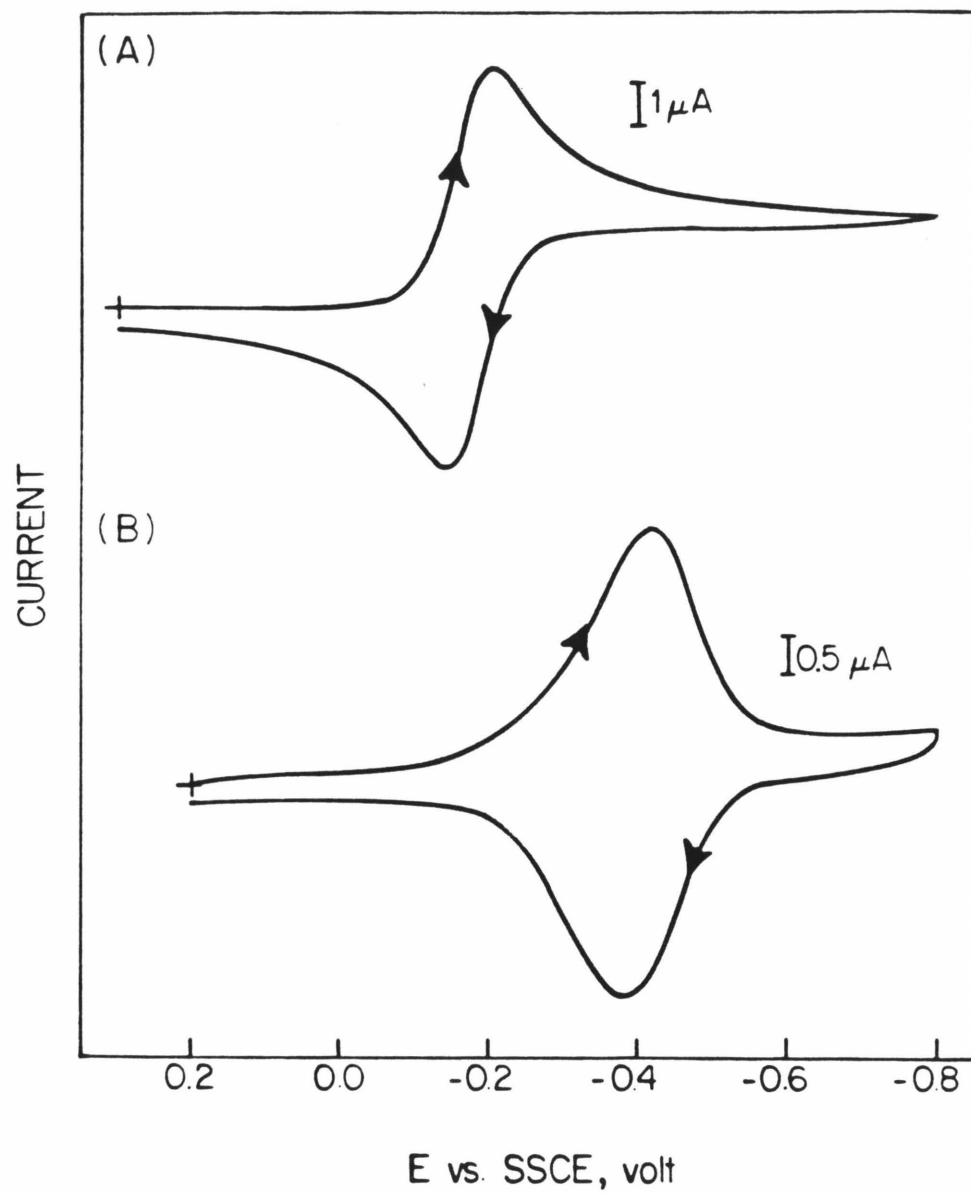
the electrode used to record the voltammograms in Figure 2.1 is transferred to a pure supporting electrolyte solution. Similar behavior was reported earlier for the voltammetry of $\text{Ru}(\text{NH}_3)_6^{3+/2+}$ at electrodes coated with polyvinylsulfate^{3a}. The responses which persist after transferring originate from the redox reactants which act as counterions of the polyelectrolytes¹². The wave that exists only in solutions containing $\text{Ru}(\text{NH}_3)_6^{3+/2+}$ is believed to arise from the diffusion penetration of the polymer coating by the complex so that it is reduced and reoxidized directly at the electrode surface. That the peak does not arise from a reaction at the bare patches of the electrode exposed by imperfections in the coating was indicated by tests of coated electrodes with nonincorporating anions, such as $\text{Fe}(\text{CN})_6^{4-}$, which exhibited much smaller peak currents and much greater peak separations at coated than at bare electrodes. In any case, this work was devoted to comparisons between the voltammetric responses of redox couples at bare electrodes and those taken after their incorporation into coatings on electrodes which are subsequently transferred to a pure supporting electrolyte solution. Thus, the penetration peak evident in Figure 2.1 presented no problems.

In Figure 2.2 the cyclic voltammogram for $\text{Ru}(\text{NH}_3)_6^{3+/2+}$ at a bare graphite electrode is compared with that for the same couple incorporated in a coating of the carboxylate polyelectrolyte, II. The large difference in the average of anodic and cathodic peak potentials (i.e., formal potentials) of the couple in the two cases is evident. This difference in formal potentials should reflect the difference in the strength of the binding of each half of the redox couple to the polyelectrolyte coating. Thus, if $[\text{O}]_s/[\text{R}]_s$ and $[\text{O}]_p/[\text{R}]_p$ are the equilibrium ratios of the concentrations of the oxidized and reduced forms of a couple in the solution (s) and polyelectrolyte (p) phases, respectively, the difference in

Figure 2.2

A. Cyclic voltammograms for 0.5 mM $\text{Ru}(\text{NH}_3)_6^{3+}$ at a bare graphite electrode.

B. Repeat after the electrode was coated with polyelectrolyte II (8.4×10^{-8} mole cm^{-2} of carboxylate groups), soaked in the $\text{Ru}(\text{NH}_3)_6^{3+}$ solution for five minutes and transferred to pure supporting electrolyte (0.02 M CH_3COONa at pH 5.5). Scan rate: 5 mV s^{-1} for both curves.



the formal potentials observed in the phases can be expressed as in equation (2.1).

$$E_p^f - E_s^f = \frac{RT}{F} \left(\ln \frac{[O]_s}{[R]_s} - \ln \frac{[O]_p}{[R]_p} \right) \quad (2.1)$$

Experimental values of E_p^f and E_s^f were obtained from the average of the peak potentials of voltammograms such as those in Figure 2.2. The voltammograms for redox couples incorporated in polyelectrolyte coatings were recorded at sufficiently small scan rates ($< 5 \text{ mV s}^{-1}$) so that all of the incorporated complex was reduced or oxidized during every half-cycle. The peak currents were proportional to scan rate, as expected under these conditions¹³, and the formal potential was taken as the simple average of the peak potentials, which were typically separated by 10 to 30 mV by residual ohmic potentials present in the cell and coating. At bare electrodes, the peak potentials were usually separated by 60-70 mV, as expected¹⁴. The formal potential (E_s^f) was obtained from the average of the peak potentials corrected for the difference in the solution diffusion coefficients of the two halves of the redox couple¹⁴. This correction typically amounted to 1 to 2 mV.

The open-circuit equilibrium potential assumed by bare (or coated) electrodes in solutions containing both O and R is given by

$$E_{eq} = E_s^f - \frac{RT}{F} \ln \frac{[R]_s}{[O]_s} \quad (2.2)$$

Thus, equation (2.1) can be rewritten as

$$E_p^f = E_{eq} + \frac{RT}{F} \ln \frac{[R]_p}{[O]_p} \quad (2.3)$$

where E_{eq} is the equilibrium potential of the coated (or bare) electrode in an incorporation solution which leads to the concentration ratio $[R]_p/[O]_p$ in the polyelectrolyte phase. In order to test the important equation (2.1), coated electrodes were equilibrated in incorporation solutions containing various ratios of the oxidized to reduced form of the redox couple. The formal potentials of the redox couple in the coating (E_p') were then compared with the values, $E_{eq} + \frac{RT}{F} \ln \frac{[R]_p}{[O]_p}$, calculated from the observed values of E_{eq} and the measured concentrations of R and O in the polyelectrolyte phase. The latter were determined chronopotentiometrically⁹ after the equilibrated electrode was transferred to a pure supporting electrolyte solution. The constant current intensity (i) utilized in the chronopotentiometric measurements were kept small enough to make sure that all the incorporated reactant in the coatings had been oxidized or reduced at the transition time (τ). Under this condition the quantity of reactant could be calculated as $i\tau/nF$.

At the transition time, a constant current in the opposite direction was passed through the coating until a second transition corresponding to the sum of the oxidized and reduced reactant initially present in the coatings resulted. For example, if the first transition time (τ) was obtained with an anodic current (i_1), and the second, (τ_2) resulted from a subsequent cathodic current (i_2), $[O]_p/[O]_R$ was calculated as

$$\frac{[O]_p}{[R]_p} = \frac{i_2\tau_2 - i_1\tau_1}{i_1\tau_1} \quad . \quad (2.4)$$

Two typical chronopotentiograms are shown in Figure 2.3; in these coatings $Ru(NH_3)_6^{3+/2+}$ or $Os(bpy)_3^{3+/2+}$ had been incorporated. Table 2.1 summarizes the results of a series of such experiments with three redox couples to test

Figure 2.3

Chronopotentiograms for the $\text{Ru}(\text{NH}_3)_6^{3+/2+}$ and $\text{Os}(\text{bpy})_3^{3+/2+}$ couples in coatings of polyelectrolyte II.

A. Electrode coated with 2.1×10^{-7} mole cm^{-2} of carboxylate group equilibrated with a solution containing $\text{Ru}(\text{NH}_3)_6^{3+}$ and $\text{Ru}(\text{NH}_3)_6^{2+}$ ($E_{\text{eq}} = 312$ mV; $[\text{Ru}(\text{NH}_3)_6^{3+}] + [\text{Ru}(\text{NH}_3)_6^{2+}] = 1.0$ mM) before transfer to pure supporting electrolyte solution (0.02 M CH_3COONa at pH 5.5). Constant current density = $1.15 \mu\text{A cm}^{-2}$ for oxidation of Ru(II) and $23.0 \mu\text{A cm}^{-2}$ for reduction of Ru(III).

B. Electrode coated with 8.4×10^{-8} mole cm^{-2} of carboxylate groups equilibrated with a solution of $\text{Os}(\text{bpy})_3^{3+}$ and $\text{Os}(\text{bpy})_3^{2+}$ ($E_{\text{eq}} = 602$ mV; $[\text{Os}(\text{bpy})_3^{3+}] + [\text{Os}(\text{bpy})_3^{2+}] = 0.5$ mM). Constant current density = $2.87 \mu\text{A cm}^{-2}$ throughout.

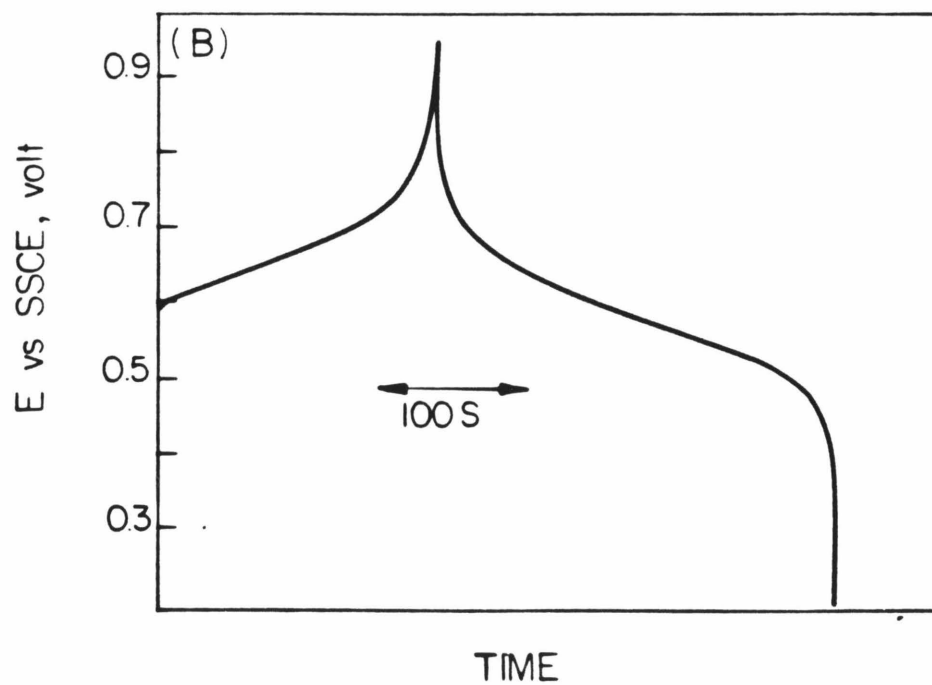
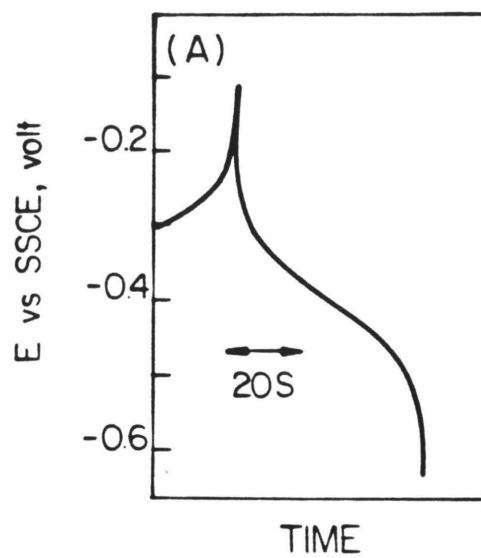


Table 2.1

Calculated and Observed Shifts in Formal Potentials
of Redox Couples Incorporated in Coating of Polyelectrolyte II^a

Redox Couple	E_{eq}^b mV	$\frac{[R]_p^c}{[O]_p}$	$E_{eq} + \frac{RT}{F} \ln \left(\frac{[R]_p}{[O]_p} \right)$, mV	E_p^d , mV
$Ru(NH_3)_6^{3+/2+}$	-312	0.024	-408	-402
$Ru(NH_3)_5isn^{3+/2+}^e$	- 60	5.0	- 20	- 21
	- 43	2.57	- 20	- 21
	- 40	2.45	- 17	- 21
	- 37	1.80	- 22	- 21
	- 24	0.90	- 23	- 21
	- 19	0.90	- 20	- 21
	0	0.63	- 12	- 21
	+ 10	0.42	- 12	- 21
$Os(bpy)_3^{3+/2+}$	602	2.38	624	609
	605	2.21	625	609

a. The coatings contained $8.4 \times 10^{-8} \text{ mol} \cdot \text{cm}^{-2}$ of carboxyl groups in every case except $Ru(NH_3)_6^{3+/2+}$ where the coating contained $2.1 \times 10^{-7} \text{ mol} \cdot \text{cm}^{-2}$. Supporting electrolyte for both the incorporation and chronopotentiometric assay was 0.02 M CH_3COONa at pH 5.5.

b. Open circuit equilibrium potential (vs. SSCE) of the electrode in the solution from where the incorporation was carried out.

- c. Ratio of the reduced to the oxidized form of the redox couple in the polyelectrolyte phase. Determined by chronopotentiometric assay using equation 4.
- d. Formal potential (vs SSCE) of the redox couple within the polyelectrolyte coatings.
- e. isn = isonicotinamide

whether equation (2.1) and (2.3) provide an adequate description of the behavior of the coated electrodes. The agreement between the calculated and the observed potentials in the last two columns of Table 2.1 is, in most cases, within the experimental precision of $\pm 5\text{mV}$, so the equations (2.1) and (2.3) appear to be obeyed over a reasonably wide range of $[\text{R}]_{\text{P}}/[\text{O}]_{\text{P}}$ ratios. Thus, it may be concluded that the difference in measured formal potentials of redox couples in solution and incorporated within polyelectrolyte II reliably reflects the difference between the free energy changes associated with the incorporation of the two halves of the redox couple by the polyelectrolyte.

Effect of changes in ionic strength

The incorporation of cationic redox couples by polyelectrolyte II is an ion exchange process. Equivalent amounts of unipositive counterions initially present in the polyelectrolyte were replaced by an incorporated multiply-charged redox complex. Therefore, the extent of incorporation of each half of a redox couple would be expected to vary with ionic strength of the incorporation solution. This prediction was tested by measuring the differences between the formal potentials of several redox couples in homogeneous solution and within the polyelectrolyte coating as a function of ionic strength. The results, summarized in Table 2.2, show that the difference in formal potentials measured inside and outside of the polyelectrolyte coating is strongly dependent on the ionic strength and on the nature of the redox couple.

Temperature dependence of the formal potential

Table 2.2

Ionic Strength Dependence of the Difference Between
Redox Formal Potentials in Solution and Within
Coatings of Polyelectrolyte II ^a

Redox Couple	Supporting Electrolyte Conc., ^b M	E _s ^{f, c} mV vs SSCE	E _p ^{f, d} mV vs SSCE	E _p ^f -E _s ^f = ΔE ^f , mV
Ru(NH ₃) ₆ ^{3+/2+}	0.02	-169	-402	-233
	0.2	-185	-347	-162
	2.0	-220	-290	- 70
Ru(NH ₃) ₅ isn ^{3+/2+}	0.02	158	- 21	-179
Os(bpy) ₃ ^{3+/2+}	0.02	619	609	- 10
	0.2	608	632	24
	2.0	607	683	76
CpFeCpCH ₂ N- ^e (CH ₃) ₃ ^{2+/+}	0.2	388	381	- 7

a. All coatings contained 8.4×10^{-8} mole cm⁻² of carboxyl groups.

b. The supporting electrolyte was CH₃COONa and all solutions were at pH 5.5.

- c. Formal potential of the couple in homogeneous solution, obtained from the average of cyclic voltammetric peak potentials and corrected for differences in diffusion coefficients (13).
- d. Formal potential of the redox couple with the polyelectrolyte coating as obtained from cyclic voltammograms recorded at low scan rate.
- e. C_p = cyclopentadienide

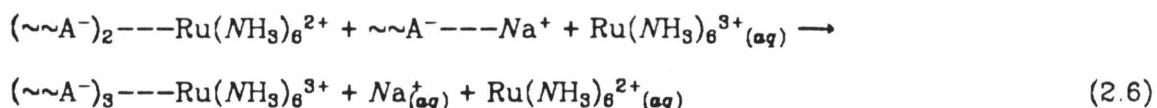
It is important to obtain more insight into the thermodynamic parameters responsible for the opposite shifts in formal potentials of $\text{Ru}(\text{NH}_3)_6^{3+/2+}$ and $\text{Os}(\text{bpy})_3^{3+/2+}$ couples upon their incorporation in the polyelectrolyte coatings under some conditions (Table 2.2). The temperature dependence of the formal potentials of the two couples were measured within the coatings and at a bare electrode. As shown in Figure 2.4, a very interesting behavior is observed. Increases in temperature cause the formal potentials for both couples to shift to more negative values within coatings of polyelectrolyte II, but in the homogeneous solution an opposite direction of shift was realized.

According to Weaver et al.¹⁰, the slopes of lines in Figure 2.4 can be used to evaluate the half-reaction entropies for redox couples (ΔS_{rc}°) by equation (2.5)

$$\Delta S_{rc}^\circ = nF \left(\frac{dE^\circ}{dT} \right) \quad . \quad (2.5)$$

The results are summarized in Table 2.3. The value of ΔS_{rc}° for $\text{Ru}(\text{NH}_3)_6^{3+/2+}$ at the bare electrode agrees well with that reported by Weaver et al.¹⁰, and the value for $\text{Os}(\text{bpy})_3^{3+/2+}$ is not far from their value for the isostructural $\text{Fe}(\text{bpy})_3^{3+/2+}$ couple¹⁰.

The difference between the values of ΔS_{rc}° at bare and coated electrodes ($\Delta \Delta S_{rc}^\circ$) (Table 2.3) represents the entropy change associated with an overall reaction such as



where $\sim\sim\text{A}^-$ represents one of the anionic fixed charge groups of the polyelectrolytes, and (aq) denotes the hydrated ion in the bulk of the solution.

Figure 2.4

Temperature dependences of the formal potentials of the $\text{Ru}(\text{NH}_3)_6^{3+/2+}$ and $\text{Os}(\text{bpy})_3^{3+/2+}$ couples.

A. $\text{Ru}(\text{NH}_3)_6^{3+/2+}$.

B. $\text{Os}(\text{bpy})_3^{3+/2+}$.

(■) bare electrode; (▲) electrode coated with polyelectrolyte II; (●) electrode coated with Nafion.

Supporting electrolyte: 0.02 M CH_3COONa at pH 5.5.

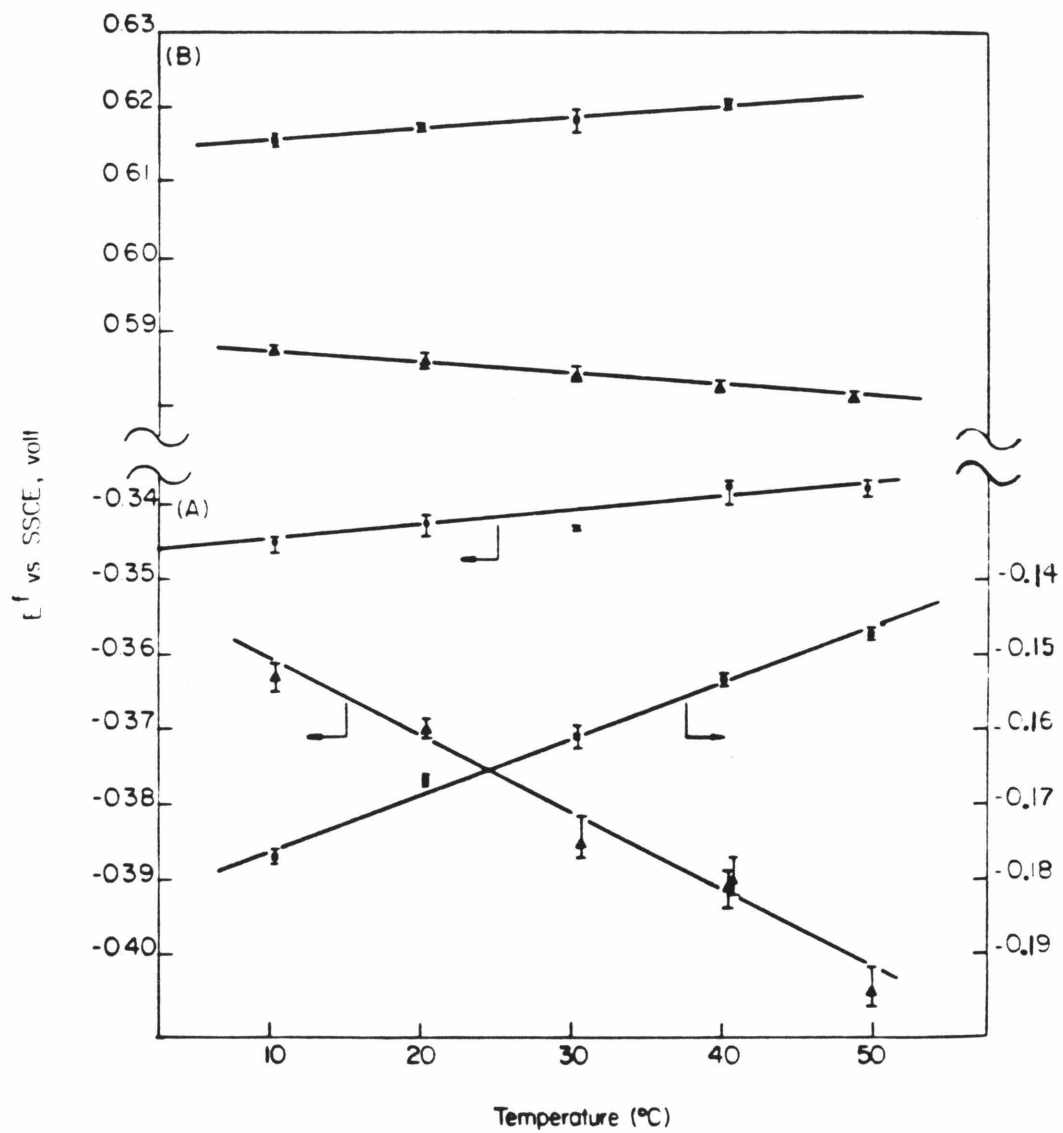


Table 2.3

Differences in Half-Reaction Entropies and Enthalpies for the $\text{Ru}(\text{NH}_3)_6^{3+/2+}$ and $\text{Os}(\text{bpy})_3^{3+/2+}$ Couples in Coatings of Nafion and Polyelectrolyte II ^a

Redox Couple	Electrode Coating	$\Delta S_{\text{rc}}^\circ$, ^b e.u.	$\Delta\Delta S_{\text{rc}}^\circ$, ^c e.u.	$\Delta\Delta H_{298}^\circ$, ^d kcal mole ⁻¹	$\Delta\Delta G_{298}^\circ$, ^e kcal mole ⁻¹
$\text{Ru}(\text{NH}_3)_6^{3+/2+}$	bare	+17.1 (0.99)			
	Nafion	+ 4.6 (0.90)	+12.5	-0.36	-4.09
	II	-23.5 (0.98)	+40.6	+7.22	-4.88
$\text{Os}(\text{bpy})_3^{3+/2+}$	bare	+3.5 (0.90)			
	II	-3.8 (0.95)	+ 7.3	+1.42	-0.75

a. Supporting electrolyte: 0.02 M CH_3COONa at pH 5.5.

b. The entropy change for the half-reaction: $\text{M}^{3+} + \text{e}^- \rightleftharpoons \text{M}^{2+}$.

Calculated from the slopes of the lines in Figure 4. Linear correlation coefficients are given in parentheses.

c,d,e. Differences between $\Delta S_{\text{rc}}^\circ$, ΔH_{298}° and ΔG_{298}° at coated and bare electrodes.

Calculated from $\Delta\Delta H^\circ = \Delta\Delta G^\circ - T\Delta\Delta S_{\text{rc}}^\circ$; $\Delta\Delta G_{298}^\circ = -nF\Delta E^f$.

The ionic aggregates inside the polyelectrolyte, denoted by $(\sim\sim A^-)_n$ $Ru(NH_3)_6^{3+}$, are also hydrated to an extent that is great enough to affect both their entropies and enthalpies significantly.

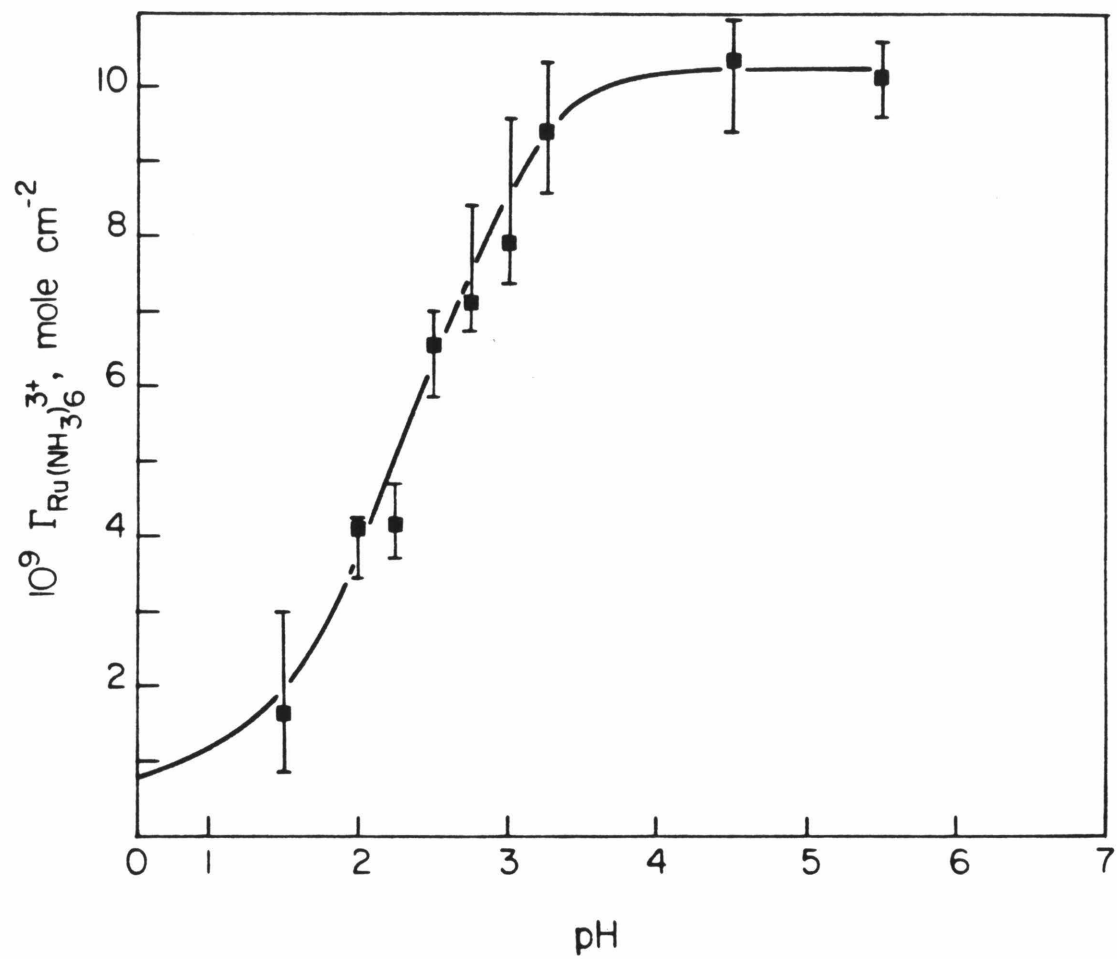
As shown in Table 2.3, the positive values of $\Delta\Delta S_{rc}^\circ$ indicate that the substitution for one incorporated cation complex of its redox partner with the higher charge causes a net increase in entropy for each case. The corresponding enthalpic differences, $\Delta\Delta H_{298}^\circ$, are positive in the case of polyelectrolyte II. The combination of unusually large positive reaction entropy and large positive reaction enthalpy for $Ru(NH_3)_6^{3+/2+}$ couple is especially noteworthy.

pH dependence of the incorporation

The apparent pK_a of the carboxylic acid groups in polyelectrolyte II can be investigated by measuring the effect of pH on the incorporation of cations by the polyelectrolyte. This experiment was performed by using $Ru(NH_3)_6^{3+}$ as a probe. Coatings of polyelectrolyte II was exposed to a solution of $Ru(NH_3)_6^{3+}$; pH of the solution was adjusted to a value between 1.5 and 5.5. After the incorporation equilibrium had been attained (30 min of exposure proved adequate), the coated electrode was transferred to a pure supporting electrolyte solution at the same pH, and the amount of the incorporation $Ru(NH_3)_6^{3+}$ was determined by stepping the electrode potential to -0.6V and measuring the total cathodic charge that passed until the current dropped to background levels. Figure 2.5 presents the results. The pH at which the incorporation reaches one-half of its maximum value (only ca. 36% of the total carboxylate groups in the coating bound $Ru(NH_3)_6^{3+}$ which were detected by the

Figure 2.5

Incorporation of $\text{Ru}(\text{NH}_3)_6^{3+}$ by polyelectrolyte II as a function of pH. Electrode coating contained 8.4×10^{-8} mole cm^{-2} of carboxylate groups. Electrode was equilibrated for 30 minutes with a 5 mM solution of $\text{Ru}(\text{NH}_3)_6^{3+}$ at each pH before transfer to pure supporting electrolyte for measurement of the quantity incorporated. Supporting electrolyte: $\text{pH} \geq 4.5$: acetate buffer; $2.25 \leq \text{pH} \leq 3.25$: phosphate buffer; $\text{pH} < 2$: $\text{HCl} + \text{NaCl}$. The ionic strength was maintained at 0.2 M.



electrochemical reduction) is 2.2. This value is close to the pK_a of 1.9 measured more directly for a similar perfluorocarboxylate polyelectrolyte¹⁵. However, the shape of the plot in Figure 2.5 does not match that of a typical pH titration curve. This is presumably due to the mutual interactions among the high concentration of carboxylate groups within the polyelectrolyte. A similar phenomenon was observed recently for coatings of protonated polyvinylpyridine¹⁶. The "effective pK_a " was seen to vary with the degree of protonation and with ionic strength¹⁶. Thus, it is not appropriate to identify the pH corresponding to half-maximum incorporation in Figure 2.5 with a single pK_a of the functional group. Nevertheless, it is clear that at pH values as low as 1, protons compete quite successfully with $Ru(NH_3)_6^{3+}$ ions for counter-ionic sites within the polyelectrolyte.

Discussion

The important conclusion obtained from the combination of Table 2.1 and Table 2.2 is that the equilibrium constants governing the incorporation of cations by coatings of polyelectrolyte II control the changes in the formal potentials of redox couples extracted into the coatings. This gives the formal potential of a redox couple in the polyelectrolyte coating a firm thermodynamic basis and demonstrates that it is accessible from a simple cyclic voltammetric experiment. As will be shown below, electrochemical techniques combined with polyelectrolyte modified electrodes such as in the present study are very useful in obtaining thermodynamic parameters associated with the binding of polyelectrolytes with counterions.

Recently Peter et al.¹⁷ reported that the formal potentials of $\text{Ru}(\text{CN})_6^{4-/3-}$ and $\text{Fe}(\text{CN})_6^{4-/3-}$ couples shifted significantly in the presence of protonated macrocyclic nitrogen donor ligands. The formation of "ionic complexes" was interpreted to account for the formal potential shifts. Although the situation is not the same as the present study, some similarities between these two systems are noteworthy.

The values of $E_p^f - E_s^f (= \Delta E^f)$ in Table 2.2 demonstrate that the relative equilibrium binding constants for two halves of a redox couple are not determined solely by the magnitude of their positive charges. For example, although the two couples, $\text{Ru}(\text{NH}_3)_6^{3+/2+}$ and $\text{Os}(\text{bpy})_3^{3+/2+}$, have the same pair of charge types, at ionic strength above ca. 0.05M the formal potentials of the couples are shifted in opposite directions upon incorporation.

The additional factor controlling the formal potential shifts seems likely to be hydrophobic interactions between the fluorocarbon component of the polyelectrolyte coating and the incorporated cations. These kinds of hydrophobic interactions have been interpreted to be the cause of the blue shift in the luminescence of $\text{Ru}(\text{bpy})_3^{2+}$ incorporated in Nafion membranes compared with the red shift observed with other, less hydrophobic polyelectrolyte¹⁸.

A parallel observation in an electrochemical study appeared recently. Faulkner et al.¹⁸ reported that the formal potential of $\text{Ru}(\text{bpy})_3^{3+/2+}$ exhibited a very negative shift upon incorporation into a polystyrenesulfonate coating, in contrast with the behavior of $\text{Os}(\text{bpy})_3^{3+/2+}$ couple in polyelectrolyte II coatings in the present study. This indicates that strong hydrophobic interactions only occur in certain cases such as perfluorocarbon polyelectrolytes. Other evidence is the much smaller diffusion coefficients within Nafion coatings of

cationic complexes with hydrophobic ligands²⁰. This was believed to originate from the strong interaction between the diffusing ions and the hydrophobic fluorocarbon portions of the interior of the polyelectrolyte.

The trends evident in the data of Table 2.2 can be rationalized in terms of the relative importance of hydrophobic and electrostatic interactions between the incorporated cations and the polyelectrolyte. For example, at an ionic strength of 0.2M, ΔE^f is positive for $\text{Os}(\text{bpy})_3^{3+/2+}$, near zero for $\text{CpFeCpCH}_2\text{N}(\text{CH}_3)_3^{2+/+}$ and negative for $\text{Ru}(\text{NH}_3)_6^{3+/2+}$. The less highly charged (i.e., reduced) form of each couple would be more hydrophobic and therefore be preferentially stabilized by hydrophobic interaction compared with its more highly charged partner. On the other hand, the electrostatic interactions are expected to act in the opposite direction. Thus, the values of ΔE^f for the three couples mentioned above imply the dominance of hydrophobic interactions for $\text{Os}(\text{bpy})_3^{3+/2+}$ and hydrophilic interaction for $\text{Ru}(\text{NH}_3)_6^{3+/2+}$, with the two factors exerting approximately equal and opposite influences for $\text{CpFeCpCH}_2\text{N}(\text{CH}_3)_3^{2+/+}$. This rationalization is consistent with the order of increasing hydrophobicity predicted from the structures, $\text{Ru}(\text{NH}_3)_6^{3+/2+} < \text{CpFeCpCH}_2\text{N}(\text{CH}_3)_3^{2+/+} < \text{Os}(\text{bpy})_3^{3+/2+}$.

The influences of ionic strength on the values of ΔE^f in Table 2.2 for the $\text{Os}(\text{bpy})_3^{3+/2+}$ and $\text{Ru}(\text{NH}_3)_6^{3+/2+}$ couples can be understood on the same basis. Alterations in the intensity of hydrophobic interactions induced by changes in ionic strength are not likely to be as large as the expected²¹ decreases in electrostatic interaction as the ionic strength increases. The latter changes can be substantial as illustrated by the behavior of $\text{Os}(\text{bpy})_3^{3+/2+}$ couple. ΔE^f in 2M supporting electrolyte solution is more positive, indicating the

strongest hydrophobic stabilization, while in the 0.02M solution ΔE^f becomes slightly negative, suggesting that under this condition the strength of the electrostatic interaction has increased sufficiently to overcome the hydrophobic interactions that operate in the opposite direction. The ΔE^f values for the much more hydrophilic $\text{Ru}(\text{NH}_3)_6^{3+/2+}$ couple show great dominance by electrostatic interactions at all ionic strengths investigated.

The intensity of these interactions is evidently quite large for this couple, as indicated by the unusually large value of ΔE^f in the 0.02M supporting electrolyte.

It is interesting to investigate the interactions between $\text{Ru}(\text{NH}_3)_6^{3+/2+}$ and other polyelectrolytes to gain additional information about the factors controlling the intensity of the electrostatic interactions. Thus, ΔE^f was measured for $\text{Ru}(\text{NH}_3)_6^{3+/2+}$ couple in Nafion coatings. At 0.2 M ionic strength the value observed was - 100 mV compared with -164mV for polyelectrolyte II under the same conditions. Previously similar differences between the strength of the binding of alkali cations by ion exchange resins on sulfonate and carboxylate groups have been observed. The behavioral difference has been attributed to differences in the structure of the primary hydration spheres of the cations induced by the two types of anionic binding groups²². This will be discussed in detail later. In the present study, where both hydrophobic and electrostatic factors are believed to influence the strength of cation binding, the difference in ΔE^f for Nafion and polyelectrolyte II for $\text{Ru}(\text{NH}_3)_6^{3+/2+}$ couple may reflect a greater control by electrostatic binding in the latter coating.

Let us now turn to the entropic and enthalpic changes associated with the incorporation equilibria, such as that in equation (2.6). Table 2.3 clearly

reveals the great entropic control of the equilibria. The discussion will be first focused on the results from the polycarboxylates.

Table 2.4 lists the thermodynamic parameters of the substitution of divalent cations for a monovalent cation (Na^+) as counterions of a carboxymethylcellulose (CMC), taken from Ref. 23a, along with those of $\text{Ru}(\text{NH}_3)_6^{3+/2+}$ in polyelectrolyte II from Table 2.3. It is evident in Table 2.4 that the overall free energy change which favors the higher charged cation is composed of a favorable entropy term and an unfavorable enthalpy term. As did Rinaudo and Milas^{23a} the major entropic contribution is attributed to the release of water molecules from both the charged binding sites and the hydration spheres of the bound cations. Evidence has been presented for the release of water molecules upon counterion binding by the ultrasonic absorption^{23c} and molar volume^{23d} measurements in some previous studies. Presumably the extent of desolvation is larger when a cation of higher charge density is the counterion; this can account for the results in Table 2.4. It is also noted that in Table 2.4 that the entropic term in the $\text{Ru}(\text{NH}_3)_6^{3+/2+}$ case is much larger than the others. This possibly indicates an unusually large extent of the desolvation of tripositive $\text{Ru}(\text{NH}_3)_6^{3+}$. Since the structures of the two polyelectrolytes are different, further speculation is unwarranted. The enthalpy term will be discussed later.

Table 2.3 shows that the binding of the $\text{Ru}(\text{NH}_3)_6^{3+/2+}$ couple by Nafion produces a much smaller value of $\Delta\Delta S^\circ_c$ than for binding to the polyelectrolyte, II. This may be a reflection of a higher charge density on the fixed anionic sites in polyelectrolyte II compared with Nafion. This could produce tighter ion pairing with multiply-charged cations within polyelectrolyte II and greater loss of

Table 2.4
Thermodynamic Parameters in Ion Exchange Reactions

Polyelectrolyte	Exchanges	ΔG°	ΔH°	ΔS°
		Kcal mol ⁻¹	Kcal mol ⁻¹	cal/K mol
CMC ^{a, b}	$2\text{Na}^+ \rightarrow \text{Ca}^{2+}$	-3.28	+1.54	+16.2
CMC ^{a, b}	$2\text{Na}^+ \rightarrow \text{Sr}^{2+}$	-3.16	+0.90	+13.7
CMC ^{a, b}	$2\text{Na}^+ \rightarrow \text{Ba}^{2+}$	-3.30	+0.34	+12.2
polyelectrolyte II ^c	$\text{Na}^+ + \text{Ru}(\text{NH}_3)_6^{2+} \rightarrow \text{Ru}(\text{NH}_3)_6^{3+}$	-4.88	+7.22	+40.6

a. CMC = Carboxymethylcellulose

b. From M. Rinaudo and M. Milas, "Macromolecules", 6, 879 (1973).

c. From Table III, $\Delta G^\circ = \Delta\Delta G^\circ_{298}$, $\Delta H^\circ = \Delta\Delta H^\circ_{298}$, $\Delta S^\circ = \Delta\Delta S^\circ_{rc}$.

water molecules from the outer coordination spheres of the incorporated complexes. Differences in the partial molar volumes of sulfonate and carboxylate bearing polyelectrolytes upon incorporation of cations were explained in similar terms by Tondre and Zana^{23f}. It is noteworthy that although the free energy changes involved in the incorporation equilibria of $\text{Ru}(\text{NH}_3)_6^{3+/2+}$ couple in Nafion and in polyelectrolyte II are not very different, their enthalpic and entropic changes are drastically different. This points to the fact that a clear picture of counterion binding by polyelectrolytes can not be obtained solely by the free energy changes. Similar comments have been made previously^{23b}. That the entropic change associated with the incorporation of $\text{Os}(\text{bpy})_3^{3+/2+}$ couple is smaller than that for $\text{Ru}(\text{NH}_3)_6^{3+/2+}$ couple is presumably due to the lower charge density and/or higher hydrophobicity of the former couple. This will make a smaller difference in the solvation structures of the two halves.

The positive value of $\Delta\Delta H^\circ$ for incorporation of the $\text{Ru}(\text{NH}_3)_6^{3+/2+}$ couple by polyelectrolyte II (Table 2.3) is interesting not only due to its sign but also due to its being so large. This (as well as other positive values of entropic change in Tables 2.3 and 2.4) represents the net result of a variety of coulombic and dipolar interactions whose individual contributions to the measured values of $\Delta\Delta H^\circ$ would be different to disentangle.

Since, as discussed above, the release of the water molecules from the hydration spheres of both fixed charged groups and the incorporated ions can account for the large entropy changes, water molecules could also possibly be an important factor to the observed positive enthalpy. Changes in the ion-dipole interaction between water molecules and the fixed ionic groups and those

between water molecules and the incorporated ions may make important contributions to the enthalpy changes. Hydrogen bonding may also make some contributions²⁴.

Concluding remarks

The present study has demonstrated that modified electrodes based on deposited polyelectrolyte films are very useful in the study of the interaction between polyelectrolytes and multiply-charged counterions. The difference in the measured formal potential of a redox couple in solution and incorporated within a polyelectrolyte was shown to reliably reflect the difference between the free energy changes associated with the incorporation of the two halves of the redox by the polyelectrolyte.

It is interesting to note that the factors governing the relative binding interaction of polyelectrolytes and complex ions can involve much more than the concept of coulombic interaction. Water molecules have been found to be a very important factor in governing the incorporation equilibria involving multiply-charged ions. Further studies might be made on the effects of the polyelectrolyte structure on the thermodynamic parameters for the incorporation equilibria. This needs the availability of stable polyanion films other than perfluoro polyelectrolytes.

References

- 1 N. Oyama and F. C. Anson, *J. Electrochem. Soc.*, 127(1980)247.
- 2 F. C. Anson, T. Ohsaka and J.-M. Saveant, *J. Am. Chem. Soc.*, 105(1983)4883.
- 3 (a) N. Oyama, T. Shimomura, K. Shigehara and F. C. Anson, *J. Electroanal. Chem.*, 112(1980)271; (b) K.-N. Kuo and R. W. Murray, *ibid.*, 131(1982)37.
- 4 H. Braun, W. Storck and K. Doblhofer, *J. Electrochem. Soc.*, 130(1983)807.
- 5 D. A. Buttry and F. C. Anson, *J. Am. Chem. Soc.*, 104(1982)4824.
- 6 N. Oyama and F. C. Anson, *ibid.*, 101(1979)3450.
- 7 R. G. Gaunter and H. Taube, *Inorg. Chem.*, 9(1970)2627.
- 8 C. Creutz, M. Chou, T. L. Netzel, M. Okumura and N. J. Sutin, *J. Am. Chem. Soc.*, 102(1980)1309.
- 9 A. J. Bard and L. R. Faulkner, " *Electrochemical Methods*, " John Wiley and Sons, Inc., New York (1980), p.536.
- 10 E. L. Yee, R. J. Cave, K. L. Guyer, P. D. Tyma and M. J. Weaver, *J. Am. Chem. Soc.*, 101(1979)1131.
- 11 (a) N. Sutin, M. J. Weaver and E. L. Yee, *Inorg. Chem.*, 19(1980)1096; (b) E. L. Yee and M. J. Weaver, *ibid.*, 19(1980)1077; (c) M. J. Weaver and S. M. Nettles, *ibid.*, 19(1980)1641; (d) S. Sahami and M. J. Weaver, *J. Electroanal. Chem.*, 122(1981)155,171; (e) V. T. Taniguchi, W. R. Ellis, Jr., V. Cammarata,

- J. Webb, F. C. Anson and H. B. Gray, *Adv. Chem. Ser.*, 201(1982)51.
- 12 F. C. Anson, J.-M. Saveant, K. Shigehara, *J. Am. Chem. Soc.*, 105(1983)1096.
- 13 N. Oyama and F. C. Anson, *J. Electrochem. Soc.*, 127(1980)640.
- 14 A. J. Bard and L. R. Faulkner, " *Electrochemical Methods*, " John Wiley and Sons, Inc., New York (1980), Chap. 6.
- 15 Z. Twardowski, H. L. Yeager and B. O'Dell, *J. Electrochem. Soc.*, 129(1982)328.
- 16 H. Zumbrennen and F. C. Anson, *J. Electroanal. Chem.*, 152(1983)111.
- 17 F. Peter, M. Gross, M. W. Hosseini and J. M. Lehn, *J. Electroanal. Chem.*, 144(1983)279.
- 18 P. C. Lee and D. Meisel, *J. Am. Chem. Soc.*, 102(1980)5477.
- 19 M. Majda and L. R. Faulkner, *J. Electroanal. Chem.*, 169(1984)77.
- 20 D. A. Buttry and F. C. Anson, *J. Am. Chem. Soc.*, 105(1983)685.
- 21 F. G. Helfferich, " *Ion Exchangers*, " McGraw-Hill, New York (1962), Chap. 4.
- 22 (a) H. Morawetz, " *Macromolecules in Solution*, " 2nd ed., John Wiley and Sons, Inc., New York (1975), p.369; (b) L. Lazare, B. R. Sundheim and H. P. Gregor, *J. Phys. Chem.*, 60(1956)641; (c) I. Michalei and A. Katchalsky, *J. Polym.Sci.*, 23(1957)683; (d) F. Nelson and K. A. Kraus, *J. Am. Chem. Soc.*, 80(1958)4154; (e) M. H. Gottlieb and H. P. Gregor, *ibid.*, 76(1954)4639.

- 23 (a) M. Rinaudo and M. Milas, *Macromolecules*, 6(1973)879; (b) G. E. Boyed and D. P. Wilson, *ibid.*, 15(1982)78; (c) R. Zana, C. Tondre, M. Rinaudo and M. Milas, *J. Chim. Phys.*, 68(1971)1258; (d) M. Rinaudo and C. Pierre, *C. R. Acad. Sci., Ser. C*, 269(1970)1170; (e) J. Hen and U. P. Strauss, *J. Phys. Chem.*, 78(1974)1013; (f) C. Tondre and R. Zana, *J. Phys. Chem.*, 76(1972)3451.
- 24 (a) H. S. Frank and M. W. Evans, *J. Chem. Phys.*, 13(1945)507; (b) C. Tanford, " *The Hydrophobic Effect: Formation of Micelles and Biological Membranes*, " 2nd ed., John Wiley and Sons, New York (1980), p.27.

CHAPTER III

Outer-Sphere Oxidation of Ascorbate with $\text{Os}(\text{bpy})_3^{3+}$

Incorporated in Nafion Coatings

on Graphite Electrodes

Introduction

A large number of recent studies on polymer modified electrodes have focused on their possible uses in electrocatalysis¹. The original motivation for developing polymer modified electrodes was the intention to enlarge the capacities of the catalytic systems derived from monolayer catalysts. Attaching the catalyst to the electrode surface offers two advantages: (1) the easy separation of the catalyst from the product (2) providing a high local concentration of catalyst with the use of a very small total quantity of it. The multilayer nature of polymer modified electrodes provides one more advantage which is carrying out the catalytic reaction in a three-dimensional fashion compared with a two-dimensional fashion for monolayer derived electrodes. This prediction was based on a model of electrocatalytic reactions at redox polymer electrodes in which the rate-limiting process was the electrocatalytic reaction itself. But it was soon realized that two other processes may also be the rate-limiting processes, namely, the diffusion of the substrate from the film-solution interface to the electrode surface, and the rate of charge propagation between the electrode-film and the film-solution interface.

A more sophisticated model was thus presented by Saveant and co-workers². The model was analyzed in the context of rotating disk voltammetry at the level(s) of plateau current. It rigorously accounted for the interplay of

these three factors, together with the diffusion of the substrate in the solution. Another interesting point which has not been commonly realized is that these studies also provide the opportunities for understanding the effects of polyelectrolyte environments on redox reactions. Despite the availability of the theoretical model, few experimental studies have been undertaken in order to test the theory^{1,2f,g}. No quantitative kinetic experiments have been carried out with coatings prepared from Nafion, the perfluoropolyelectrolyte (see section II for the structure) that has been shown to provide very stable and chemically inert films^{3,4}.

In this study $\text{Os}(\text{bpy})_3^{2+}$ ($\text{bpy}=2, 2'$ -bipyridine) is incorporated in Nafion coatings on graphite electrodes, where it can be electro-oxidized to $\text{Os}(\text{bpy})_3^{3+}$ and used to oxidize ascorbate to dehydroascorbic acid. In a previous study the $\text{Os}(\text{bpy})_3^{3+/2+}$ couple was found to be quite stable in Nafion coatings and yield reversible cyclic voltammograms^{3c} at potentials well removed from the background which frequently interferes in experiments with the corresponding $\text{Ru}(\text{bpy})_3^{3+/2+}$ couple. In addition, the relatively slow propagation of charge through Nafion coatings by the $\text{Os}(\text{bpy})_3^{3+/2+}$ couple^{3c} offered the possibility for experimental examination of the case in which the rate of charge propagation (i.e., the rate of regeneration of the catalyst $\text{Os}(\text{bpy})_3^{3+}$), rather than the rate of the electron-transfer cross-reaction itself, limited the measured currents.

Ascorbate was chosen as the substrate because its unassisted electro-oxidation at Nafion-coated electrodes is very slow, and the kinetics of the oxidation of ascorbate in homogeneous solution by a variety of outer-sphere oxidants have been thoroughly studied^{5,6}. In the present study the experiments were conducted at pH values where the ascorbate was anionic and presumably

was not incorporated into the polyanionic Nafion coatings. Thus, the electron transfer cross-reaction was assumed to involve $\text{Os}(\text{bpy})_3^{3+}$ bound to the coating and ascorbate dissolved in the supporting electrolyte solution that permeates the hydrophilic channels that are characteristic features of the structure of Nafion membranes.⁷

Experimental

Material

$\text{Os}(\text{bpy})_3\text{I}_2 \cdot 3\text{H}_2\text{O}$ was prepared as described by Creutz et al.⁷ The iodide was converted to the p-toluenesulfonate (pTS) salt by addition of a stoichiometric amount of $\text{Ag}(\text{pTS})$ to an aqueous solution of the iodide and filtering to remove AgI . $\text{NaFe}(\text{edta}) \cdot 2\text{H}_2\text{O}$ was prepared according to Ref. 8. Other chemicals were reagent grade and were used as received. Soluble Nafion was available as a 5.2 wt.% solution obtained a number of years ago from E.I. du Pont de Nemours & Co. Similar material is now commercially available (C.G. Processing, Inc., Rockland, DE). Coatings were prepared from a stock solution of Nafion prepared by diluting this solution 10-fold with isopropanol. Pyrolytic graphite electrodes (Union Carbide Co.) were cut into 0.17 cm^2 disks and mounted as previously described^{1a} to expose the basal planes of the graphite to the test solutions.

Apparatus and procedures

The electrochemical apparatus and procedures employed have been previously described^{1a}. During measurements by chronocoulometry⁹ of charge propagation rates in Nafion- $\text{Os}(\text{bpy})_3^{2+}$ coatings, positive feedback was added to the potentiostatic circuit to compensate for as much of the coating resistance

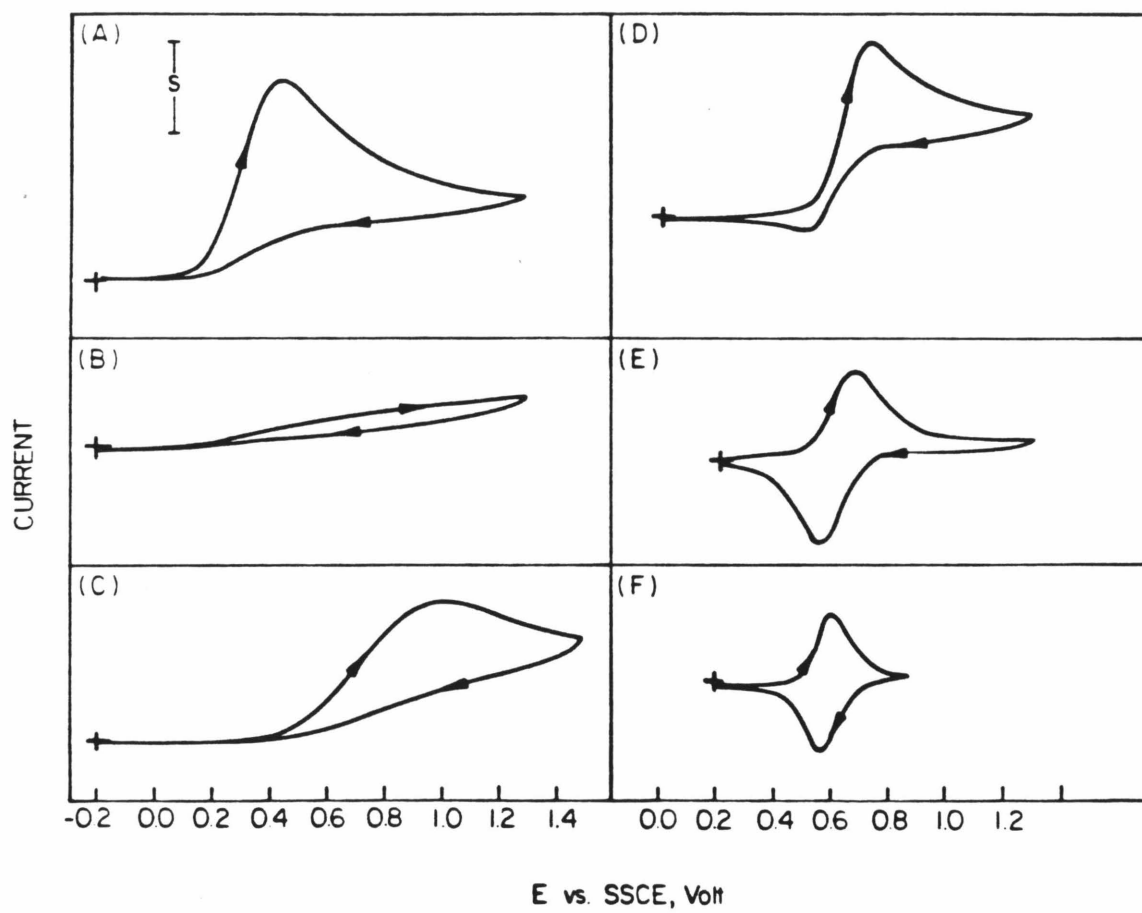
as possible. Preparation of the Nafion coatings and incorporation of the $\text{Os}(\text{bpy})_3^{2+}$ complex followed the procedures described earlier^{4c}. The most stable coatlings were obtained by allowing the Nafion to incorporate $\text{Os}(\text{bpy})_3^{2+}$ to its saturation level (typically amounting to 25-30% of the sulfonate groups in the coating). This also produced a standard coating for the measurement of substrate diffusion rates. For these reasons all measurements were conducted with coatings saturated with $\text{Os}(\text{bpy})_3^{2+}$. The quantities of electroactive $\text{Os}(\text{bpy})_3^{2+}$ incorporated in the coatings were measured coulometrically after the loaded coating was transferred to pure supporting electrolyte solution. Test solutions were de-aerated with pre-purified argon. Potentials are quoted with respect to a sodium chloride saturated calomel electrode, SSCE.

Result and discussion

A set of cyclic voltammograms obtained from the oxidation of ascorbate at several types of graphite electrodes is presented in Figure 3.1. The large anodic wave in curve A is obtained at the freshly cleaved,uncoated basal plane of the pyrolytic graphite electrode. Coating this electrode with Nafion causes the direct oxidation to be severely inhibited as shown in curve B. The inhibition is presumably the result of barriers encountered by ascorbate anions which must cross the polyanionic coating to reach the electrode surface (where the oxidation occurs), as well as possible decreases in the rate constant for the electrode reaction produced by the Nafion coating. At lower pH values where the ascorbate is converted to uncharged ascorbic acid, a larger current for direct oxidation at Nafion-coated electrodes is observed (curve C), indicating less difficulty for ascorbic acid to permeate the coating. Comparison of curves

Figure 3.1

Cyclic voltammograms for the oxidation of 8.2 mM ascorbate at basal plane graphite electrodes in 0.4 M CH_3COONa (pH 5.5).
(A) Freshly cleaved uncoated electrode;
(B) Repeat of A after coating the electrode with Nafion to the extent of $1.5 \times 10^{-7} \text{ mol cm}^{-2}$ of sulfonate groups;
(C) Repeat of B except the supporting electrolyte is 0.2 M NaHSO_4 at pH 2;
(D) Repeat of B after $1.7 \times 10^{-8} \text{ mol cm}^{-2}$ of $\text{Os}(\text{bpy})_3^{2+}$ was incorporated in the Nafion;
(E, F) Repeat of D in the absence of ascorbate.
Scan rate: (A) - (E) 100 mV s^{-1} ; (F) 5 mV s^{-1} . S: $150 \mu\text{A}$ for (A) - (D); $75 \mu\text{A}$ for (E); $7.5 \mu\text{A}$ for (F).



B and D shows that rapid oxidation of ascorbate results when $\text{Os}(\text{bpy})_3^{2+}$ is incorporated into the Nafion coating. However, the oxidation now proceeds at potentials quite close to the formal potential of the $\text{Os}(\text{bpy})_3^{3+/2+}$ couple (curve E) instead of the less positive potential observed at the uncoated graphite electrode (curve A). That the shape of the cyclic voltammogram for $\text{Os}(\text{bpy})_3^{3+/2+}$ exhibits significant tailing at potentials beyond the peaks indicates a diffusion limited response despite the fact that the reactant is confined within the Nafion coating on the electrode. The reason is that the very small rate of propagation of $\text{Os}(\text{bpy})_3^{2+}$ within Nafion coatings causes the delivery of the complex to the electrode surface to match that obtained for true semi-infinite linear diffusion at the scan rate employed in curve E. If the cyclic voltammetry is performed at a sufficiently low scan rate, such that the dimension of the diffusion layer at the electrode surface becomes commensurate with the thickness of the Nafion coatings, a more symmetrical response is obtained (curve F) as is expected for a surface-confined reactant that is exhaustively oxidized and re-reduced during the recording of the cyclic voltammogram ¹⁰. In any case the close correspondence of the anodic peak potential in curve E to the potential where the anodic current begins to flow in curve D clearly shows that the $\text{Os}(\text{bpy})_3^{3+/2+}$ couple is mediating the oxidation of the ascorbate in curve D. The remainder of this chapter III is focused on the attempts to account for the magnitude of the mediated ascorbate oxidation currents in terms of the model and theory presented by Andrieux, Saveant and co-workers^{2a,b,c}. The polyanionic Nafion coatings appear to have structures and associated properties that cause their behavior to deviate significantly from that expected from existing models^{2a,b,c} in which some mediated reactions in other polyelectrolyte coatings have shown good agreement.

Rotating disk voltammetry

Catalyzed and mediated current responses at polymer-coated electrodes can be analyzed most simply and appropriately by a steady-state method at a rotating disk electrode¹¹. This method has been widely employed in electrochemistry¹¹. Moreover, recently it has proved to be extremely powerful in obtaining kinetic information of mediated reaction at polymer-coated electrodes¹. Therefore, this method was used quite frequently to obtain quantitative data. Rotating disk voltammetry is the most convenient and widely used electrochemical technique involving convective mass transfer of reactants and products. In this technique a disk electrode is rotated about an axis through its center and normal to its surface. The applicable range of rotation rates is between 100 and 10,000 revolutions per minute (RPM).

At a rotating bare electrode the spinning electrode flings the solution outwards from the center in a radial direction and the solution at the electrode surface is replenished by a flow normal to its surface. The essential point is that the rate of the mass transport of the species interested in the solution can be controlled by the rotation rate of the electrode.

The great advantage of rotating disk voltammetry is that a measurement is made at a quickly attained steady state. This usually allows currents to be measured with high precision. Moreover, the interference from double-layer charging can be avoided. In a typical rotating disk experiment at a bare electrode, the electrode is rotated at a fixed rate while the electrode potential is slowly scanned through the potential range of interest. For a simple electrochemical redox reaction, the current rises near the redox potential of

the species and finally the current levels off to a limiting current plateau, giving an s-shaped current-potential curve. When the limiting current flows at a bare electrode for the simple electrode redox reaction, the electrode process is occurring at the maximum rate possible, i.e., under the totally mass-transfer-limited condition. In other words, the species is reduced (or oxidized) as fast as it can be brought to the electrode surface. This limiting current is given by the Levich equation¹²

$$i_{Lev} = 0.62nFA D^{2/3} \omega^{1/2} \nu^{-1/6} C^* \quad (3.1)$$

where i_{Lev} is the Levich current (amp), n is the number of electron(s) consumed in the redox process, F is the Faraday constant, A is the electrode area (cm^2), D and C^* are the diffusion coefficient ($\text{cm}^2 \text{ s}^{-1}$) and bulk concentration (mole cm^{-3}), respectively, of the redox species, ω is the angular velocity (sec^{-1}) and ν is the kinematic viscosity of the solution ($\text{cm}^2 \text{ s}^{-1}$). The Nernst diffusion layer model¹³ can be applied to express the Levich equation in a conceptually simple way. This model assumes that a stagnant layer of thickness, δ , exists near the electrode surface. Outside this layer, convective transport maintains the concentration uniform at the bulk concentration, C^* . Within the layer mass transfer occurs only by diffusion. The model expresses the limiting current¹³ as

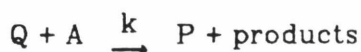
$$i_{Lev} = nFA \left(\frac{D}{\delta} \right) C^*$$

where δ is the diffusion layer thickness. Therefore, for a rotating disk electrode the diffusion layer thickness is $\delta = 1.61 D^{1/3} \omega^{-1/2} \nu^{1/6}$. The concept of the Nernst diffusion-layer model is very useful. It makes the treatment of kinetic behavior of electrochemical reactions mediated by redox polymer films easier.

Description of the model for electrochemical reactions mediated by redox

polymer films in a rotating disk voltammetric experiment^{2a}

The catalyzed (mediated) reaction is expressed as follows:



where P/Q is the catalyst couple and A is the substrate in the case of an oxidation process. The second-order rate constant (k) is for the reaction between the substrate and Q, i.e. the active form of the mediation in the film.

The film is assumed to be loaded uniformly with a fixed amount of catalyst (Γ^0 , mole cm⁻²) which corresponds to a concentration $C^0 = \Gamma^0/\varphi$ (mole cm⁻³), where φ (cm) is the film thickness.

The various characteristic currents are described now. The rate at which the catalyst in the coating can be electro-oxidized (or electro-reduced) is regarded as having a diffusion-like character. In their treatments², Andrieux et al. have used a general term, "the propagation of the electrons through the film," or "diffusion of electrons" to denote this rate. These general terms were introduced to emphasize that the treatments could be applied to any charge propagation mechanism in the redox polymer films (the rate-limiting steps can be physical motion, electron hopping, some other mechanism(s) or a combination of them). In any case, an "effective diffusion coefficient" which can be measured by electrochemical methods is sufficient to evaluate the rate.

The diffusion of the substrate from the film-solution interface through the film toward the electrode is assumed to be linear and characterized by a diffusion coefficient, D_s , different from that in the solution.

Diffusion of the substrate from the bulk of the solution to the film-solution interface is regarded as stationary and is treated by the Nernst linear diffusion-layer model¹⁹. The concentration gradient is determined by the substrate bulk concentration and its concentration at the film-solution interface which is controlled by the relative magnitudes of the characteristic currents.

The catalytic reaction is assumed to occur according to the scheme depicted above. The regions in the film where the reaction occurs as well as the concentration profiles of the catalyst and the substrate in the film depend on the relative magnitudes of the characteristic currents.

The equilibrium concentration of substrate (A) in the solution and in the film are not necessarily regarded as equal. A partition coefficient is defined as $\kappa = [A_{film}]_{eq} / [A_{sol}]_{eq}$.

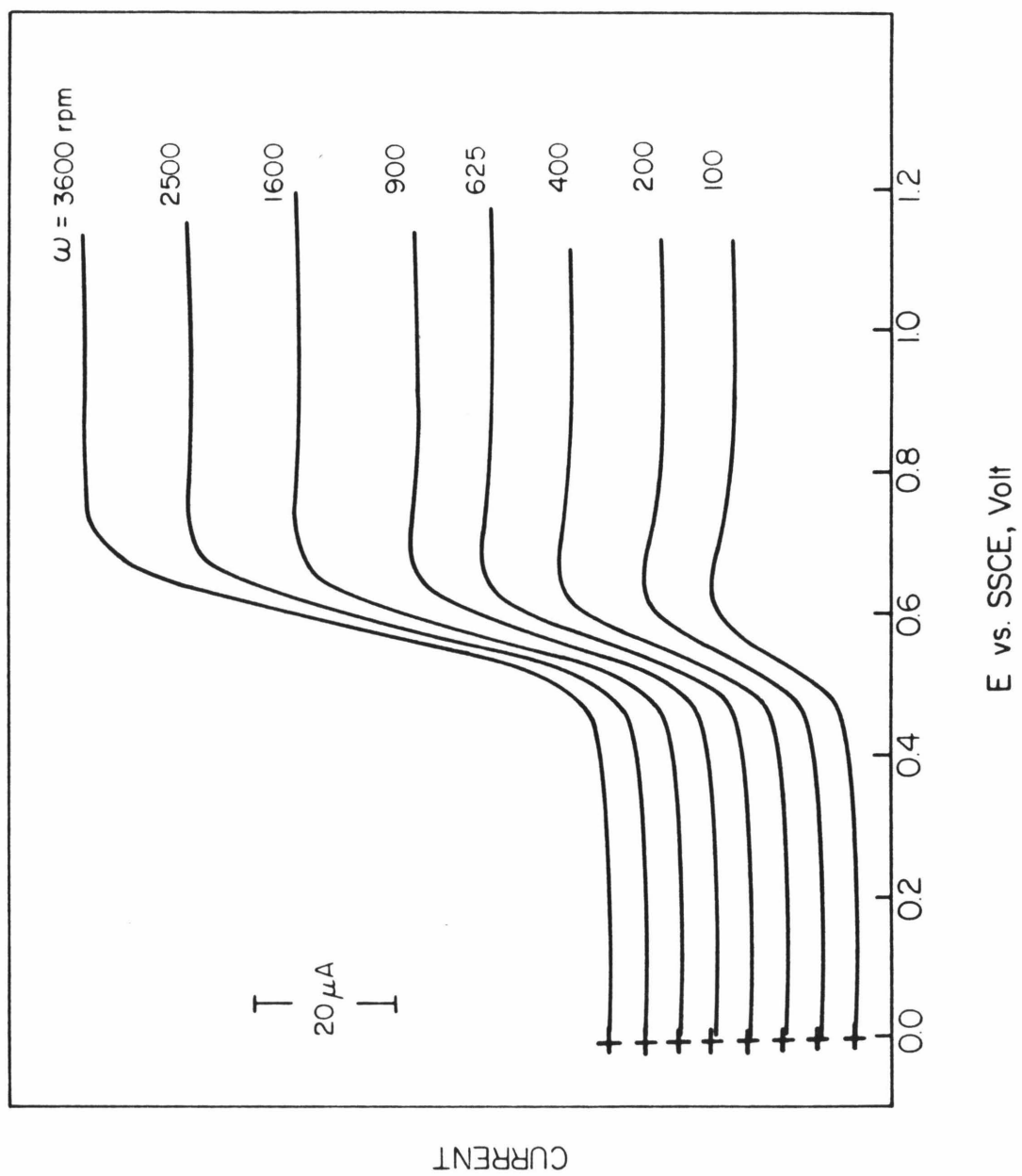
The expressions for these characteristic currents will be discussed in the corresponding sections.

Analysis of the rotating disk voltammetric data

Figure 3.2 shows a set of current-potential curves for ascorbate oxidation at a rotating graphite disk electrode coated with Nafion-Os(bpy)₃²⁺. No significant current flow was observed before the Os(bpy)₃²⁺-mediated wave. Presumably this is because the incorporation of Os(bpy)₃²⁺ in the coating introduces electrostatic cross-linking that diminishes the already low rate of penetration of the coating by ascorbate anions to a very low level. The similar phenomena observed by Oyama and Anson^{1a} in the system of the oxidation of

Figure 3.2

Current-potential curves for oxidation of 0.38 mM ascorbate at a rotating graphite disk electrode coated with 1.5×10^{-7} mole cm^2 of Nafion in which 1.8×10^{-8} mole cm^{-2} of $\text{Os}(\text{bpy})_3^{2+}$ was incorporated. Supporting electrolyte: 0.1 M CF_3COONa + 0.1 M CH_3COONa (pH 5.5). Scan rate 5 mV s^{-1} . Electrode rotation rates, ω , are listed for each curve.



$\text{Fe}^{2+}(\text{aq})$ by the protonated polyvinylpyridine- IrCl_6^{3-} was explained in similar terms. Levich plots¹² of the limiting disk currents vs. $\omega^{1/2}$, where ω is the electrode rotation rate, are non-linear as shown in Figure 3.3. The non-linearity indicates the presence of current-limiting factors other than the rate of convective transfer of ascorbate to the coating/electrolyte solution interface. The current-rotation rate responses obtained were then analyzed by means of Koutecky-Levich plots¹⁴ of $(i_{\text{lim}})^{-1}$ vs. $\omega^{-1/2}$ for comparison with the relevant theoretical treatment^{2a}. At concentrations of ascorbate below ca. 0.2 mM, linear Koutecky-Levich plots such those shown in Figure 3.4A were obtained with slopes that matched that expected for the two-electron oxidation of ascorbate (the diffusion coefficient is $5.7 \times 10^{-6} \text{ cm}^2\text{s}^{-1}$ ¹⁵) and intercepts that are inversely proportional to the concentration of ascorbate. At higher concentrations the data exhibited deviant behavior that will be described later.

Before a thorough analysis of the data can be performed, the relative magnitudes of the various characteristic current densities described earlier have to be evaluated (or estimated). This is described as follows:

Measurement of the characteristic current density for catalyst oxidation

The rate at which $\text{Os}(\text{bpy})_3^{2+}$ in the coating can be electro-oxidized is governed by the characteristic current density, i_E (A cm^{-2}), as defined by Andrieux et al.^{2b}

$$i_E = FD_E\Gamma_{\text{Os}}/\varphi^2 \quad (3.1)$$

where F is the Faraday constant, D_E (cm^2s^{-1}) is the effective diffusion coefficient of the $\text{Os}(\text{bpy})_3^{2+}$, Γ_{Os} (mole cm^{-2}) is the total surface concentration

Figure 3.3

Levich plots for the oxidation of ascorbate at a rotating graphite disk electrode coated with Nafion-Os(bpy)₃²⁺. Ascorbate concentrations: 1 - 0.032; 2 - 0.063; 3 - 0.13; 4 - 0.26; 5 - 0.38; 6 - 0.51; 7 - 1.03 mM. Other conditions as in Figure 3.2.

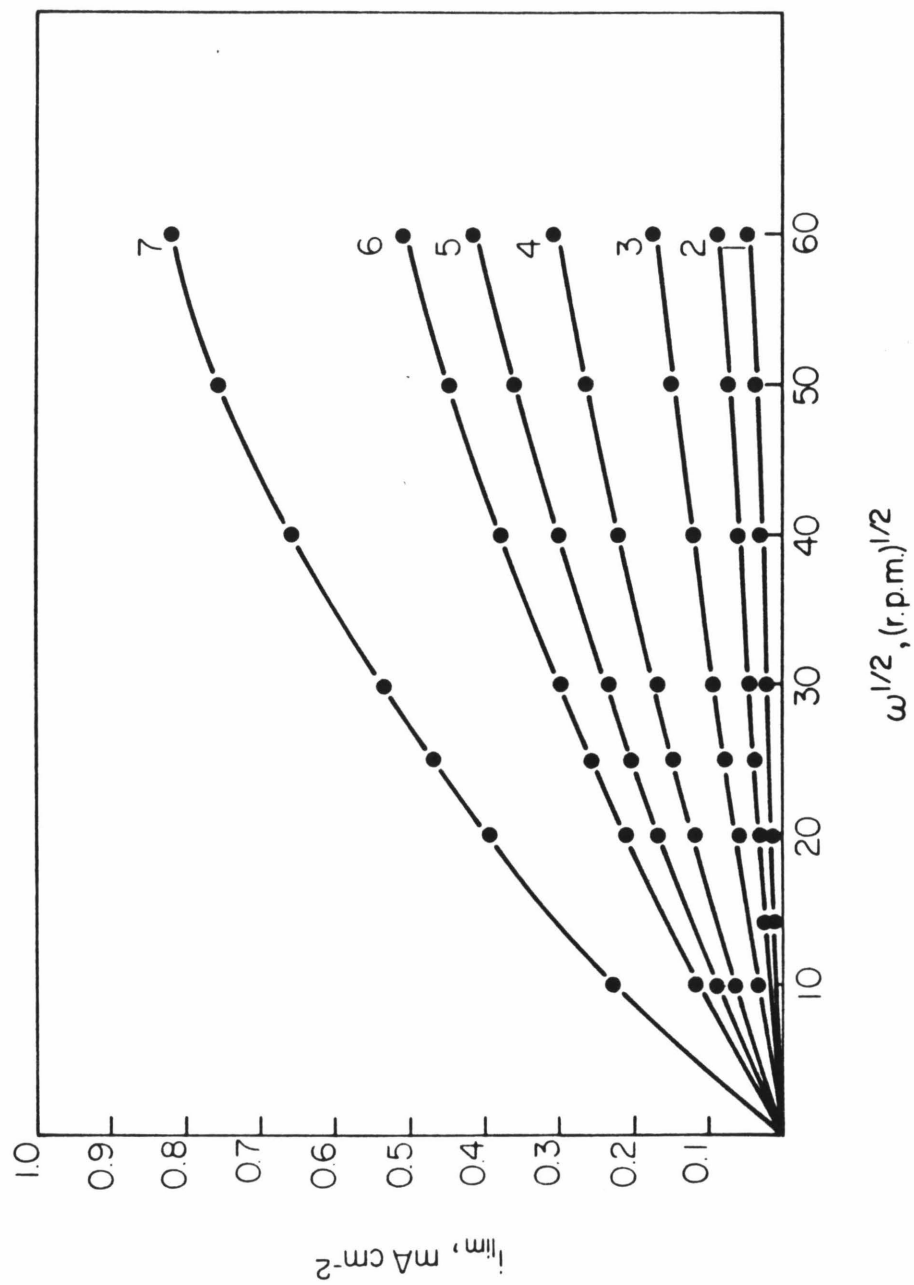
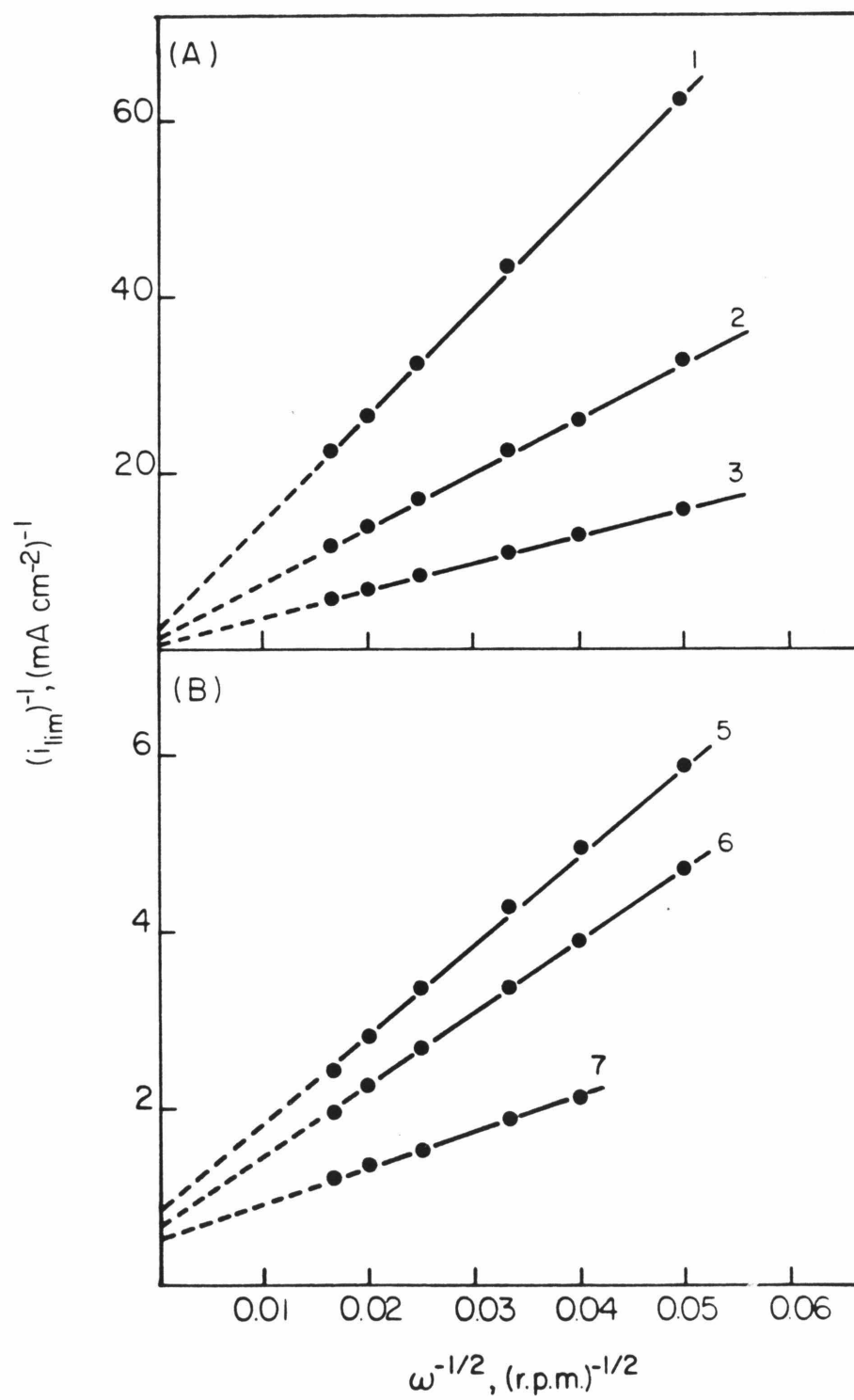


Figure 3.4

Koutecky-Levich plots of some of the data from Figure 3.3
The numbers on the lines correspond to the concentrations
listed in Figure 3.3.



of the complex in the coating, and φ (cm) is the coating thickness. For isotropic coatings of uniform thickness, i_E could be evaluated (without having to know the film thickness) from transient potential step measurements with the catalyst-loaded films in the pure supporting electrolyte solution. In the present work chronocoulometric method ¹⁶ was performed. In this method the potential of Nafion-Os(bpy)₃²⁺ coated electrode is initially equilibrated at a potential well negative of the redox potential; at $t=0$, its potential is stepped to a value well beyond the redox potential so that Os(bpy)₃²⁺ is oxidized at a diffusion-controlled rate. The resulting linear plot of charge vs. (time)^{1/2} has a slope, S , which is related to i_E by equation (3.2)^{16,17}.

$$i_E = \pi S^2 / 4F\Gamma_{Os} \quad (3.2)$$

An assumption made in writing equation (3.2) is that the effective diffusion coefficient of Os(bpy)₃²⁺ in the small portion of the coating sampled during the transient chronocoulometric measurement is representative of the coefficient governing the complex throughout the entire film.

If an anisotropic structure of the coatings renders the diffusion coefficient of incorporated complex varies with its position in the coating, equation (3.2) would not apply. It is suspected that this could well be the case for Nafion. For the coatings utilized to obtain the data in Figures 3.1-3.4, where Γ_{Os} was 1.7 to 1.8×10^{-8} mole cm⁻², the values of i_E evaluated were in the range of 1.0 to 1.3 mA cm⁻².

Estimation of the characteristic current density for substrate diffusion through the film

The rate at which a substrate penetrates a coating on the electrode is governed by the characteristic current density, i_s , as defined by equation (3.3)^{1f,2b}.

$$i_s = nF\kappa D_S C_A^0 / \varphi \quad (3.3)$$

where n is the number of electrons involved in the substrate reaction and C_A^0 is the concentration of the substrate in the bulk of the solution, D_S is the diffusion coefficient of the substrate within the coating, and κ the coefficient governing the partitioning of the substrate between the solution inside and outside the coating. The value of i_s can be directly evaluated in favorable cases where the wave (with a well-defined plateau) corresponding to the direct oxidation (or reduction) precedes its catalyst-mediated reaction^{1f}. Otherwise, its direct reaction can be measured with a coating containing a complex that is structurally similar to the actual catalyst, but inactive toward the substrate. Alternatively, a surrogate substrate of approximately the same diffusional characteristics^{1e,17} as the substrate can be employed with actual catalyst-bearing coatings if there is no reaction between the surrogate and the catalyst. Unfortunately, neither of these strategies could be successfully applied to the case of ascorbate.

The Nafion coatings, both with and without incorporated $\text{Os}(\text{bpy})_3^{2+}$, repressed the unassisted oxidation of ascorbate at potentials preceding the catalytic wave so severely that no reliable evaluation of the current due to the direct oxidation of ascorbate was possible. The situation was marginally better for the surrogate substrate $\text{Fe}(\text{edta})^-$ (edta = ethylenediamminetetraacetate) which bears the same uni-negative charge as ascorbate anion. Its unassisted reduction to $\text{Fe}(\text{edta})^{2-}$ at electrodes coated with Nafion- $\text{Os}(\text{bpy})_3^{2+}$ proceeds at

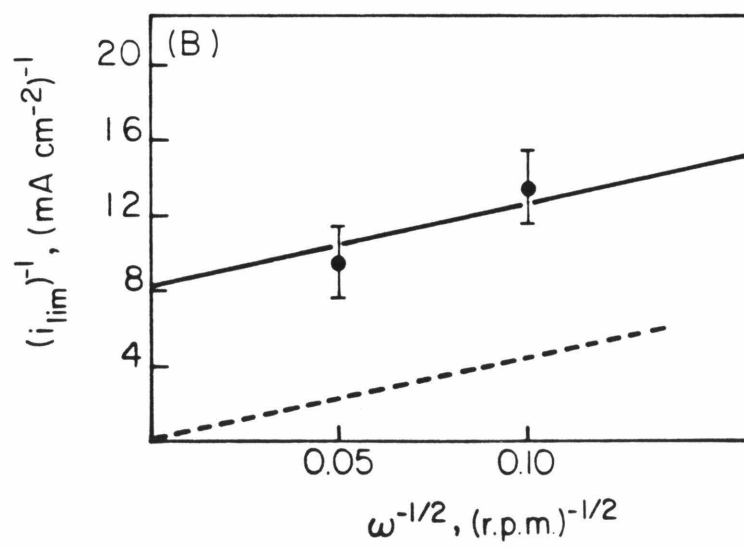
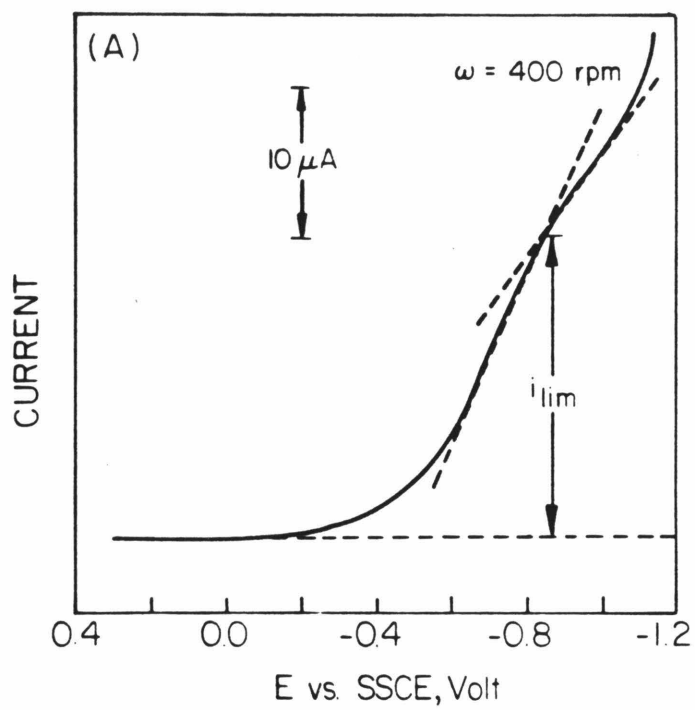
potentials far negative to the potential where the response from the $\text{Os}(\text{bpy})_3^{3+/2+}$ couple occurs and provides a measure of diffusion rate in the coating. A typical rotating disk current-potential curve for the reduction of $\text{Fe}(\text{edta})^-$ is shown in Figure 3.5A. The empirical procedure used to estimate the limiting current as indicated by the dotted lines is also included. Figure 3.5B shows a typical Koutecky-Levich plot of data obtained from waves such as that in Figure 3.5A. The intercept of the plot was assumed to represent i_s^{-1} for $\text{Fe}(\text{edta})^-$. The value of i_s for ascorbate (for which $n = 2$) was taken as 2.8 times the estimated value for $\text{Fe}(\text{edta})^-$ at the same concentration. The factor of 2.8 represents the product of the ratios of n -values (2.0) and diffusion coefficients (1.4) for the two reactants in homogeneous solutions. Although in favorable cases^{1f} the rate of permeation of a substrate through an electrode coating can be easily determined, in cases where an ionic substrate penetrates polyelectrolyte coatings bearing ionic groups of the same sign, poorly formed current-potential curves such as that in Figure 3.5A are usually obtained. However, the resulting uncertainties in the estimated values of i_s are of little consequence if the substrate permeation is very slow and the cross-reaction between it and the catalyst incorporated in the coating is fast such that the reaction occurs very near the outer surface of the coating. This proved to be true of the $\text{Os}(\text{bpy})_3^{2+}$ -ascorbate system at Nafion-coated electrode (vide infra) so that the uncertainties associated with the evaluated i_s (estimated to be 50% at most) did not impede the analysis of the data.

Rate law and characteristic kinetic current density for ascorbate oxidation

The outer-sphere homogeneous oxidation of ascorbate by metal polypyridine complexes was thoroughly studied recently⁵. Pelizzetti et al.^{5a,b}

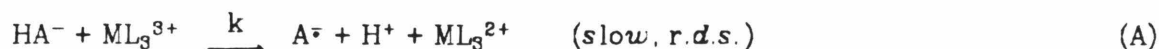
Figure 3.5

- A. Current-potential curve for the reduction of 2.3 mM $\text{Fe}(\text{edta})^-$ at a rotating graphite disk electrode coated with Nafion- $\text{Os}(\text{bpy})_3^{2+}$. Supporting electrolyte: 0.1 M CF_3COONa + 0.1 M CH_3COONa (pH 5.5). Rotation rate: 400 rpm. The graphical construction utilized to estimate the limiting current is shown.
- B. Koutecky-Levich plot for limiting current data obtained from curves such as the one in A. The line drawn through the data points was constrained to lie parallel to the dashed plot for the uncoated electrode.



studied the oxidation of ascorbate by a series of iron(III)-phenanthroline complexes. Macartney and Sutin et al.^{5c} extended the investigation to tris(2,2'-bipyridine) and tris(4,4'-dimethyl-2,2'-bipyridine) complexes of osmium (III), ruthenium (III), and nickel (III).

The reactions are believed to proceed by the following mechanism⁵ :



where A^- is ascorbate radical anion and A is dehydroascorbic acid. If a rate law of the same type is assumed to apply to the reaction between ascorbate and $\text{Os}(\text{bpy})_3^{3+}$ within Nafion coating the characteristic kinetic current density can be expressed as in equation(3.4)^{2b}:

$$i_k = 2F\kappa k C_A \Gamma_{\text{Os}} \quad (3.4)$$

where k is the second-order rate constant for reaction (A). For $\text{Os}(\text{bpy})_3^{3+}$ k is $4 \times 10^7 \text{ M}^{-1}\text{s}^{-1}$ at 1 M ionic strength^{5c}.

Comparison with the model of Andrieux et al.

After the evaluations of various characteristic current densities, we are ready to compare the experimental limiting currents at the coated rotating disk electrode with the predictions resulting from the models presented by Andrieux et al.².

For the electrode coatings and solutions utilized in obtaining the data in Figure 3.4A, $i_E = 10^3 \mu\text{A cm}^{-2}$. At the highest concentration and rotation rate employed in Figure 3.4A, $i_S = 17 \mu\text{A cm}^{-2}$ (taking $\kappa = 1$) and $i_A = 198 \mu\text{A cm}^{-2}$ (i_A ,

is the uncomplicated diffusion-convection-controlled reaction of ascorbate at an uncoated electrode¹⁵). If the value $k = 4 \times 10^7 \text{ M}^{-1}\text{s}^{-1}$ is used to calculate i_k from equation (3.4) one obtains $i_k = 20 \text{ A cm}^{-2}$ at the highest ascorbate concentration in Figure 3.4A, 0.13 mM. The situation now can be summarized as follows: i_E is much larger than both i_s and i_A , and i_k is much larger than all the other characteristic current densities. This situation corresponds to that labeled "SR" by Andrieux et al.^{2a,b}. However, the very small ratio of i_s to i_k implies that the reaction between ascorbate and $\text{Os}(\text{bpy})_3^{3+}$ is confined within a very thin reaction layer at the coating/solution interface. The reaction layer thickness for substrate diffusion in the film, μ , can be calculated by²ⁱ $\mu = \varphi (i_s/i_k)^{1/2}$ where φ is the coating thickness. The values of i_s and i_k quoted above combined with the estimated film thickness ($3 \times 10^{-5} \text{ cm}$) yield a reaction layer thickness of only 0.3 nm. Therefore, instead of the "SR" case, the kinetic situation is more appropriately described as that in which the substrate does not penetrate the coating. Mathematically, the catalytic reaction in this situation must be treated as a surface reaction instead of a volume reaction. Andrieux et al.^{2a,b} also treated this "surface catalytic reaction" case. According to their derivations^{2a,b}, the intercepts of linear Koutecký-Levich plots are equal to i_k^{-1} so long as i_E remains much larger than i_A and i_k ^{2a,b}. The intercepts of the plots in Figure 3.4A were interpreted on this basis to obtain values of k summarized in Table 3.1. The average value of k obtained, $2.9 \times 10^5 \text{ M}^{-1}\text{s}^{-1}$, is smaller than that used in the estimation of the reaction layer thickness. However, even with this smaller value of k , the estimated value of μ is only about 3 nm which is also about the average distance between monolayers of the catalyst (assuming a cubic lattice). Thus, the assumption that the reaction occurs only at the coating/solution interface seems well justified. The physical

Table 3.1

Rate Constant for the Reaction of Ascorbate with $\text{Os}(\text{bpy})_3^{3+}$
on the Surface of a Nafion Coating on a Graphite Electrode ^a

C^0 , ^b mM	i_k , ^c mA cm ⁻²	$10^{-5} k$, ^d M ⁻¹ s ⁻¹
0.032	0.39	3.0
0.063	0.75	2.9
0.13	1.53	<u>2.9</u>
		av. $2.9 \times 10^5 \text{ M}^{-1} \text{ s}^{-1}$

- a. The electrode coating consisted of 1.5×10^{-7} moles cm⁻² of Nafion and 1.8×10^{-8} moles cm⁻² of $\text{Os}(\text{bpy})_3^{2+}$.
- b. Ascorbate concentration in the solution.
- c. Calculated from the intercept of a Koutecky-Levich plot.
- d. Calculated from eqn. 4 taking Γ_{Os} for one monolayer as 2×10^{-10} mole cm⁻² (the incorporated $\text{Os}(\text{bpy})_3^{2+}$ complexes were assumed to reside on a cubic lattice).

picture is that the consumption of ascorbate by the catalytic reaction is so fast that, once it reaches the coating/solution interface, its concentration drops rapidly to a negligible level after penetration of the coating by about one monolayer.

The average value of k in Table 3.1 is much smaller than the corresponding value in homogeneous solution^{5c}. Examples of reaction rate constants within polymer coatings that are smaller than their counterparts in homogeneous solution are becoming commonplace^{1a,ef}. The possible reasons, as have been discussed recently, are different environment (e.g., ionic strength) and different accessibilities of reactants to each other^{1a,ef}.

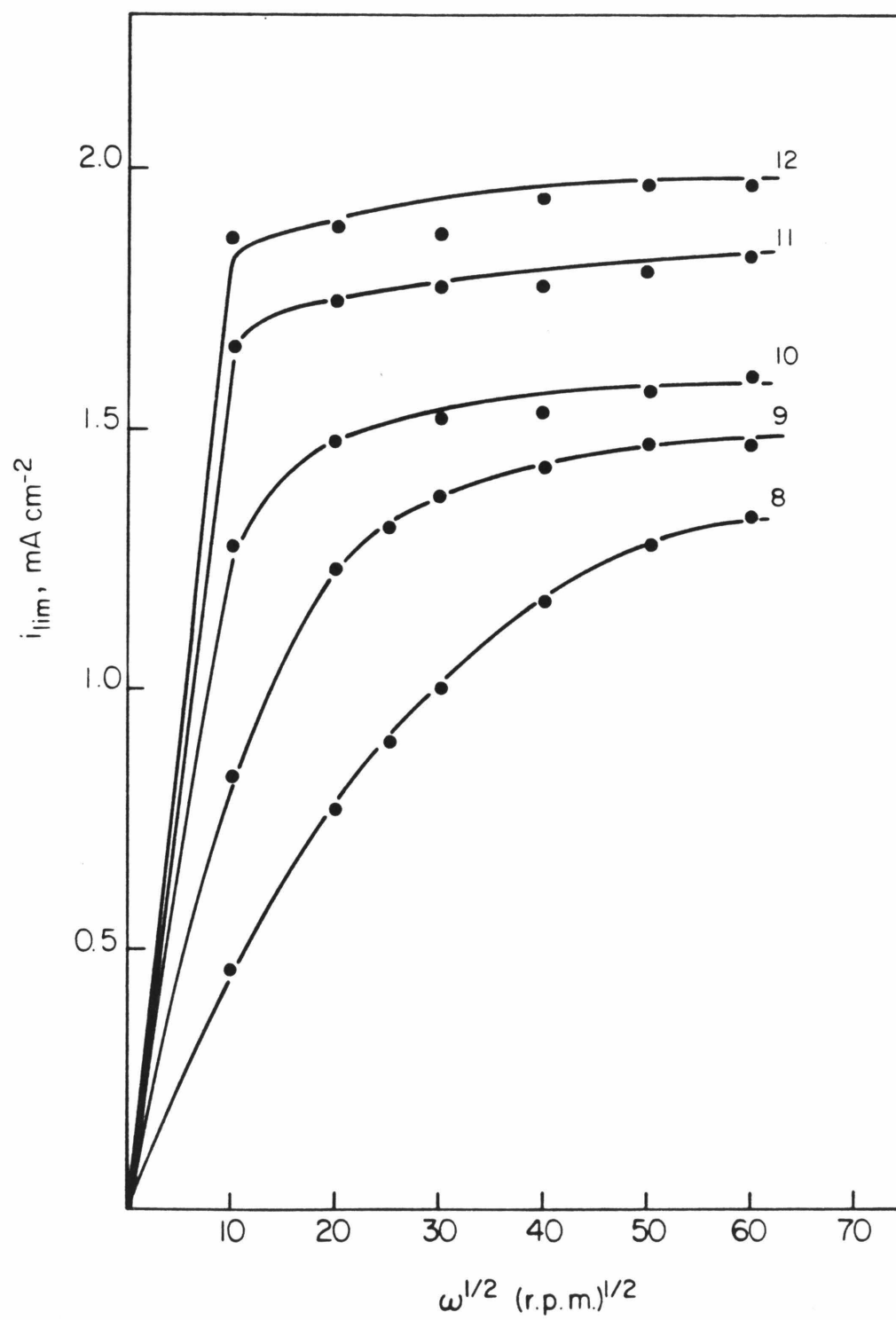
Kinetic behavior at higher substrate concentration

The Koutecky-Levich plots at ascorbate concentrations greater than ca. 0.2 mM (Figure 3.4B) appeared to be linear, but their slopes and intercepts did not match those expected for a simple surface reaction. As the ascorbate concentration was raised above 1.0 mM the plateau currents at the rotating disk electrode became less sensitive to changes in rotation rate (Figure 3.6) and the corresponding Koutecky-Levich plots were far from linear. These qualitative features are expected when the increase in substrate concentration raises i_A to values comparable to i_E (i_E is independent of the substrate concentration^{2b}.) Under these circumstances the current for a surface reaction is expected^{2b} to obey equation (3.5).

$$\frac{1}{i_{lim}} = \frac{1}{i_A} + \frac{i_E}{i_k(i_E - i_{lim})} \quad (3.5)$$

Figure 3.6

Levich plots for ascorbate oxidation at higher concentrations of ascorbate: 8 - 2.0; 9- 4.2; 10 - 8.2; 11 - 16; 12 - 32 mM. Supporting electrolyte: 0.4 M CH_3COONa (pH 5.5). Other conditions as in Figure 3.2 .



Attempts were made to fit the kinetic data for higher ascorbate solutions to equation (3.5). A careful examination of equation (3.5) reveals that it is not possible for i_{lim} to exceed i_E when the reaction occurs at the coating/solution interface. However, limiting plateau currents well above the value of i_E obtained by the chronocoulometric method (1.1 mA cm^{-2}) were observed (Figure 3.6). A possible explanation could be that i_E obtained from the transient potential step experiments is smaller than the actual sustainable charge propagation current because of non-uniformity in the thickness of cast Nafion coatings. If the coatings were thinner in the center and thicker near their edges because of uneven evaporation of the solution^{4b}, there would be no effect on the value of i_E measured by transient potential step experiments (at suitably short times), but the value of i_E which should be used in equation (3.5) could be larger.

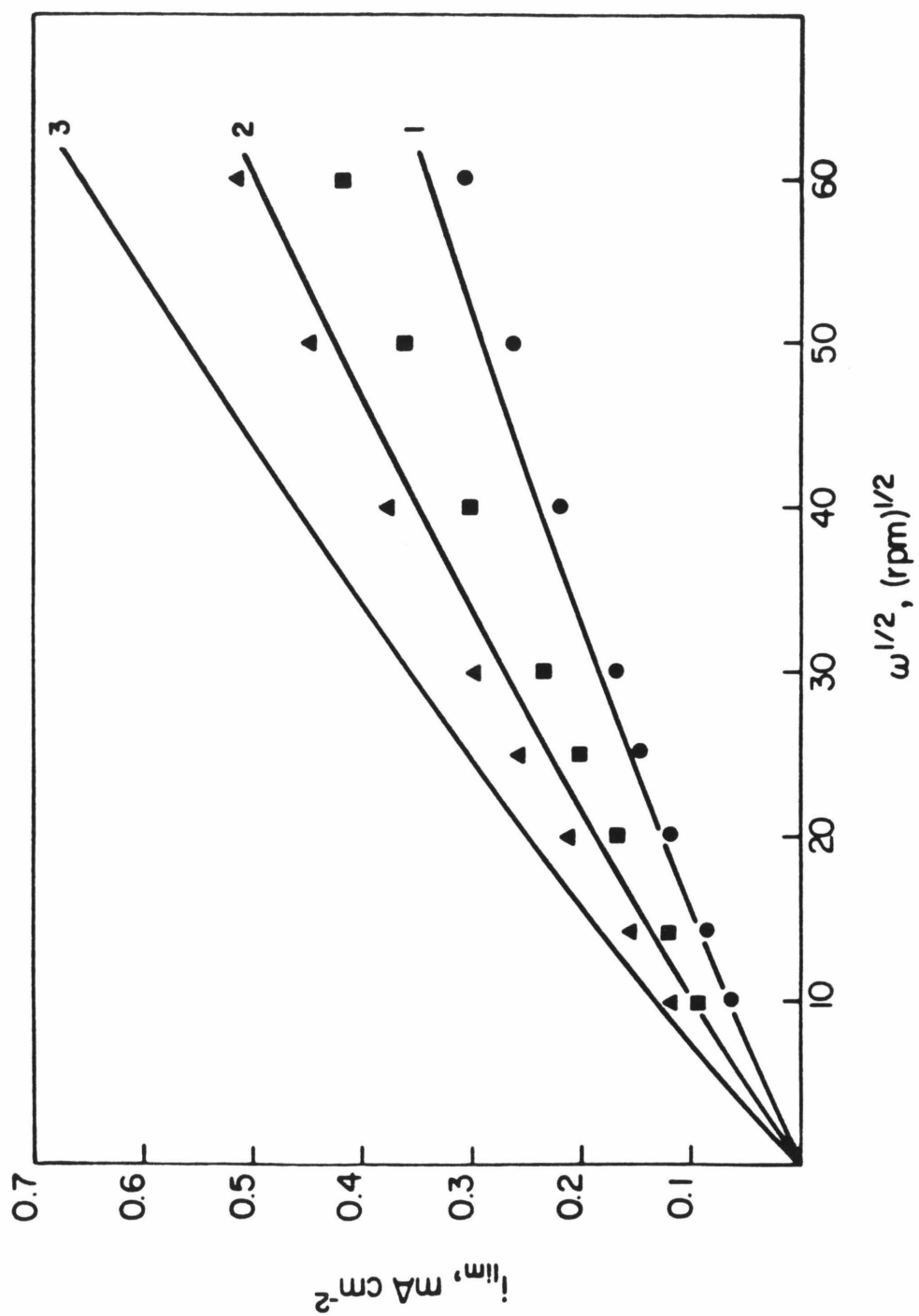
Under these circumstances the approximately rotation rate-independent current in Figure 3.6 would provide a better measure of i_E . This could be easily shown by rearranging equation (3.5) and noting that i_k is much larger than i_E . On this basis a value of 2 mA cm^{-2} for i_E was used in applying equation (3.5) rather than the lower value of i_E from the chronocoulometric data with equation (3.2).

In Figure 3.7 plots of i_{lim} vs. $\omega^{1/2}$ calculated from equation (3.5), using the value of k from Table 3.1, are compared with the experimental plateau currents. The agreement is not satisfactory and the discrepancies became larger as the concentration of ascorbate was increased. A clearer picture of the data obtained for all the ascorbate concentrations could be revealed by the rearrangement of equation (3.5) as follows:

$$\log \left[\frac{i_{lim}}{(1 - \frac{i_{lim}}{i_E})} \right] = \log C_A^o (1 - \frac{i_{lim}}{i_A}) + \log 2F\kappa k \Gamma_{0s} \quad (3.6)$$

Figure 3.7

Comparison of experimental data for the oxidation of ascorbate at Nafion-Os(bpy)₃²⁺ coatings with the behavior calculated (2a, b) for a monolayer of catalyst located at the film-solution interface. The points are experimental. The lines were calculated, taking i_E as 2.1 mA cm⁻² (see text), and k as $2.9 \times 10^5 \text{ M}^{-1} \text{ s}^{-1}$. Other experimental conditions corresponded to those of Figure 3.2.



Thus, a plot of the l. h. s. of equation (3.6) vs. $\log C_A^\circ (1 - \frac{i_{lim}}{i_A})$ for all concentrations of ascorbate and electrode rotation rates should yield a single line of unit slope if equation (3.5) is obeyed.

Figure 3.8 contains all the experimental data plotted in this format. The lack of adherence is very clear. The data appear to fall on different lines with different concentrations of ascorbate and only at the lowest concentrations do they fall close to a line of unit slope. The analysis seems to indicate clearly that Nafion-Os(bpy)₃³⁺-ascorbate system does not show good agreement with that expected from theoretical models.

Discussion of the discrepancies

The anomalous behavior evident in Figure 3.7 and 3.8 seems likely to be a peculiarity of Nafion coatings. Kuo and Murray^{1d} reported only linear Koutecky-Levich plots in their study of the catalysis of ascorbic acid oxidation by Fe(CN)₆³⁻ incorporated in a polycationic siloxane coating at an ascorbic acid concentration as high as 10 mM and they showed their data can be reasonably explained by the theoretical models^{1d}. Therefore, the possibility that the peculiarity might originate from ascorbic acid can be ruled out.

The behavior may originate from the unusual two-phase structure that Nafion membranes are known to adopt⁶. Nafion membranes are believed to consist of hydrophilic channels containing most of the sulfonate groups and largely charge-free hydrophobic regions composed of fluorocarbon portions of the polyelectrolyte. Between these two regions lies a transitional "interfacial region"⁶ containing some of the sulfonate groups but offering a more

Figure 3.8

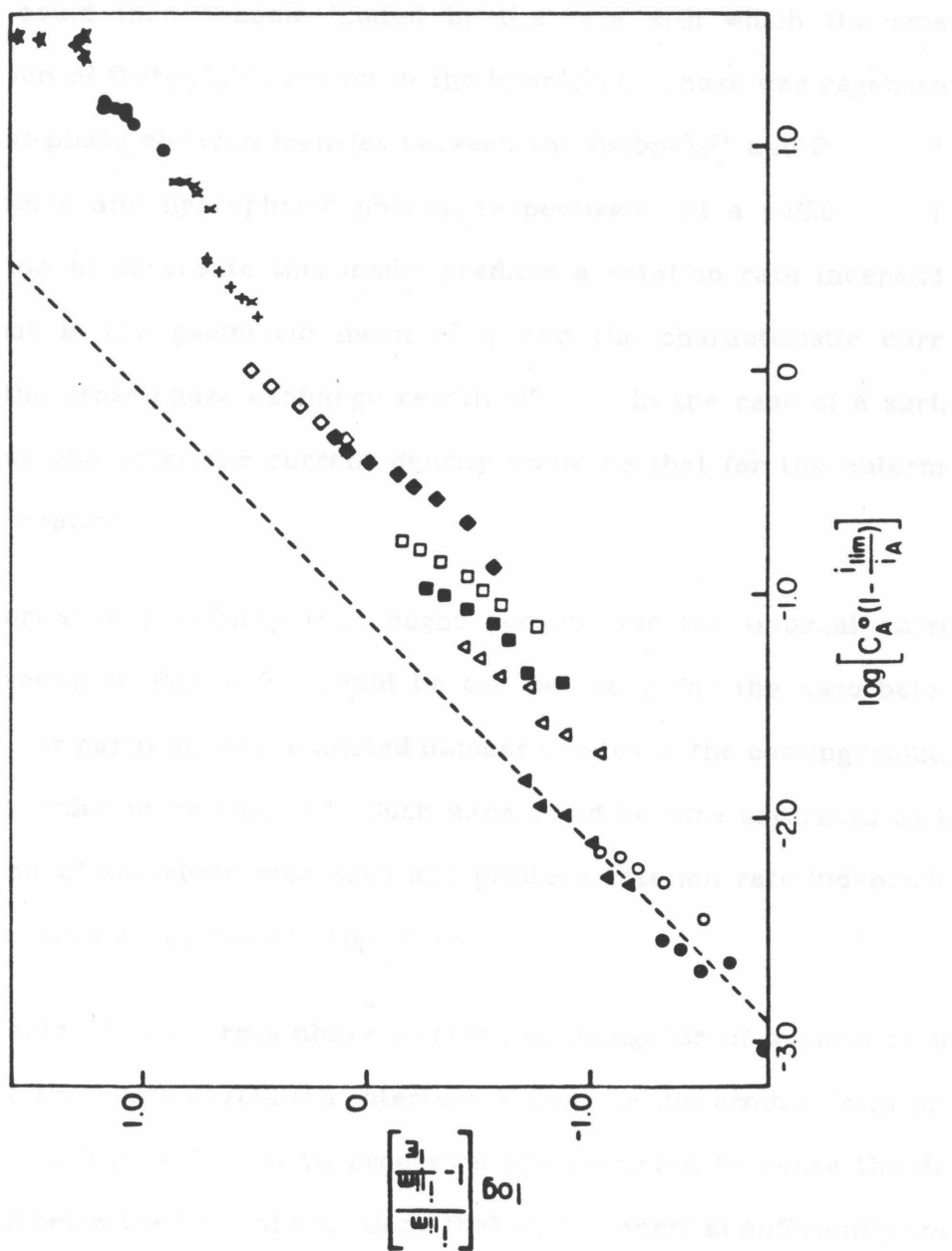
A plot of all the experimental data according to equation 3.6 . The concentrations of ascorbate were:

(●) 0.032 (○) 0.063 (▲) 0.13 (△) 0.26 (■) 0.38

(□) 0.52 (◆) 1.03 (◇) 2.0 (+) 4.2 (x) 8.2

(θ) 16 (★) 32 mM. $\Gamma_{0s} = 1.8 \times 10^{-8}$ mole cm⁻².

The dashed line is drawn with unit slope.



hydrophobic environment than the hydrophilic channels. Hydrophobic cations such as $\text{Os}(\text{bpy})_3^{2+}$ would be expected to partition preferentially into the more hydrophobic interfacial regions within the Nafion coatings^{4c} which may be less accessible to hydrophilic reactants such as ascorbate. The rate of oxidation of ascorbate could then become limited by the rate with which the smaller concentration of $\text{Os}(\text{bpy})_3^{3+}$ catalyst in the hydrophilic phase was regenerated by the cross-phase electron transfer between the $\text{Os}(\text{bpy})_3^{2+}$ and $\text{Os}(\text{bpy})_3^{3+}$ in the hydrophilic and hydrophobic phases, respectively. At a sufficiently high concentration of ascorbate this model predicts a rotation rate independent current that is the geometric mean of i_E and the characteristic current governing the cross-phase exchange reaction¹⁸. In the case of a surface reaction this characteristic current density would be that for the outermost layer of the coating.

An alternative possibility that might account for the unusual current responses shown in Figure 3.7 could be the necessity for the ascorbate to absorb onto, or partition into, a limited number of sites at the coating/solution boundary in order to be oxidized. Such sites could become saturated as the concentration of ascorbate increased and produce rotation rate-independent plateau currents such as those in Figure 3.5.

The effects of slow cross-phase electron exchange or of adsorption-like equilibria at the coating/solution interface should be discernible from plots such as that in Figure 3.8. Both processes are predicted to cause the data points to fall below the lines of unit slope that should apply at sufficiently small values of C_A ^{o18}. The data in Figure 3.8 do exhibit some of the predicted trends, but their evident failure to adhere to a single curve is not expected, and more

detailed analysis seems unwarranted until the origin of this discrepant behavior can be identified with more certainty.

Concluding remarks

One of the most attractive features of Nafion coatings in electrocatalytic application is their great stability in aqueous media, which all investigations^{3,4}, including the present study have affirmed. However, the present study has revealed some aspects of the behavior of Nafion coatings that should be carefully considered. The observation that Nafion coatings exhibit behavior that cannot be accommodated by the kinetic models² that have proved successful with other polymer-coated electrodes¹ presents a problem which will make the analysis of the kinetic data of electrocatalytic reactions in Nafion more difficult than in other polymer coatings. Both the internal and surface structure of Nafion are probably not as uniform and isotropic as is assumed in all the models that have been proposed to date. In addition, there is reason to doubt that the thickness of cast films are equal at the center and the edges of the coatings. The small diffusion coefficients of the hydrophobic reactants that appear most stable when incorporated in Nafion coatings raise another problem, but this could be improved by using thin coatings since the rate of regeneration of catalyst is inversely proportional to the coating thickness.

References

- 1 (a) N. Oyama and F. C. Anson, *Anal. Chem.*, 52(1980)1192; (b) K. Shigehara and F. C. Anson, *J. Electroanal. Chem.*, 132(1982)107; (c) P. Martigny and F. C. Anson, *J. Electroanal. chem.*, 139(1982)37; (d) K. Kuo and R. W. Murray, *J. Electroanal. Chem.*, 131(1982)37; (e) F. C. Anson, J.-M. Saveant and K. Shigehara, *J. Am. chem. Soc.*, 105(1983)1096; (f) F. C. Anson, T. Ohsaka and J.-M. Saveant, *J. Am. Chem. Soc.*, 105(1983)4883; (g) R. N. Dominey, N. S. Lewis, J. A. Bruce, D. C. Bookbinder and M. S. Wrighton, *J. Am. Chem. Soc.*, 104(1982)467; (h) R. H. Schmehl and R. W. Murray, *J. Electroanal. Chem.*, 152(1983)97.
- 2 (a) C. P. Andrieux, J.-M. Dumas-Bouchiat and J.-M. Saveant, *J. Electroanal. Chem.*, 131(1982)1; (b) C. P. Andrieux and J.-M. Saveant, *J. Electroanal. Chem.*, 134(1982)163; (c) C. P. Andrieux and J.-M. Saveant, *J. Electroanal. Chem.*, 142(1982)1; (d) R. W. Murray, *Phil. Trans. R. Soc. London A*, 302(1981)253; (e) E. Laviron, *J. Electroanal. Chem.*, 131(1982)61; (f) R. D. Rocklin and R. W. Murray, *J. Phys. Chem.*, 85(1981)2104; (g) P. Daum and R. W. Murray, *J. Phys. Chem.*, 85(1981)389; (h) C. P. Andrieux, J.-M. Dumas-Bouchiat and J.-M. Saveant, *J. Electroanal. Chem.*, 114(1980)159; (i) C. P. Andrieux and J.-M. Saveant, *J. Electroanal. Chem.*, 93(1978)163.
- 3 (a) T. P. Henning, H. S. White and A. J. Bard, *J. Am. Chem. Soc.*, 103(1981)3937; (b) *ibid.*, 104(1982)5862; (c) H. S. White, J. Leddy and A. J. Bard, *J. Am. Chem. Soc.*, 104(1982)4811; (d) C. R. Martin, I. Rubinstein and A. J. Bard, *J. Am. Chem. Soc.*, 104(1982)4817; (e) I. Rubinstein and A. J. Bard, *J. Am. chem. Soc.*, 102(1980)6641; (f) *ibid.*, 103(1981)5007; (g) T. P.

- Henning and A. J. Bard, *J. Electrochem. Soc.*, 130(1983)613.
- 4 (a) D. A. Buttry and F. C. Anson, *J. Electroanal. Chem.*, 130(1981)333; (b) D. A. Buttry and F. C. Anson, *J. Am. Chem. Soc.*, 104(1982)4824; (c) D. A. Buttry and F. C. Anson, *J. Am. Chem. Soc.*, 105(1983)685.
- 5 (a) E. Pelizzetti, E. Mentasti and E. Pramauro, *Inorg. Chem.*, 15(1976)2898, (b) E. Pelizzetti, E. Mentasti and E. Pramauro, *ibid.*, 17(1978)1181; (c) D. H. Macartney and N. Sutin, *Inorg. Chim. Acta*, 74(1983)221.
- 6 (a) T. D. Gierke, G. E. Munn and F. C. Wilson, *J. Polym. Sci. Phys. Ed.*, 19(1981)1687; (b) H. L. Yeager and A. Steck, *J. Electrochem. Soc.*, 128(1981)1880.
- 7 C. Creutz, M. Chou, T. L. Netzel, M. Okumura and N. J. Sutin, *J. Am. Chem. Soc.*, 102(1980)1309.
- 8 D. T. Sawyer and J. M. McKinnie, *J. Am. Chem. Soc.*, 82(1960)4191.
- 9 G. Lauer, R. Abel and F. C. Anson, *Anal. Chem.*, 39(1967)765.
- 10 E. Laviron, Roullier and C. Degrand, *J. Electroanal. Chem.*, 112(1980)11.
- 11 A. J. Bard and L. R. Faulkner, " *Electrochemical Methods*, " John Wiley and Sons, New York, 1980, Ch. 1.
- 12 V. G. Levich, " *Physicochemical Hydrodynamics*, " Prentice-Hall, Englewood Cliffs, 1962, Ch.1, p. 69.
- 13 Ref. 11, p. 32.

- 14 J. Koutecky and V. G. Levich, *Zh. Fiz. Khim.*, 32(1956)1565; Ref. 12, pp. 345-357.
- 15 W. S. Gilliam, *Ind. Eng. Chem. Anal. Ed.*, 17(1945)217.
- 16 F. C. Anson, *Anal. Chem.*, 38(1966)54.
- 17 F. C. Anson, T. Ohsaka and J.-M. Saveant, *J. Phys. Chem.*, 87(1983)640.
- 18 J.-M. Saveant and F. C. Anson, work in progress.

CHAPTER IV

Charge-Transport Rates in Nafion Coatings on Electrodes

Disparate Diffusion Coefficients for a Single Molecule

Containing Two Electroactive Centers

Introduction

The rates of charge propagation through redox polymer coatings on electrode surfaces have been the subject of numerous recent investigations¹⁻¹¹. Some of these studies have attempted to identify the elementary steps responsible for charge-transport while others have focused on the possible use of redox polymer coatings in the applications¹². Where the electroactive reactants incorporated in coatings are not part of the polymeric structure or permanently attached to functional groups present in the coatings, their diffusion within the polymeric matrix can include contributions from both molecular motion and electron exchange between adjacent pairs of the oxidized and reduced reactant^{2a,b,d,g,f,3a,b,4a,b,5,8}.

Buttry and Anson measured the diffusion coefficients of a number of inorganic complexes in Nafion coatings^{2a,b} and rationalized the results by considering the physical structures and self-exchange constants of these complexes^{2a,b}. Martin and Dollard⁸, and Bard and co-workers^{3a,b}, have also made some efforts on this subject.

Due to the contribution from physical motion, the apparent diffusion coefficients of two redox couples can not be compared only on the basis of their self-exchange constants. This is because the rate of physical motion of a complex depends heavily on its physical structure, i.e., its interaction with the

polyelectrolyte film^{2a,b,8}. Only in several particular cases, the influence of self-exchange could be recognized without ambiguity^{2a,b,4a}.

A particular clear example of the important contribution that electron exchange can make to diffusional rates measured for redox couples in polymeric coatings was provided by the $\text{Co}(\text{bpy})_3^{2+}$ complex (bpy=2,2'-bipyridine)^{2b}. It exhibited a much larger diffusion coefficient when the electrochemical measurement was performed by reducing it to $\text{Co}(\text{bpy})_3^+$ than when the measurement was performed by oxidizing it to $\text{Co}(\text{bpy})_3^{3+}$. The difference was attributed to the very different self-exchange rate of $\text{Co}(\text{bpy})_3^{2+}/^+$ couple compared with that of $\text{Co}(\text{bpy})_3^{3+}/^{2+}$ couple^{2b}. In the present study, a similar strategy has been adopted by synthesizing a molecule bearing two separate reversible redox groups and measuring the diffusion coefficient of the molecule in all three of its possible redox states ($\text{Ox}_1\text{-Ox}_2$; $\text{Ox}_1\text{-Red}_2$; $\text{Red}_1\text{-Red}_2$). The results revealed large differences in diffusional rates among the various oxidation states. The relative magnitudes of the differences among the diffusion coefficients and their concentration dependences were compared with those to be expected in cases where intermolecular electron self-exchange contributes significantly to the diffusional rates.

Besides the diffusion coefficients of redox couples, electron-transfer coupling by redox cross-reactions between reactants incorporated in polyelectrolyte coatings has also been described in some recent studies^{4b,13a,b}. Electron-transfer coupling denotes the coupling of the diffusional rates of pairs of reacting redox couples with disparate individual diffusion coefficients. Previously the phenomenon was observed in homogeneous solution. It was first reported by Miller and Orelmann in the case of dc polarography^{14a} and


subsequently examined by several groups in studies of ac polarography of mixtures of redox reagents^{14b-f}.

Recently, the advent of polymer-coated electrodes has renewed interest in the phenomenon. The wide range of diffusion coefficients^{13b} for different compounds in polymer films makes this phenomenon more likely to be encountered. Enhanced currents at electrodes coated with a quinoid polymer were reported recently by Miller and co-workers¹⁵ when a rapidly diffusing redox mediator, (bis(hydroxymethyl)ferricenium), was added to the solution in which the coating was being reduced. They clearly identified the cross-reaction between the mediator and the essentially immobile quinoid groups as the source of the current enhancement. Facci and Murray^{4a,b} studied $\text{IrCl}_6^{3-}/\text{Fe}(\text{CN})_6^{3-}$ mixtures electrostatically incorporated into a polycationic film on an electrode and presented qualitative evidence for mediation of charge transport to each redox couple by the other. Buttry, Saveant and Anson^{13b} examined the electron-transfer cross-reactions between $\text{Co}(\text{terp})_2^{3+/2+}$ (terp=2,2',2''-terpyridine) and $\text{Ru}(\text{NH}_3)_6^{3+/2+}$, where the diffusion coefficient of the latter is significantly larger than the former. Comparison of the current enhancements in the chronocoulometric experiments with those calculated from the model resulted in a moderately good agreement^{13b}.

In the present study the enhancement (or depression) of the measured diffusion currents by means of intermolecular electron cross-exchange reactions was detected and its magnitude compared with that calculated on the basis of a simple model.

Experimental

Material

$[\text{Ru}(\text{NH}_3)_5\text{py}](\text{ClO}_4)_3$ (py=pyridine)¹⁶ and $[\text{Ru}(\text{NH}_3)_6\text{OH}_2](\text{PF}_6)_2$ ¹⁷ were prepared as described in the cited references. (Ferrocenylmethyl)trimethylammonium hexafluorophosphate, $[\text{CpFeCp-CH}_2\text{N}(\text{CH}_3)_3]\text{PF}_6 \equiv [\text{Cp}_2\text{FeTMA}]\text{PF}_6$, (Cp=cyclopentadienide) was obtained by metathesis of the corresponding bromide (Research Organic/Inorganic Company) using NH_4PF_6 . The crude product was recrystallized from water. N-(4-picolinic)-ferrocenylformamide, $\text{CpFeCp-CNHCCH}_2\text{-}$  was prepared by slight modifications in conventional procedures for peptide synthesis^{18,19}: 11 millimoles of N,N'-dicyclohexylcarbodiimide (Aldrich) dissolved in 10 ml of CH_2Cl_2 were added slowly to a well-stirred mixture of 10 millimoles of ferrocenylcarboxylic acid (Aldrich) and 10 millimoles of 4-aminomethylpyridine (Aldrich) in 10 ml of CH_2Cl_2 . The resulting mixture was allowed to react for 48 hours at 0°C. Most of the solvent was removed by evacuation and the residue was dissolved in CHCl_3 . A small amount of acetic acid was added to convert the excess carbodiimide to the corresponding urea which precipitated and was removed by filtration. The filtrate was extracted with several portions of 1 M hydrochloric acid.

The combined aqueous extracts were neutralized with NaOH to pH>10 to precipitate the crude product which was dissolved in CHCl_3 and the extraction-precipitation-redissolution procedure repeated 5 to 6 times. The final CHCl_3 solution was extracted with several portions of aqueous NaOH (1 M) followed by H_2O . The product obtained by evaporation of CHCl_3 was recrystallized from toluene, washed with ethyl ether and dried at 70°C in a vacuum oven. Elemental analysis: C, 63.79; H, 5.10; N, 8.71. Calculated for $\text{FeC}_{17}\text{H}_{16}\text{N}_2\text{O}$: C, 63.78; H, 5.04;

N, 8.75. ^1H NMR data (in CDCl_3 , δ (ppm) vs. Me_4Si): 4.19(s, 5H, C_5H_5), 4.37(t, 2H, $\beta\text{-C}_5\text{H}_4$), 4.55(d, 2H, CH_2), 4.73(t, 2H, $\alpha\text{-C}_5\text{H}_4$), 6.49(br t, 1H, NH), 7.26(d, 2H, 3,5-py), 8.54(d, 2H, 2,6-py).

$$[(\text{NH}_3)_5\text{RuN} \text{---} \text{C}_6\text{H}_4 \text{---} \text{CH}_2\text{HNC} \text{---} \text{CpFeCp}](\text{PF}_6)_3 \equiv [(\text{NH}_3)_5\text{RuPFF}](\text{PF}_6)_3$$
 was prepared by adaptation of the procedure of Sutton and Taube for similar substituted pyridine complexes¹⁷ except that the oxidation of Ru(II) product to Ru(III) was performed electrochemically instead of chemically in order to avoid the oxidation of the ferrocene center. An excess of PFF (3 mmole) was reacted with 0.6 mmole of $[(\text{NH}_3)_5\text{RuOH}_2](\text{PF}_6)_2$ in 30 ml of (1:1) acetone-ethanol in an argon atmosphere and in absence of light for 6 hours. The reaction was monitored by means of an absorption band at 415 nm²⁰. The product was collected by adding the reaction solution to a large volume (250 ml) of rapidly stirred ether. The precipitate was dissolved in 20 ml of 1 M HCl and oxidized at a platinum gauze electrode maintained at 0.23 volt until the current had decreased to background levels. The desired Ru(III) product was precipitated as the chloride by pouring the electrolysis solution into ~200 ml of rapidly stirred acetone. The resulting solid was converted to the PF_6^- salt by metathesis with NH_4PF_6 and recrystallization from water. To prepare a solution for voltammetric experiments, the solid salt was dissolved in water and passed through a Sephadex-SPC25-120 cation exchange column in the Na^+ form. Residual impurities were eluted with 0.15 M NaCl followed by the desired complex, $[(\text{NH}_3)_5\text{RuPFF}]^{3+}$ with 0.6M NaCl. Isolation of the purified complex as a solid were unsuccessful because of the apparent decomposition of the ferrocene moiety at the temperature required to remove the solvent. The purified complex was therefore stored as a solution at ~5°C.

Nafion coatings were cast from 5.2 wt.% solutions of a soluble form of the polymer (eq. wt. = 970) obtained from E. I. du Pont de Nemours & Co. a number of years ago. Similar material is presently available from C. G. Processing Inc., (Rockland, DE). Solutions were prepared from distilled water that was further treated by passage through a purification train (Barnsted Nanopure). Electrodes were prepared from basal plane pyrolytic graphite obtained from Union Carbide Co. (Chicago).

Procedures

Electrodes were cut and mounted as previously described^{12a} to yield exposed areas of 0.17 cm². Nafion coatings were obtained by transferring 2 μ l of the stock solution to a freshly cleaved electrode and allowing the solvent to evaporate. Metal complexes were incorporated in the coatings by soaking them in aqueous solutions of the complexes (\sim 1 mM). The quantities of complex incorporated were measured coulometrically as previously described^{2b}. Cyclic and normal pulse voltammetry and coulometry were conducted with appropriate combinations of PAR instruments (E G & G, Inc.). Chronocoulometry was conducted with a computer-controlled apparatus previously described²¹. All experiments were conducted at ambient temperature ($22 \pm 2^\circ\text{C}$) in solutions that had been de-aerated with pre-purified argon. Potentials are quoted with respect to a sodium chloride-saturated calomel electrode, SSCE.

Results and discussion

The binuclear complex, $[(\text{NH}_3)_5\text{RuN} \langle \text{C}_6\text{H}_4 \rangle \text{CH}_2\text{-NH-C(=O)-CpFeCp}]^{3+}$, which will be denoted Ru^{III}Fe^{II} hereafter, contains one oxidized and one reduced redox

center. Uncoated electrodes placed in solutions of this complex assume open circuit potentials near 0.2 volt. Cyclic voltammograms initiated from the open circuit potential contain an anodic peak (with its cathodic counterpart) when scanned to more positive potentials and a cathodic peak (with its anodic counterpart) when scanned to more negative potentials (Figure 4.1A). The response at 0.4 volt corresponds to the one-electron oxidation of the ferrocene center in the complex and that at 0.05 volt can be assigned to the one-electron reduction of the $\text{Ru}(\text{NH}_3)_5\text{py}^{3+}$ center because its formal potential matches that of the corresponding mononuclear complex in which a phenyl group replaces the ferrocene moiety²². To obtain reliable estimates of the diffusion limited currents corresponding to each of the peaks in Figure 4.1A normal pulse voltammograms²³ were also recorded (Figure 4.1B). The anodic and cathodic plateau currents in Figure 4.1B are identical (within the experimental precision of 1%) as expected because the same molecule diffuses to the electrode surface whether it is oxidized or reduced there.

This simple symmetrical pattern was broken when the same $\text{Ru}^{\text{III}}\text{LFe}^{\text{II}}$ complex was incorporated in a Nafion coating on the graphite electrode as shown in Figure 4.2. The cathodic peak for the reduction of the Ru^{III} center is now significantly larger than the anodic peak for the oxidation of the Fe^{II} center. Despite the differences in peak currents, coulometric measurements demonstrated, as expected, that exactly as much charge was required to oxidize all of the $\text{Fe}(\text{II})$ centers or to reduce all of the $\text{Ru}(\text{III})$ centers in the coating. The shapes of the voltammograms in Figure 4.2 indicate that the currents are controlled by the diffusion of the complex within the coating^{2b,11} so that the unequal peak currents must reflect unequal rates of diffusional charge transport even though the same molecule is "diffusing" in both cases. If we

Figure 4.1

- (A) Cyclic voltammograms for a 0.28 mM $\text{Ru}^{\text{III}}\text{LFe}^{\text{II}}$ solution at a bare graphite electrode. Scan rate: 100 mV s^{-1} .
- (B) Normal pulse voltammograms for a 0.7 mM $\text{Ru}^{\text{III}}\text{LFe}^{\text{II}}$ solution at a bare graphite electrode. Scan rate: 2 mV s^{-1} .
- Supporting electrolyte: 0.6 M NaCl + 0.05 M CH_3COONa at pH 4.5 for both curves.

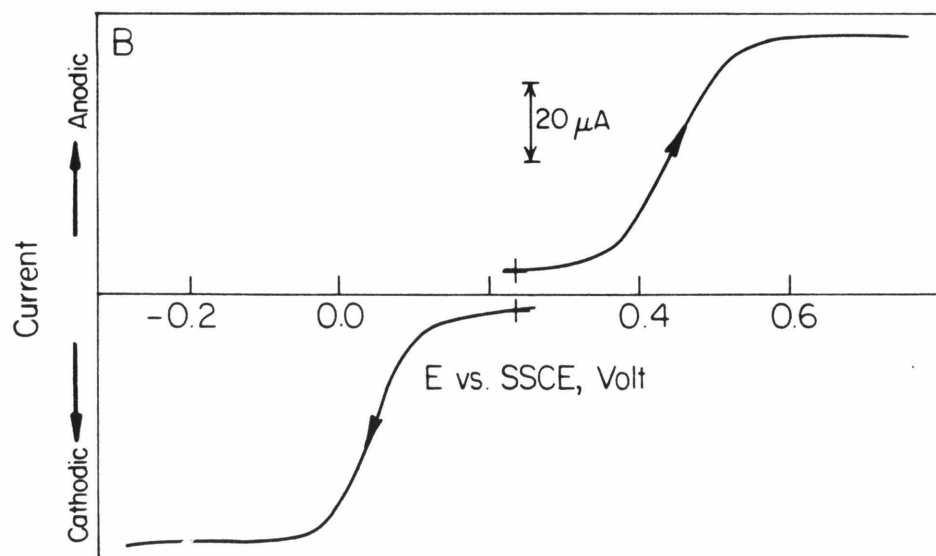
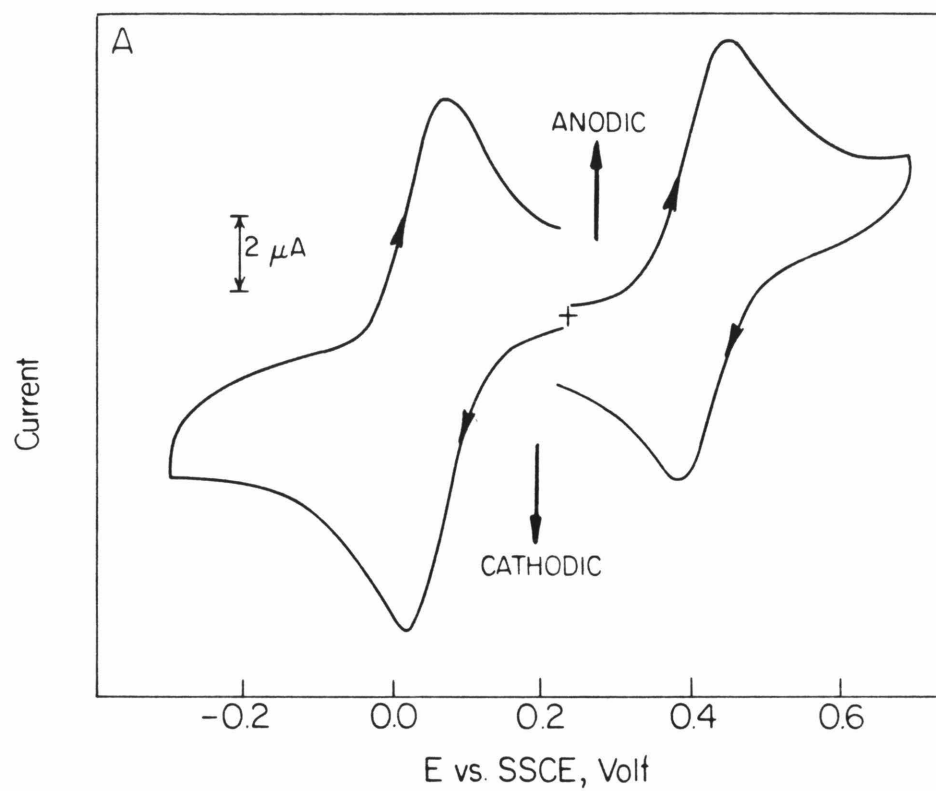
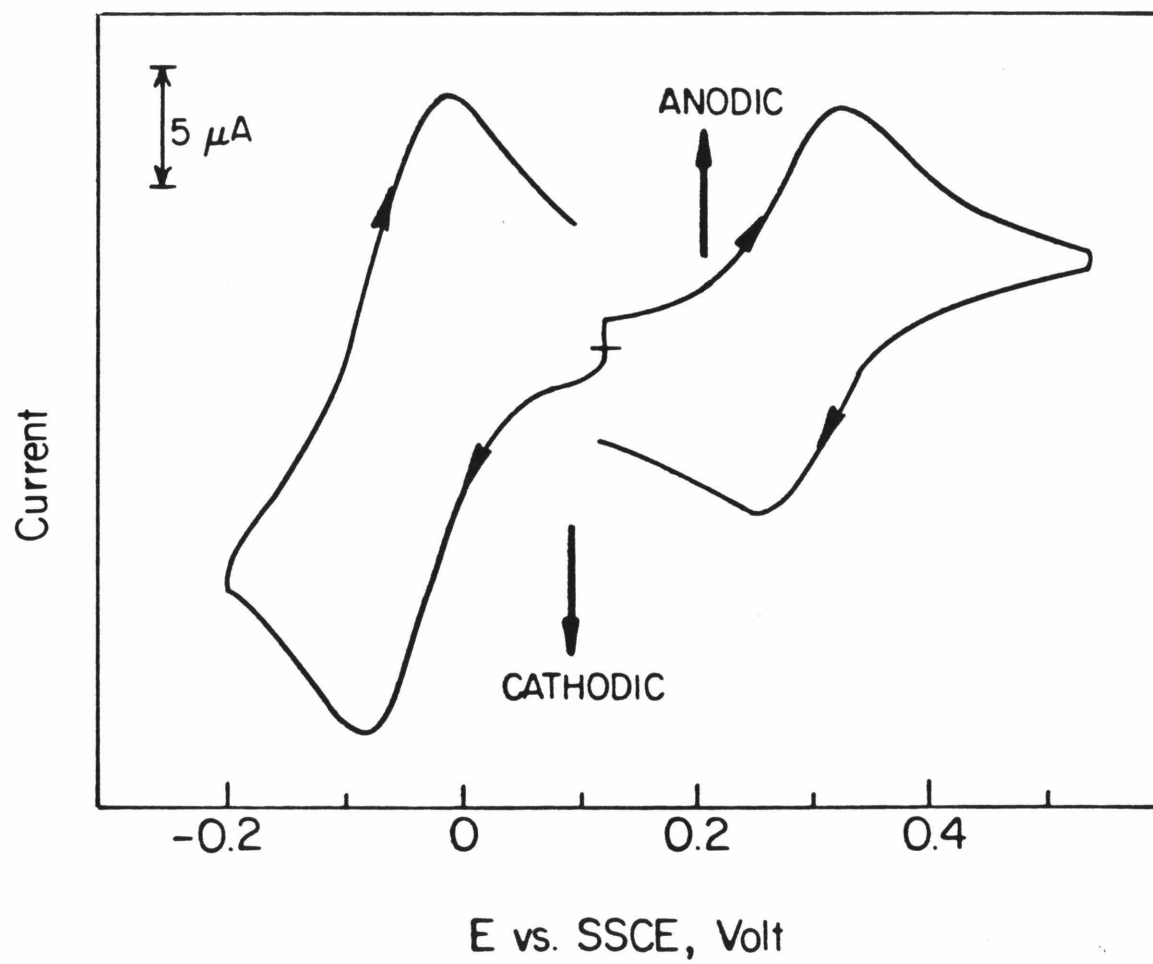


Figure 4.2

Cyclic voltammograms for 6.6×10^{-9} mole cm^{-2} of $\text{Ru}^{\text{III}}\text{LFe}^{\text{II}}$ incorporated in a Nafion coating on a graphite electrode containing 6.0×10^{-7} mole cm^{-2} of sulfonate groups. Supporting electrolyte = 0.1 M CF_3COONa + 0.1 M CH_3COONa at pH 4.5. Scan rate: 100 mV s^{-1} .



denote by $D_{III^{\bullet}-II}$ and $D_{III-II^{\bullet}}$ the diffusion coefficients corresponding to the reduction of the Ru(III) center and the oxidation of the Fe(II) center, respectively, the peak currents in Figure 4.2 indicate that $D_{III^{\bullet}-II} > D_{III-II^{\bullet}}$.

Evaluation of diffusion coefficients

To allow more quantitative comparisons of diffusional rates, diffusion coefficients were measured by potential-step chronocoulometry²⁴. The measured parameter was the slope, S , of linear chronocoulometric charge-(time)^{1/2} plots recorded at times short enough to ensure that the conditions for semi-infinite linear diffusion were obtained despite the finite volume of the thin Nafion coating to which the diffusion was confined^{10a,12l}. Equation (4.1) gives the relationship between S and the corresponding diffusion coefficient:

$$D = \left[\frac{S \varphi \pi^{1/2}}{2 F \Gamma} \right]^2 \quad (4.1)$$

where F is the Faraday constant, φ is the (uniform) thickness of the electrode coating and Γ is the total quantity of the (uniformly distributed) diffusing reactant in the coating. Coating thicknesses were estimated from the quantity of Nafion present in the coatings and the previous profilometer measurements of Buttry on similar coatings^{2b}. The quantity of reactant incorporated in the coatings was obtained by coulometric assay^{2d}.

The binuclear complex can be prepared in three different combinations of oxidation states of the two metal centers: $Ru^{III}LFe^{III}$, $Ru^{III}LFe^{II}$ and $Ru^{II}LFe^{II}$ (the $Ru^{II}LFe^{III}$ state is unstable with respect to $Ru^{III}LFe^{II}$). Four diffusion coefficients can therefore be measured for these three oxidation states: $D_{III^{\bullet}-II}$ and $D_{III-II^{\bullet}}$, defined above; $D_{III-III^{\bullet}}$, corresponding to the reduction of the Fe(III) center in the

$\text{Ru}^{\text{III}}\text{LFe}^{\text{III}}$, and $D_{\text{II}^{\bullet}-\text{II}}$, corresponding to the oxidation of the $\text{Ru}(\text{II})$ center in $\text{Ru}^{\text{II}}\text{LFe}^{\text{II}}$. Values were obtained for these four diffusion coefficients by adjusting the initial potential of the coated electrode to convert the incorporated complex into each of the possible oxidation states. The results, listed in Table 4.1, are remarkable for several reasons. The measured diffusion coefficients vary by a factor of 4.5 even though the diffusing species differ only in their net charges. The diffusing species in experiments 1 and 4 are, in fact, identical in all respects, yet the values of $D_{\text{III}^{\bullet}-\text{II}}$ and $D_{\text{III}-\text{II}^{\bullet}}$ differ by a factor of ~ 2.3 . This observation is of primary interest in the present study. The possible origins of the disparate diffusion coefficients for the identical species, $\text{Ru}^{\text{III}}\text{LFe}^{\text{II}}$, are discussed now.

The larger values of D obtained when the ruthenium center is the site of the electron transfer reaction ($D_{\text{III}^{\bullet}-\text{II}}$) than those obtained when the ferrocene center is the site of the electron transfer reaction ($D_{\text{III}-\text{II}^{\bullet}}$) could be explained as the result of the faster electron exchange between $\text{Ru}^{\text{III}}\text{LFe}^{\text{II}}$ and $\text{Ru}^{\text{II}}\text{LFe}^{\text{II}}$ than that between $\text{Ru}^{\text{III}}\text{LFe}^{\text{II}}$ and $\text{Ru}^{\text{III}}\text{LFe}^{\text{III}}$. The enhancement of diffusional rates by electron self-exchange was proposed by Dahms²⁵ and Ruff et al.²⁶ in the earlier works. They derived the following relation for the experimentally observed diffusion coefficient for one-half of a redox couple, D_{exptl} , in terms of the second-order self-exchange rate constant for the redox couple, k_{ex} , and the diffusion coefficient that would be measured in the absence of self-exchange, D_0 :

$$D_{\text{exptl}} = D_0 + (\pi/4)k_{\text{ex}}\delta^2C \quad (4.2)$$

C is the sum of the concentration of the oxidized and reduced forms of the redox couple and δ is the distance between the centers of the reactants when the electron transfer occurs. (Equation (4.2) is a simplified version of a more

Table 4.1

Diffusion Coefficients for the RuLFe Complex Within a Nafion Coating ^a

Expt. No.	E _i , ^b mV	E _f , ^c mV	Oxidation State		10 ⁹ D, ^d cm ² s ⁻¹	Symbol for D
1	0.12	-0.20	Ru ^{III} LFe ^{II}	Ru ^{II} LFe ^{II}	1.3	D _{III*-II}
2	-0.20	0.12	Ru ^{II} LFe ^{II}	Ru ^{III} LFe ^{II}	2.1	D _{II*-II}
3	0.55	0.12	Ru ^{III} LFe ^{III}	Ru ^{III} LFe ^{II}	0.46	D _{III-III*}
4	0.12	0.55	Ru ^{III} LFe ^{II}	Ru ^{III} LFe ^{III}	0.57	D _{III-II*}

a. The Nafion coating contained 6×10^{-7} mol cm⁻² of sulfonate groups and 4.9×10^{-9} mol cm⁻² of the RuLFe complex.

b. Initial electrode potential.

c. Final electrode potential.

d. Calculated from eqn. (1) with $\phi = 1.2 \times 10^{-4}$ cm.

general expression. It applies to cases where the ratio of the concentration gradients of the oxidized and reduced forms of the reactant are everywhere equal to -1.) (vide infra). This expression has been shown to be applicable to the $\text{Co}(\text{bpy})_3^{2+}/+$ couple in Nafion coatings^{2b}.

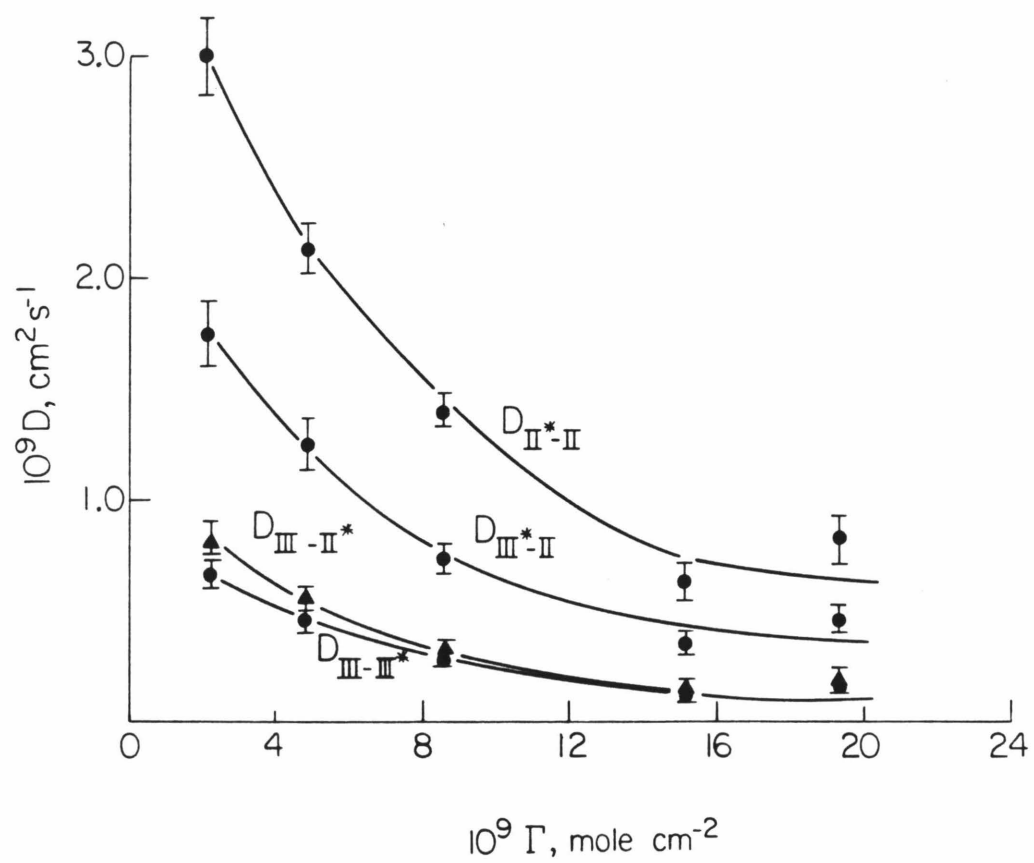
However, the concentration dependence of D_{III-II} shown in Figure 4.3 seems not to agree with that expected from equation (4.2). The measured values of D_{III-II} decrease as the concentration of the complex is increased instead of increasing in the manner as predicted by equation (4.2). But it should be noted that in this simple comparison D_0 and k_{ex} have been taken as concentration-independent. The assumption is possibly not true, since almost all previously reported diffusion coefficients for redox couples in Nafion coatings^{2a,b,3a,b,8,18} have exhibited similar decreases as the reactant concentration is increased. These decreases have been attributed to the effects of electrostatic cross-linking^{2e,f,4a,10,12a,g} and/or of single-file diffusion^{2b,27}. With larger and more highly charged redox couples such as $[\text{RuLFe}]^{4+}/3+$ the factors responsible for decreases in diffusion coefficients with concentration may become dominant so that the contributions of electron self-exchange, which act in the opposite direction, may be masked. Thus, while measured diffusion coefficients that increase with concentration seem a reliable indicator of the presence of contributions from electron self-exchange to the diffusional process, the converse is not necessarily true. Diffusion coefficients that decrease as the reactant concentration increases may nevertheless be enhanced by contributions from electron self-exchange reactions.

Although it has been instructive in previous studies^{2b,3a,b,4b,c} to employ the simplest version of the equation of Dahms and Ruff^{25,26} to compare measured

Figure 4.3

Concentration dependences of the four diffusion coefficients
evaluated for the binuclear RuLFe complex (see text).

Supporting electrolyte as in Figure 4.2 .



and calculated values of diffusion coefficients when contributions from electron self-exchange are suspected, it is not appropriate to do the same analysis for the present system because the disparate magnitudes and concentration dependences of the diffusion coefficients obtained seem incompatible with the assumptions that underlie the Dahms-Ruff analysis. For example, the rate constants governing self-exchange reactions for such intrinsically reactive couples as Ru(III/II) and ferricenium/ferrocene^{28,29} are apt to be close to the diffusion-controlled limit in Nafion coatings^{2b}. (The diffusion-controlled limit in Nafion coatings is much lower than that in homogeneous solution because the diffusion coefficients of multiply-charged ions in Nafion coatings are much smaller than those in homogeneous solution ($10^{-5} \sim 10^{-6} \text{ cm}^2 \text{ s}^{-1}$).) Since the diffusion coefficients of the couples decrease with concentration, the diffusion-controlled rate constants must also decrease, so that the assumption of a concentration-independent self-exchange rate constant in the Dahms-Ruff equation will be invalid.

Another difficulty is posed by the fact that significant differences were observed between $D_{III^{\bullet}-II}$ and $D_{II^{\bullet}-II}$ and between $D_{III-II^{\bullet}}$ and $D_{III-III^{\bullet}}$ (Table 4.1). The Dahms-Ruff equation employed therefore^{2b,3a,b,4b,c} was derived for the case $D_{ox} = D_{red}$. When this is not the case, a more complex equation results^{26c} that has yet to be solved and tested.

A further factor that may cause the difference between $D_{III^{\bullet}-II}$ and $D_{III-II^{\bullet}}$ is coupling between the diffusive fluxes of the oxidized and reduced forms of the redox couple when both are confined within polyelectrolyte matrices by electrostatic force (and other interactions). This proposition has never been presented before. The diffusion of a reactant ion accompanying an electrode

reaction is necessarily coupled with its redox counterpart. For example, in an electrochemical oxidation the reduced species diffuses toward the electrode and the oxidized species diffuses outward (vice versa). Under this circumstance, if the concentration of multiply-charged diffusants increases to the point that the number of available electrostatic binding sites is limited, one might well expect the diffusive motion of one-half of a redox couple to be influenced by that of the other half which proceeds in the opposite direction. Such coupling is not encountered when diffusion coefficients in homogeneous solution are measured by electrochemical techniques or in cases where only one-half of a redox couple is present during the measurement (by non-electrochemical methods). The existence of this type of coupling could help to explain the large difference between $D_{III\bullet-II}$ and $D_{III-II\bullet}$ (Table 4.1) which both apply to the same $Ru^{III}LFe^{II}$ complex. $D_{III\bullet-II}$ is measured by converting $Ru^{III}LFe^{II}$ to the less highly charged $Ru^{II}LFe^{II}$ so that the electrode reaction product would require fewer electrostatic binding sites than the reactant from which it originated. As a result, the diffusion of the reactant might be affected less than when $D_{III-II\bullet}$ is measured and the more highly charged $Ru^{III}LFe^{III}$ complex is the reaction product. Moreover, the diffusion route of $Ru^{III}LFe^{II}$ might be more compact when $Ru^{III}LFe^{III}$ is the product than when $Ru^{II}LFe^{II}$ is the product because the extent of cross-linking of the film by $Ru^{III}LFe^{III}$ is higher. The situation is further complicated by the likelihood that contributions to ion transport in polymer coatings by migration may not be easy to eliminate³¹, especially when highly charged diffusants are involved.

The fact that $D_{II\bullet-II} > D_{III\bullet-II}$ for all the concentrations (Figure 4.3) employed implies that physical motion makes significant contribution to the diffusional rates of both $Ru^{II}LFe^{II}$ and $Ru^{III}LFe^{II}$.

Comparison with Mononuclear Complexes

For the purpose of comparison, diffusion coefficients were also evaluated for various concentrations of mononuclear complexes which were structurally analogous to either end of the binuclear RuLFe complex. The results, summarized in Figure 4.4, show the mononuclear complexes to diffuse more rapidly than the binuclear complex under all conditions, but both types of complex have diffusion coefficients that decrease with concentration. The much smaller concentration dependence of the diffusion coefficient for the singly charged, reduced form of the monomeric ferrocene derivative may be the result of its low cationic charge which causes the effects of electrostatic cross-linking and (possible) electron self-exchange to be more nearly balanced. The large difference in the magnitudes of diffusion coefficients for the oxidized and reduced forms of the monomeric ferrocene complex has been previously reported⁸ and attributed to differences in hydrophobic interactions between the two complexes and the hydrophobic portions of the Nafion matrix³².

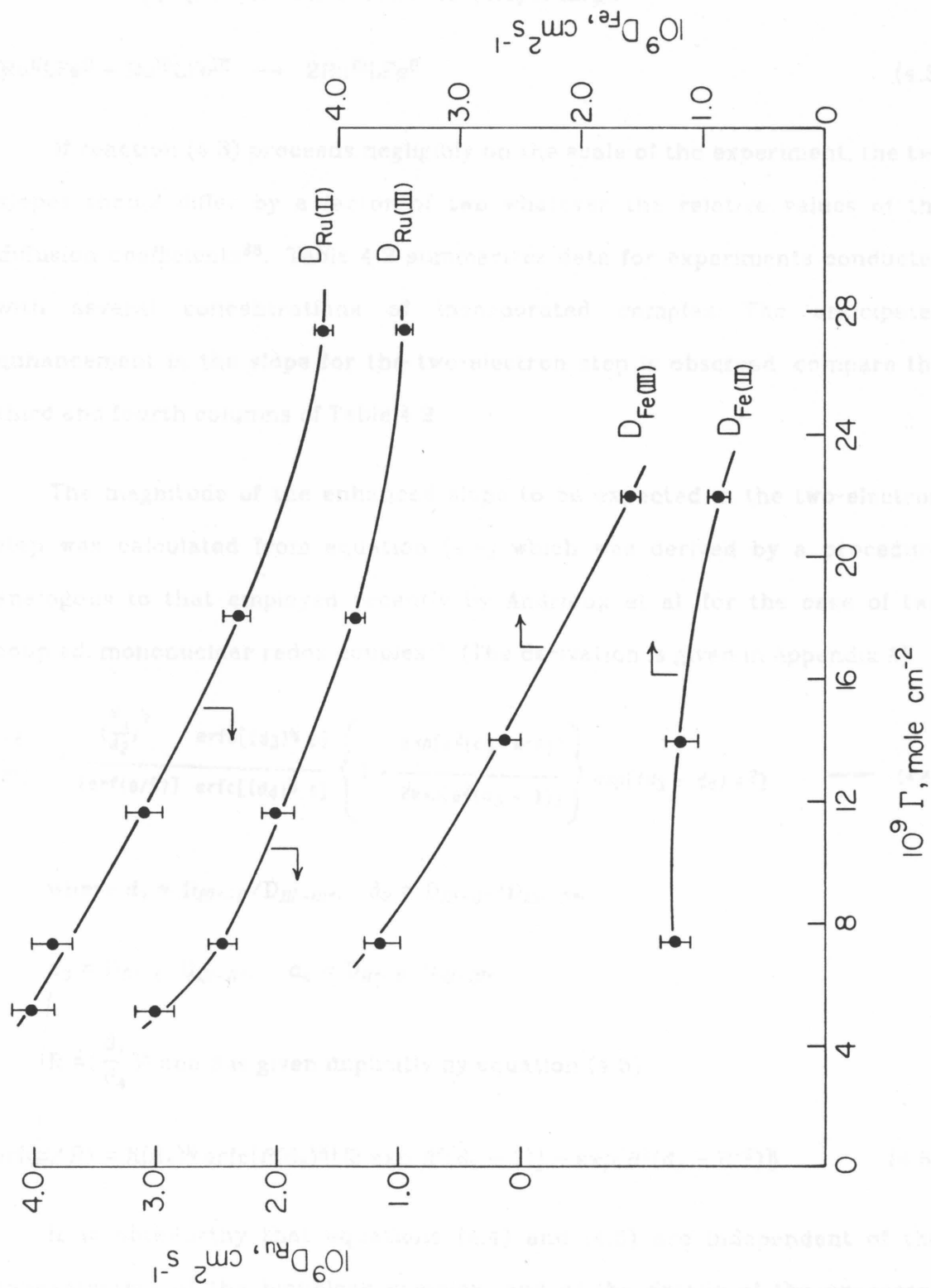
Effect of electron cross-reactions on diffusion currents

The widely differing diffusion coefficients exhibited by the binuclear complex prepared in this study (Table 4.1) are expected to result in the coupling of diffusive fluxes by electron transfer in the appropriate experiments. To test this expectation, the chronocoulometric slope for the one-electron reduction of $\text{Ru}^{\text{III}}\text{LFe}^{\text{III}}$ to $\text{Ru}^{\text{III}}\text{LFe}^{\text{II}}$ was compared with the slope obtained in an experiment where the potential was stepped across both reduction waves so that a two-electron reduction to $\text{Ru}^{\text{II}}\text{LFe}^{\text{II}}$ proceeded at the electrode. Since $D_{\text{II}^{\bullet}-\text{II}}$ is much greater than $D_{\text{III}-\text{II}^{\bullet}}$ (Table 4.1), one expects the slope measured in

Figure 4.4

Concentration dependence of diffusion coefficients for mono-nuclear (Ferrocenylmethyl)trimethylammonium and ruthenium pentaammine pyridine complexes.

Supporting electrolyte as in Figure 4.2 .



the single two-electron step, S_2 , to be larger than twice the slope of the one-electron step, S_1 , if the rate of reaction (4.3) is large¹⁶.



If reaction (4.3) proceeds negligibly on the scale of the experiment, the two slopes should differ by a factor of two whatever the relative values of the diffusion coefficients³³. Table 4.2 summarizes data for experiments conducted with several concentrations of incorporated complex. The anticipated enhancement in the slope for the two-electron step is observed: compare the third and fourth columns of Table 4.2.

The magnitude of the enhanced slope to be expected in the two-electron step was calculated from equation (4.4) which was derived by a procedure analogous to that employed recently by Andrieux et al. for the case of two coupled, mononuclear redox couples¹⁹. (The derivation is given in Appendix A).

$$\frac{S_2}{2S_1} = \frac{\left(\frac{d_1}{d_2}\right)^{1/2} \text{erfc}[(d_3)^{1/2} \beta]}{[\text{erf}(\beta/R)] \text{erfc}[(d_4)^{1/2} \beta]} \left\{ 1 - \frac{\exp[\beta^2(d_3 - R^{-2})]}{2\exp[\beta^2(d_3 - 1)]} \right\} \exp[(d_3 - d_4) \beta^2] \quad (4.4)$$

where $d_1 = D_{\text{III}^{\bullet}-\text{II}}/D_{\text{III}-\text{III}^{\bullet}}$, $d_2 = D_{\text{III}-\text{II}^{\bullet}}/D_{\text{III}-\text{III}^{\bullet}}$,

$d_3 = D_{\text{II}^{\bullet}-\text{II}}/D_{\text{III}-\text{II}^{\bullet}}$, $d_4 = D_{\text{II}^{\bullet}-\text{II}}/D_{\text{III}-\text{III}^{\bullet}}$.

$R = \left(\frac{d_1}{d_4}\right)^{1/2}$ and β is given implicitly by equation (4.5).

$$\text{erf}(\beta/R) = R(d_3)^{1/2} \text{erfc}[\beta(d_3)^{1/2}] \{2 \exp[\beta^2(d_3 - 1)] - \exp[\beta^2(d_3 - R^{-2})]\} \quad (4.5)$$

It is noteworthy that equations (4.4) and (4.5) are independent of the concentration of the binuclear complex, and of the details of the processes

Table 4.2

Chronocoulometric Slopes for the Reduction of $\text{Ru}^{\text{III}}\text{LFe}^{\text{III}}$ in Nafion Coatings

$10^9 \Gamma^a$ mole cm^{-2}	by One- or Two-Electron Steps			
	S_1^b $\mu\text{C cm}^{-2} \text{ s}^{-1/2}$	$2S_1$ $\mu\text{C cm}^{-2} \text{ s}^{-1/2}$	S_2^c $\mu\text{C cm}^{-2} \text{ s}^{-1/2}$	$(S_2)_{\text{calc}}^d$ $\mu\text{C cm}^{-2} \text{ s}^{-1/2}$
2.23	53	106	164	154
4.86	94	188	325	280
8.58	132	264	423	381
15.1	159	318	514	468
19.4	235	470	760	690

- a. Quantity of $[\text{Ru}^{\text{III}}\text{LFe}^{\text{III}}]^{4+}$ incorporated in the Nafion coating which contained 6×10^{-7} mole cm^{-2} of sulfonate groups.
- b. Slope measured for the electrode reaction: $\text{Ru}^{\text{III}}\text{LFe}^{\text{III}} + e \rightarrow \text{Ru}^{\text{III}}\text{LFe}^{\text{II}}$.
- c. Slope measured for the electrode reaction: $\text{Ru}^{\text{III}}\text{LFe}^{\text{III}} + 2e \rightarrow \text{Ru}^{\text{II}}\text{LFe}^{\text{II}}$.
- d. Calculated from eqn. 4.4 using the diffusion coefficients evaluated at the same values of Γ (Figure 4.3).

which give rise to the various diffusion coefficients. The final column of Table 4.2 lists the calculated values of S_2 for comparison with the experimental values in the fourth column. Although the calculated and experimental values differ somewhat, the general trend of the experimental results is matched by the calculated values. The agreement is regarded as reasonable considering the number of independent experimental parameters that are required in the calculation. That substantial enhancement in the overall diffusional rate results from the occurrence of reaction (4.3) within the diffusion layer at the coating/electrode interface seems clearly established by the data.

Equations (4.4) and (4.5) (with appropriate redefinition of the symbols) can also be used to calculate the depressions in the overall diffusional rate that are to be expected¹⁶ if the experiment is repeated in the reverse order; i.e., if $\text{Ru}^{\text{II}}\text{LFe}^{\text{II}}$ is oxidized to $\text{Ru}^{\text{III}}\text{LFe}^{\text{III}}$. Table 4.3 summarizes data obtained in a series of such experiments. The agreement between observed and calculated slopes is satisfactory and gives added evidence of the important effect that reaction (4.3) exerts on the diffusive flux of the reactant that arrives at the electrode surface.

Concluding remarks

The results obtained in this study have revealed that the diffusional behavior of redox reactants in Nafion coatings might be rather complicated. To identify the origins of the differences in the magnitudes of the diffusion coefficients in Figures (4.3) and (4.4) and of their concentration dependences will require considerably more quantitative data to be obtained. On the other hand, the agreement between the calculated and measured slopes in Tables 4.2

Table 4.3
Chronocoulometric Slopes for the Oxidation of $\text{Ru}^{\text{II}}\text{LFe}^{\text{II}}$
in Nafion Coatings by One- or Two-Electron Steps

$10^9 \Gamma^a$ mole cm^{-2}	S_1^b $\mu\text{C cm}^{-2} \text{ s}^{-1/2}$	$2S_1$ $\mu\text{C cm}^{-2} \text{ s}^{-1/2}$	S_2^c $\mu\text{C cm}^{-2} \text{ s}^{-1/2}$	$(S_2)_{\text{calc}}^d$ $\mu\text{C cm}^{-2} \text{ s}^{-1/2}$
2.23	111	222	166	164
4.86	204	408	314	300
8.58	293	586	470	434
15.2	350	700	523	511
19.4	511	1022	760	736

a. Quantity of $[\text{Ru}^{\text{II}}\text{LFe}^{\text{II}}]^{2+}$ incorporated in the Nafion coating which contained 6×10^{-7} mole cm^{-2} of sulfonate groups.

b. Slope measured for the electrode reaction:



c. Slope measured for the electrode reaction:



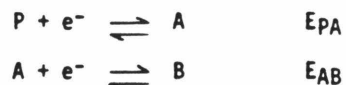
d. Calculated from eqn. 4.4 using the diffusion coefficients evaluated at the same values of Γ (Figure 4.3).

and 4.3 indicate that, despite the remarkable differences in their magnitudes, the diffusion coefficients evaluated in this study do provide accurate measures of the disparate diffusional rates exhibited by the three different oxidation states of the RuLFe complex.

In the future, more binuclear complexes might be synthesized. From the analyses and comparisons of their diffusional behavior in Nafion (or other polyelectrolyte) coatings, valuable information about various factors affecting the diffusional rates will be obtained. It is also important to see whether equations (4.4) and (4.5) are applicable to other binuclear complexes.

Appendix A

Consider a molecule, P, containing two electroactive groups that undergo the following reversible half-reactions:



where P is the fully oxidized species, A is the partially reduced species, B is the fully reduced species and the corresponding formal potentials are E_{PA} and E_{AB} . The diffusion coefficient of P as measured by its reduction to A, that of A as measured by its oxidation to P, that of A as measured by its reduction to B, and that of B as measured by its oxidation to A are D_P , D_A' , D_A and D_B , respectively. We suppose $E_{PA} \gg E_{AB}$ and wish to calculate the chronoamperometric current-time response that results when the electrode potential is stepped from a value well positive of E_{PA} to a value well negative of E_{AB} , i.e., across both reduction waves, in a solution containing only P. The cross-reaction $P + B \rightarrow 2A$ is assumed to be irreversible and to proceed at a high rate at all points within the diffusion layer. The initial conditions are:

$$t = 0; C_P = C_P^0, C_A = C_B = 0$$

where C_i is the concentration of species i and C_P^0 is the initial uniform concentration of P.

Dimensionless parameters are defined as follows:

$$\begin{aligned} p &= C_P/C_P^0; \quad a = C_A/C_P^0; \quad b = C_B/C_P^0; \quad d_a = D_A/D_P; \quad d_a' = D_A'/D_P; \\ d_b &= D_B/D_P; \quad \tau = t/\theta \quad \text{where } \theta \text{ is the total duration of the potential step, } y = x/\delta \quad \text{where } x \text{ is the distance from the electrode surface,} \\ \delta &= (D_P \theta)^{1/2}, \quad \psi = i \left[\frac{F(D_P)^{1/2} C_P^0}{\theta^{1/2}} \right]^{-1}. \end{aligned}$$

By analogy with the previous treatment of a system containing two unattached electroactive species (16), P and B are assumed to react so rapidly they do not co-exist anywhere within the diffusion layer, and μ represents the spatial position where the concentrations of both P and B are zero.

Writing Fick's Law in terms of the dimensionless parameters:

$$0 < y < \mu$$

$$\partial a / \partial \tau = d_a (\partial^2 a / \partial y^2) \quad (A1)$$

$$\partial b / \partial \tau = d_b (\partial^2 b / \partial y^2) \quad (A2)$$

$$p = 0 \quad (A3)$$

$$y < \mu < \infty$$

$$\partial a / \partial \tau = d_a' (\partial^2 a / \partial y^2) \quad (A4)$$

$$\partial p / \partial \tau = \partial^2 p / \partial y^2 \quad (A5)$$

$$b = 0 \quad (A6)$$

with

$$\tau = 0, y > 0$$

$$a = b = 0, p = 1 \quad (A7)$$

$$\tau > 0, y = 0$$

$$a = p = 0 \quad (A8)$$

$$d_a (\partial a / \partial y) = -d_b (\partial b / \partial y) \quad (A9)$$

$$y = \infty$$

$$p = 1 \quad (A10)$$

$$y = \mu$$

$$b = p = 0; (\partial p / \partial y) = -d_b (\partial b / \partial y) \quad (A11)$$

Following the previous successful approach (16) the solution of equations A1 - A11 was assumed to be of the form:

$0 < y < \mu$:

$$b = \left\{ 1 - \frac{\operatorname{erf}\left(\frac{y}{2(d_{b\tau})^{1/2}}\right)}{\operatorname{erf}\left(\frac{\mu}{2(d_{b\tau})^{1/2}}\right)} \right\} C \quad (A12)$$

$$a = \left\{ \frac{\operatorname{erf}\left(\frac{y}{2(d_{a\tau})^{1/2}}\right)}{\operatorname{erf}\left(\frac{\mu}{2(d_{a\tau})^{1/2}}\right)} \right\} C' \quad (A13)$$

$y < \mu < \infty$:

$$a = \left\{ \frac{\operatorname{erfc}\left[\frac{y}{2(d_{a'\tau})^{1/2}}\right]}{\operatorname{erfc}\left[\frac{\mu}{2(d_{a'\tau})^{1/2}}\right]} \right\} C'' \quad (A14)$$

$$p = \left\{ 1 - \frac{\operatorname{erfc}\left(\frac{y}{2\tau^{1/2}}\right)}{\operatorname{erfc}\left(\frac{\mu}{2\tau^{1/2}}\right)} \right\} \quad (A15)$$

where (A7), (A8), (A10) have been applied.

Since a is continuous at μ :

$$C' = C'' \quad (A16)$$

Substitution of (A12) and (A13) into (A9) leads to

$$C = C' (d_a/d_b)^{1/2} \left\{ \frac{\text{erf}\left[\frac{\mu}{2(d_b\tau)^{1/2}}\right]}{\text{erf}\left[\frac{\mu}{2(d_a\tau)^{1/2}}\right]} \right\} \quad (A17)$$

Conservation of matter in the cross-reaction ($P + B \rightarrow 2A$) at $y = \mu$ requires that:

$$y = \mu$$

$$d_a(\partial a/\partial y)_\mu - d_a'(\partial a/\partial y)_\mu = 2(\partial p/\partial y)_\mu \quad (A18)$$

Combining (A13), (A14), (A16) and (A18) leads to:

$$C' \left\{ \frac{(d_a)^{1/2} \exp(-\frac{\mu^2}{4d_a\tau})}{\text{erf}\left[\frac{\mu}{2(d_a\tau)^{1/2}}\right]} + \frac{(d_a')^{1/2} \exp(-\frac{\mu^2}{4d_a'\tau})}{\text{erfc}\left[\frac{\mu}{2(d_a'\tau)^{1/2}}\right]} \right\} = 2 \left[\frac{\exp(-\frac{\mu^2}{4\tau})}{\text{erfc}(\frac{\mu}{2\tau})^{1/2}} \right] \quad (A19)$$

Substitution of this expression into (A17), combination with (A11), (A12) and (A15) and rearrangement yields:

$$1 = \frac{(d_a/d_a')^{1/2} \text{erfc}\left[\frac{\mu}{2(d_a'\tau)^{1/2}}\right]}{\text{erf}\left[\frac{\mu}{2(d_a\tau)^{1/2}}\right]} \left\{ 2 \exp\left[\frac{\mu^2}{4d_b\tau} \left(\frac{d_b}{d_a'} - 1\right)\right] - \exp\left[\frac{\mu^2}{4d_b\tau} \left(\frac{d_b}{d_a'} - \frac{d_b}{d_a}\right)\right] \right\} \quad (A20)$$

By making the following identifications: $P \equiv \text{Ru}^{\text{III}}\text{LFe}^{\text{III}}$,

$A \equiv \text{Ru}^{\text{III}}\text{LFe}^{\text{II}}$, $B \equiv \text{Ru}^{\text{II}}\text{LFe}^{\text{II}}$, $d_1 = d_a$, $d_2 = d_a'$, $d_3 = d_b/d_a'$, $d_4 = d_b$

and $\mu/2(d_b\tau)^{1/2} = \beta$, eqn. (A20) becomes eqn. 4.5 in the text.

As before (16), β is a function that is independent of τ and can be evaluated from the diffusion coefficients by means of eqn. 4.5.

The dimensionless current, ψ , is obtained as follows:

$$\psi = -d_b \left(\frac{\partial b}{\partial y} \right)_{y=0} \quad (\text{A21})$$

$$\psi = \frac{2(d_1/d_2)^{1/2} \exp[(d_3-d_4)\beta^2]}{(\pi\tau)^{1/2} \text{erf}\left(\frac{\beta}{R}\right)} \left\{ 1 - \frac{\exp[\beta^2(d_3 - R^2)]}{2\exp[\beta^2(d_3 - 1)]} \right\} \frac{\text{erfc}[(d_3)^{1/2}\beta]}{\text{erfc}[(d_4)^{1/2}\beta]} \quad (\text{A22})$$

where $R = \left(\frac{d_1}{d_4}\right)^{1/2}$.

Substitution of (A22) into $i = \psi \left\{ \frac{FDp^{1/2} C_p^0}{\theta^{1/2}} \right\}$ and recasting the

result in terms of the chronocoulometric slopes leads to eqn. 4.4 in the text.

References

- 1 (a) F. B. Kaufman and E. M. Engler, *J. Am. Chem. Soc.*, 101(1979)547; (b) A. H. Schroeder, F. B. Kaufman, V. Patel and E. M. Engler, *J. Electroanal. Chem.*, 113(1980)193.
- 2 (a) D. A. Buttry and F. C. Anson, *J. Electroanal. Chem.*, 130(1981)333; (b) *ibid.*, *J. Am. Chem. Soc.*, 105(1983)685; (c) K. Shigehara, N. Oyama and F. C. Anson, *J. Am. Chem. Soc.*, 103(1981)2552; (d) K. Shigehara, N. Oyama and F. C. Anson, *Inorg. Chem.*, 20(1981)518; (e) R. J. Mortimer and F. C. Anson, *J. Electroanal. Chem.*, 138(1982)325; (f) F. C. Anson, T. Ohsaka and J.-M. Saveant, *J. Phys. Chem.*, 87(1983)640; (g) N. Oyama and F. C. Anson, *J. Electrochem. Soc.*, 127(1980)640.
- 3 (a) H. S. White, J. Leddy and A. J. Bard, *J. Am. Chem. Soc.*, 104(1982)4811; (b) C. R. Martin, I. Rubinstein and A. J. Bard, *J. Am. Chem. Soc.*, 104(1982)4817; (c) P. J. Pearce and A. J. Bard, *J. Electroanal. Chem.*, 114(1980)89; (d) T. P. Henning, H. S. White and A. J. Bard, *J. Am. Chem. Soc.*, 103(1981)3937.
- 4 (a) J. Facci and R. W. Murray, *J. Electroanal. Chem.*, 124(1981)339; (b) J. Facci and R. W. Murray, *J. Phys. Chem.*, 85(1981)2870; (c) J. Facci, H. Schmehl and R. W. Murray, *J. Am. Chem. Soc.*, 104(1982)4959; (d) P. Daum, J. R. Lenhard, D. Rolison and R. W. Murray, *J. Am. Chem. Soc.*, 102(1980)4649; (e) P. G. Pickup, W. Kutner, C. R. Leidner and R. W. Murray, *J. Am. Chem. Soc.*, 106(1984)1991.

- 5 (a) M. Majda and L. R. Faulkner, *J. Electroanal. Chem.*, 169(1984)77; (b) *ibid.*, 169(1984)97.
- 6 R. N. Dominey, N. S. Lewis, J. A. Bruce, D. C. Bookbinder and M. S. Wrighton, *J. Am. Chem. Soc.*, 104(1982)467.
- 7 W. J. Albery, M. G. Boutelle, P. J. Colby and A. R. Hillman, *J. Electroanal. Chem.*, 133(1982)135.
- 8 C. R. Martin and K. A. Dollard, *J. Electroanal. Chem.*, 159(1980)127.
- 9 E. Laviron, L. Roullier, C. DeGrand, *J. Electroanal. Chem.*, 112(1980)11.
- 10 (a) N. Oyama, S. Yamaguchi, Y. Nishiki, K. Tokuda, H. Matsuda and F. C. Anson, *J. Electroanal. Chem.*, 139(1982)371; (b) N. Oyama, T. Ohsaka, M. Kaneko, K. Sato and H. Matsuda, *J. Am. Chem. Soc.*, 105(1981)6003; (c) K. Sato, S. Yamaguchi, H. Matsuda, T. Ohsaka and N. Oyama, *Bull. Chem. Soc. Japan*, 56(1983)2004.
- 11 (a) E. Laviron, *J. Electroanal. Chem.*, 112(1980)1; (b) C. P. Andrieux and J.-M. Saveant, *ibid.*, 111(1980)377.
- 12 (a) N. Oyama and F. C. Anson, *Anal. Chem.*, 52(1980)1192; (b) K. Shigehara and F. C. Anson, *J. Electroanal. Chem.*, 132(1982)107; (c) P. Martigny and F. C. Anson, *J. Electroanal. Chem.*, 139(1980)383; (d) F. C. Anson, J.-M. Saveant and K. Shigehara, *J. Am. Chem. Soc.*, 105(1983)1096; (e) K. Kuo and R. W. Murray, *J. Electroanal. Chem.*, 131(1980)37; (f) R. H. Schmehl and R. W. Murray, *J. Electroanal. Chem.*, 152(1983)97; (g) F. C. Anson, T. Ohsaka, J.-M. Saveant, *J. Am. Chem. Soc.*, 105(1983)4883; (h) F. C. Anson, J.-M. Saveant and Y.-M. Tsou, *J. Electroanal. Chem.*, 178(1984)113; (i) M. S.

- Wrighton, *ACS Sym. Ser.*, 1982, No. 192,99; (j) F. B. Kaufman, A. H. Schroeder, E. M. Engler and V. Patel, *Appl. Phys. Lett.*, 36(1980)422; (k) K. Itaya, H. Akahoshi and S. Toshima, *J. Electrochem. Soc.*, 129(1982)762; (l) R. W. Murray in " *Electroanalytical Chemistry*, " A. J. Bard Ed., Marcel Dekker, New York, 1984, Vol. 13. (m) L. R. Faulkner, *Chem. Eng. News*, 62(1984)29.
- 13 (a) C. P. Andrieux, A. Hapiot and J.-M. Saveant, *J. Electroanal. Chem.*, 172(1984)49; (b) D. A. Buttry, J.-M. Saveant and F. C. Anson, *J. Phys. Chem.*, 88(1984)3086.
- 14 (a) S. L. Miller and E. F. Orlemann, *J. Am. Chem. Soc.*, 75(1953)3001; (b) H. Yamada, *J. Electroanal. Chem.*, 36(1972)457; (c) I. Ruzic, D. E. Smith and S. W. Feldberg, *J. Electroanal. Chem.*, 50(1974)157; (d) R. J. Schwall, I. Ruzic and D. E. Smith, *J. Electroanal. Chem.*, 60(1975)117; (e) R. J. Schwall and D. E. Smith, *J. Electroanal. Chem.*, 94(1978)227; (f) T. Matusinovic and D. E. Smith, *J. Electroanal. Chem.*, 98(1979)133.
- 15 M. Fukui, A. Kitani, C. Degrand and L. L. Miller, *J. Am. Chem. Soc.*, 104(1982)28.
- 16 R. G. Gaunder and H. Taube, *Inorg. Chem.*, 2627(1970)9.
- 17 J. E. Sutton and H. Taube, *Inorg. Chem.*, 20(1981)3125.
- 18 W. A. Bonner and P. I. McNamee, *J. Org. Chem.*, 26(1961)2554.
- 19 N. F. Albertson, *Org. Reactions*, 12(1962)205.

- 20 P. Ford, De F. P. Rudd, R. Gaunder and H. Taube, *J. Am. Chem. Soc.*, 90(1968)1187.
- 21 G. Lauer, R. Abel and F. C. Anson, *Anal. Chem.*, 39(1967)765.
- 22 C. A. Koval and F. C. Anson, *Anal. Chem.*, 50(1978)223.
- 23 A. J. Bard and L. R. Faulkner, " *Electrochemical Methods*, " John Wiley and Sons, Inc., New York (1980),p. 186.
- 24 N. Oyama and F. C. Anson, *J. Electrochem. Soc.*, 127(1980)640.
- 25 H. Dahms, *J. Phys. Chem.*, 72(1968)362.
- 26 (a) I. Ruff, *Electrochim. Acta*, 15(1970)1059; (b) I. Ruff and I. Korosi-Odor, *Inorg. Chem.*, 9(1970)186; (c) I. Ruff and V. J. Friedrich, *J. Phys. Chem.* 75(1971)3279, 3303.
- 27 (a) A. L. Hodgkin and R. D. Keynes, *J. Physiol. (London)*, 128(1955)61; (b) K. Heckmann, *Biomembranes*, A. L. Manson, Ed., Plenum Press, New York, 1972, vol. 3, p.127.
- 28 G. M. Brown, H. J. Krentzien, M. Abe and H. Taube, *Inorg. Chem.*, 18(1979)3374.
- 29 E. S. Yang, M. S. Chen and A. C. Wahl, *J. Phys. Chem.*, 84(1980)3094.
- 30 Ref. 26(c), for the case $D_{ox} \neq D_{red}$.

- 31 W. T. Yap, R. A. Durst, E. A. Blubaugh and D. D. Blubaugh, *J. Electroanal. Chem.*, 144 (1983) 69.
- 32 T. D. Gierke, G. E. Munn and F. C. Wilson, *J. Polym. Sci. Phys. Ed.*, 19(1981)1687.
- 33 Ref. 24, p.175

APPENDIX

Synthesis and Characterization of $\text{Ru}(\text{bpy})_2\text{MoS}_4$

Introduction

Extensive studies on complexes of the formula $[\text{M}'(\text{MS}_4)_2]^{2-}$ ($\text{M} = \text{Mo}$ or W , $\text{M}' = \text{Zn}, \text{Ni}, \text{Fe}, \text{Co}, \text{Pd}, \text{Pt}$) have been made.¹ They are interesting due to several reasons. Firstly, some interest originated from attempting to mimic the function of the iron-molybdenum cofactor in nitrogenase.^{1,2} Other studies were aimed at developing the inorganic chemistry of complexes containing MoS_4^{2-} and WS_4^{2-} .³ Callahan and Piliero^{4a} studied the complexes $\text{M}(\text{MoS}_4)_2^{2-}$ and $\text{M}(\text{WS}_4)_2^{2-}$, where $\text{M} = \text{Ni}, \text{Pd}, \text{Pt}$. Two well-separated one-electron reversible reductions were observed for nickel complexes. These move closer together for Pd complexes, and the second reduction becomes irreversible. Pt complexes exhibited one reversible two-electron reduction.^{4a} The reductions of Ni complexes were attributed to the addition of electrons to metal orbitals, but those of Pd, Pt complexes were proposed to involve the vacant orbitals on Mo or W.^{4a} Friesen et al.^{4b} reported the rich electrochemistry of $[\text{Fe}(\text{WS}_4)_2]^{3-}$ and $[\text{Fe}(\text{MoS}_4)_2]^{3-}$. Extensive charge delocalization from Fe to Mo (or W) has been proposed to account for these unusually low formal oxidation states.^{4b} Mossbauer spectra supported this proposition¹. A similar conclusion was also obtained for $\text{Co}(\text{WS}_4)_2^{2-}$.^{4c}

In this appendix, the synthesis of $\text{Ru}(\text{bpy})_2(\text{MoS}_4)$ ($\text{bpy} = 2,2'$ -bipyridine) is reported. The absorption spectrum and electrochemistry are also discussed briefly. Ruthenium and osmium polypyridine complexes have been extensively studied.⁵ They all have low-lying bipyridine antibonding orbitals which are

involved in their reductions. The possibilities of observing interesting interactions between HOMO and LUMO of $\text{Ru}(\text{bpy})_2$ moiety and those of MoS_4 ligand on the photophysical properties of the complex are also an important goal.

Material

$\text{Cis-Ru}(\text{bpy})_2\text{Cl}_2 \cdot 2\text{H}_2\text{O}^{5b}$ and $\text{Ru}(\text{bpy})_2\text{CO}_3 \cdot 2\text{H}_2\text{O}^{5c}$ were prepared as described in the cited references.

$\text{Ru}(\text{bpy})_2\text{MoS}_4 \cdot \text{H}_2\text{O}$: To 100 mg $\text{Ru}(\text{bpy})_2\text{CO}_3 \cdot 2\text{H}_2\text{O}$ (~ 0.02 m mole) suspended in 10 ml warm water protected from the light was added 0.5 ml neat CF_3COOH . The solution was allowed to react until all the solids were dissolved (~ 10 min). The blood red solution was carefully neutralized with aqueous NaOH to $\text{pH} = 6-8$, and the solution was allowed to cool to room temperature. Four volumes of acetone were added to the solution, and the solution was de-aerated with argon saturated with acetone for 20 minutes. Five-fold excess of $(\text{NH}_4)_2\text{MoS}_4$ was added while a slow stream of argon was continuously bubbled through the solution. The reaction solution was stirred for several hours in the dark. During this period, the product precipitated out as very small particles. After acetone was removed by evaporation, the dark green product was collected by filtration. The product was washed copiously with H_2O , then acetone, followed by ether. An analytically pure sample was obtained by recrystallization from DMF-ether. Elemental analysis : C, 36.5; H, 2.5; N, 8.5. Calculated for $\text{RuMoC}_{20}\text{H}_{18}\text{N}_4\text{S}_4\text{O}$: C, 36.6; H, 2.7; N, 8.6.

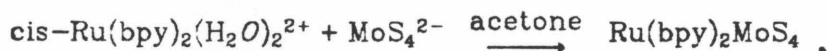
Apparatus

Absorption spectra were recorded with a Hewlett-Packard Model 8450A spectrophotometer. Cyclic voltammetry was performed with PAR instruments (EG & G Industries). The working electrode was a platinum disk, and potentials were quoted with respect to a Ag/AgCl (saturated KCl) reference electrode.

Results and Discussion

Synthesis

$\text{Ru}(\text{bpy})_2\text{MoS}_4$ was prepared by reaction of MoS_4^{2-} with $\text{cis-Ru}(\text{bpy})_2(\text{H}_2\text{O})_2^{2+}$:



Use of $\text{cis-Ru}(\text{bpy})_2\text{S}_2^{2+}$ (S = solvent) as an intermediate has been described previously^{5b,6}. The neutralization step is essential for the success since MoS_4^{2-} is very unstable in acidic solutions⁸. The use of acetone as a co-solvent was found to improve both the yield and the purity of the complex. One of the causes might be the increase of the activity of the ionic reactants by lowering the polarity of the solvent⁷.

Electronic absorption spectrum

The absorption spectrum of $\text{Ru}(\text{bpy})_2(\text{MoS}_4)$ is shown in Figure 5.1, and an enlargement is shown in Figure 5.2. There are four major absorption bands with a shoulder in the ultraviolet region that is also of importance. The two bands at 576 nm and 346 nm are assigned to the $\pi^*(\text{bpy}) \leftarrow d\pi(\text{Ru})$ charge-transfer transitions. Similar bands were observed for a lot of $\text{Ru}(\text{bpy})_2\text{X}_2$

Figure 5.1

UV-Vis absorption spectrum of $\text{Ru}(\text{bpy})_2\text{MoS}_4$ in DMSO.

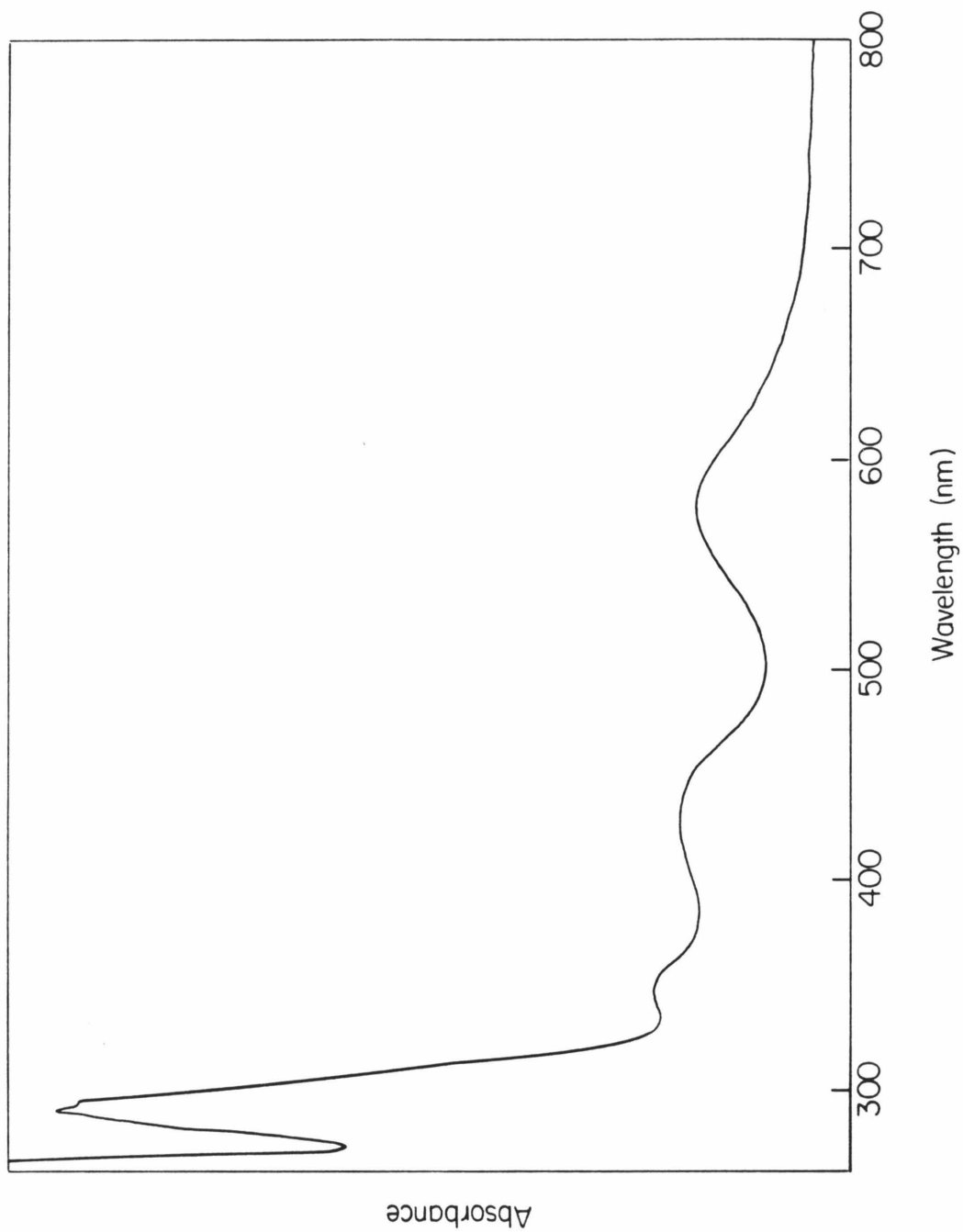
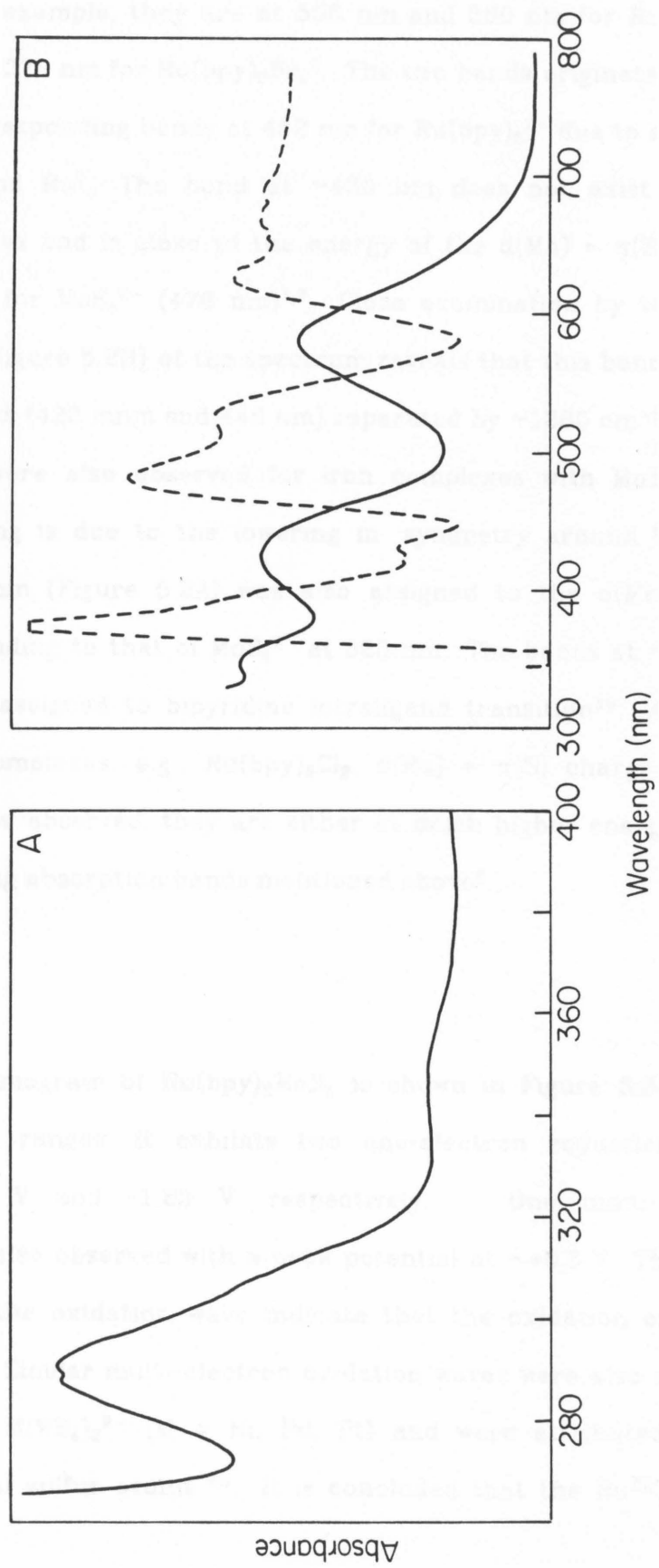


Figure 5.2

Enlargement of Figure 5.1.

(A) UV absorption spectrum .

(B) Visible spectrum: (—) absorption, (---) second derivative of absorption .



complexes⁷. For example, they are at 556 nm and 380 nm for $\text{Ru}(\text{bpy})_2\text{Cl}_2$, and at 548 nm and 378 nm for $\text{Ru}(\text{bpy})_2\text{Br}_2$ ⁷. The two bands originate from the splitting of the corresponding bands at 452 nm for $\text{Ru}(\text{bpy})_3^{2+}$ due to a lowering in symmetry around Ru⁷. The band at ~430 nm does not exist in other $\text{Ru}(\text{bpy})_2\text{X}_2$ complexes and is close to the energy of the $d(\text{Mo}) \leftarrow \pi(\text{S})$ charge-transfer transition for MoS_4^{2-} (476 nm)^{1,3}. Close examination by taking the second derivative (Figure 5.2B) of the spectrum reveals that this band actually consists of two peaks (422 nm and 446 nm) separated by $\sim 1280 \text{ cm}^{-1}$. Similar absorption bands were also observed for iron complexes with MoS_4^{2-} as a ligand¹. The splitting is due to the lowering in symmetry around Mo¹. The shoulder at ~310 nm (Figure 5.2A) was also assigned to the $d(\text{Mo}) \leftarrow \pi(\text{S})$ transition corresponding to that of MoS_4^{2-} at 323 nm. The bands at ~290 nm can be confidently assigned to bipyridine intraligand transition^{5b}. As in the other $\text{Ru}(\text{bpy})_2\text{X}_2$ complexes; e.g., $\text{Ru}(\text{bpy})_2\text{Cl}_2$, $d(\text{Ru}) \leftarrow \pi(\text{S})$ charge-transfer transition can not be observed, they are either at much higher energy or are buried in those strong absorption bands mentioned above⁸.

Electrochemistry

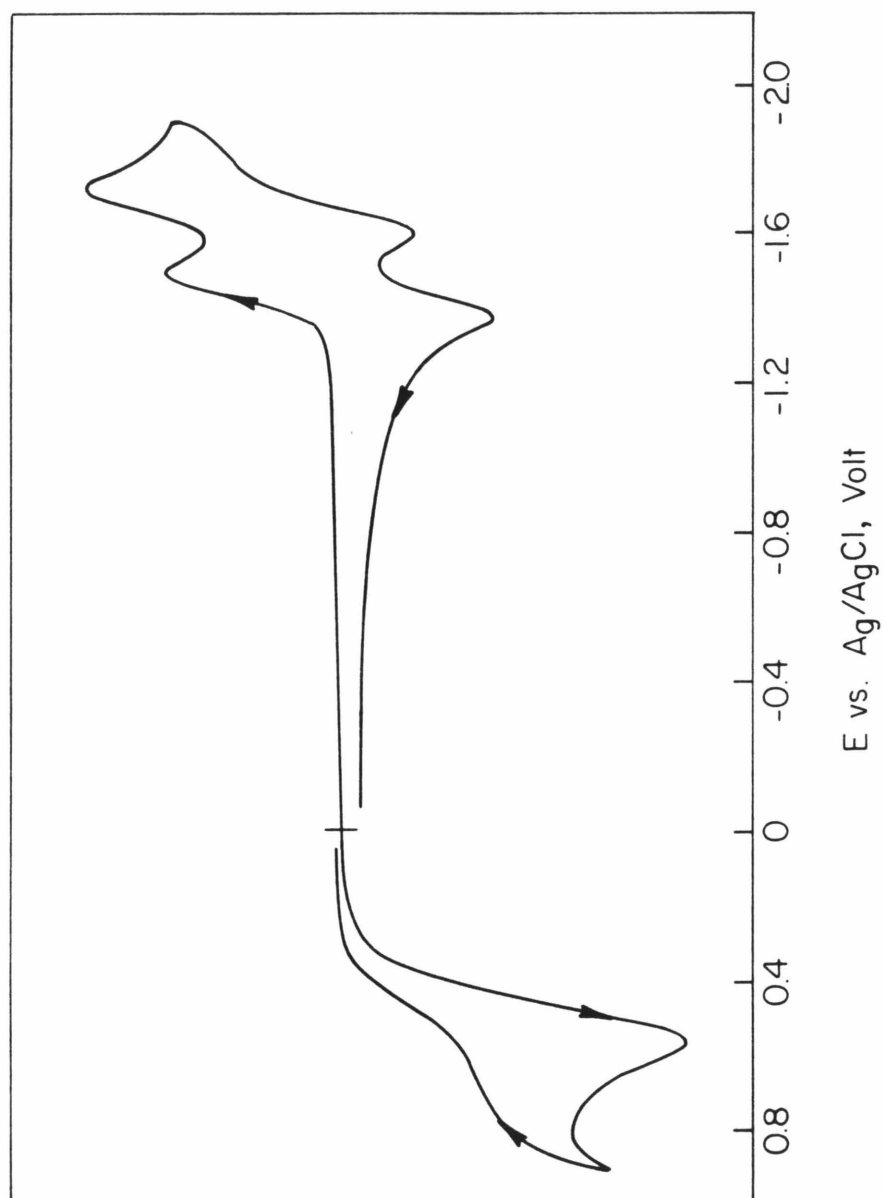
A cyclic voltammogram of $\text{Ru}(\text{bpy})_2\text{MoS}_4$ is shown in Figure 5.3. In the accessible potential ranges, it exhibits two one-electron reduction waves centered at -1.42 V and -1.65 V, respectively. One multi-electron irreversible wave is also observed with a peak potential at $\sim +0.6 \text{ V}$. The multi-electron nature of the oxidation wave indicate that the oxidation of MoS_4^{2-} moiety is involved. Similar multi-electron oxidation waves were also observed for $\text{M}(\text{MoS}_4)_2^{2-}$ and $\text{M}(\text{WS}_4)_2^{2-}$ ($\text{M} = \text{Ni}, \text{Pd}, \text{Pt}$) and were attributed to the oxidation of terminal sulfur atoms ^{4a}. It is concluded that the $\text{Ru}^{\text{III/II}}$ redox

Figure 5.3

Cyclic voltammogram of $\text{Ru}(\text{bpy})_2\text{MoS}_4$ in DMSO.

Supporting electrolyte: 0.1 M tetrabutylammonium perchlorate.

Scan rate: 200 mV s^{-1} .



potential for this complex is more positive than +0.6 V (or at least equal to +0.6 V). The easy oxidation of the terminal sulfur atoms implies that some interesting photophysical (and/or photochemical) processes might be observed following the excitation of the $\pi^*(bpy) \leftarrow d\pi(Ru)$ absorption bands.

The two reversible reduction waves can be attributed to sequential addition of electrons to the two bipyridine ligands, since the two redox potentials fall in the range of those for $Ru(bpy)_3^{2+}$ and $Ru(bpy)_2X_2^{2+}$ complexes^{5b,9}. But the possibility that MoS_4^{2-} might be involved in these reductions can not be totally ruled out. Further investigation are of course called for.

The first reduction wave was investigated closely by reversing the potential scan direction before the second reduction commenced. Figure 5.4B contains the cyclic voltammograms at different scan rates. The formal potential (the average of cathodic and anodic peak potentials) is independent of scan rate and the cathodic peak current vs. (scan rate)^{1/2} plot is linear. The peak separations at slow scan rates are ~65 mV which is close to that expected in a one-electron Nernstian wave. These confirm that the first reduction wave is a one-electron reversible (at the experimental time scale), diffusion-controlled wave. The larger peak separations at higher scan rates probably originated from the uncompensated resistance.

The behavior of the second reduction wave is essentially the same as the first one at high scan rates, but at low scan rates, a new anodic peak appears at ~-1.25 V. Comparing Figure 5.4A with 5.4B indicates that the new peak originates from some decomposition product(s) generated by the two-electron reduced species.

Figure 5.4

Cyclic voltammogram of $\text{Ru}(\text{bpy})_2\text{MoS}_4$ in DMSO.

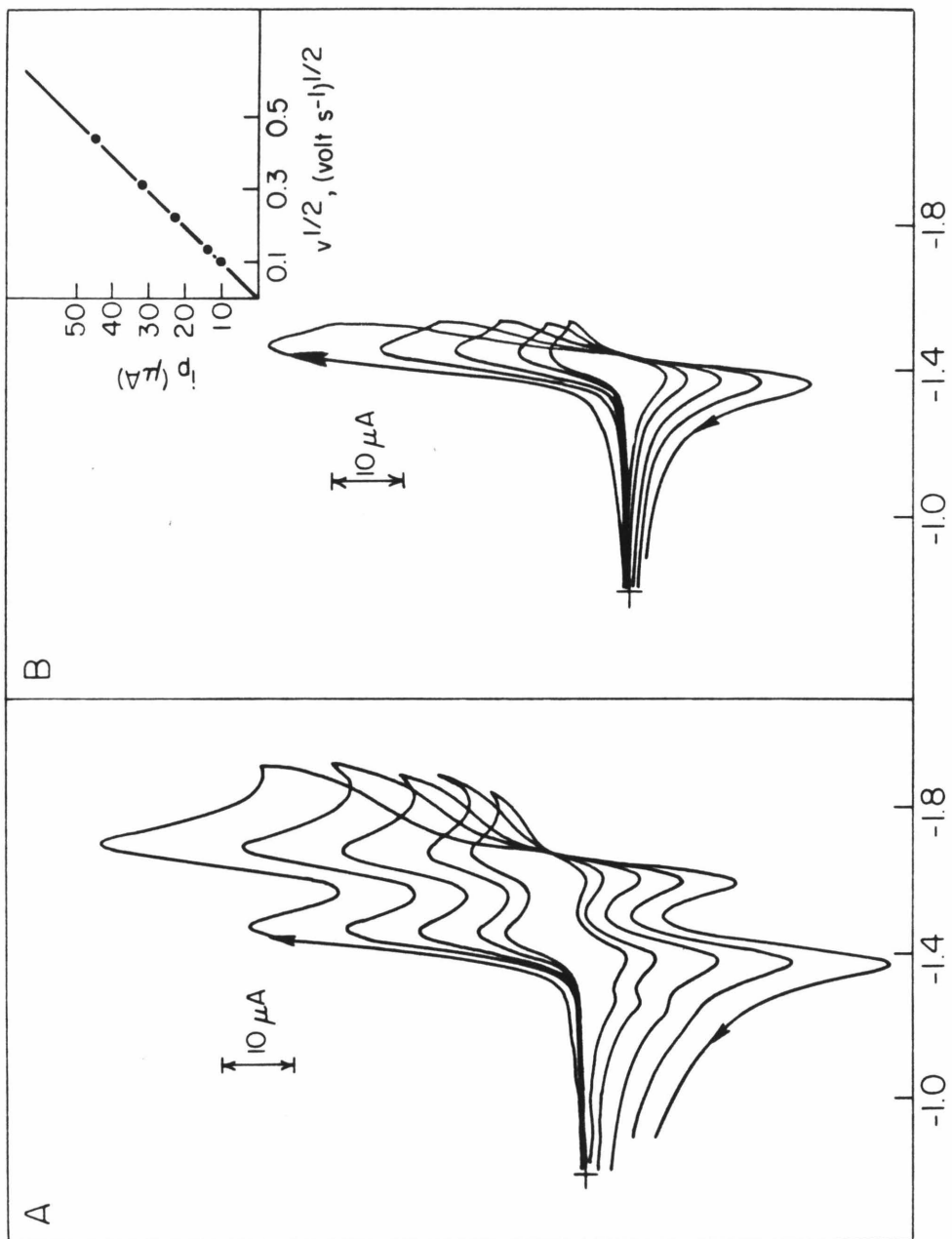
Supporting electrolyte: 0.1 M tetrabutylammonium perchlorate.

Scan rate: 10, 20, 50, 100, 200 mV s^{-1} .

(A) Reversal switching potential: - 1.9 V.

(B) Reversal switching potential: - 1.54 V.

Insert shows cathodic peak current vs. $(\text{scan rate})^{1/2}$.



E vs. Ag/AgCl, Volt

Future works

The near-infrared spectroscopic (if any) and the luminescence studies should aid in understanding more about the relative orbital energies. Resonance Raman spectroscopy may be used to detect the delocalization of electrons from the bpy^- ligands to Mo (if any) in the reduced state(s)¹⁰. The complex can be further characterized by infrared spectroscopy and x-ray crystallography¹. Structurally related complexes and the osmium analogues can be synthesized.

References

- 1 D. Coucouvanis, *Acc. Chem. Res.*, 14(1981)201.
- 2 V. K. Skah and W. J. Brill, *Proc. Natl. Acad. Sci. U.S.A.*, 74(1977)3249.
- 3 E. Diemann and A. Muller, *Coord. Chem. Rev.*, 10(1973)79.
- 4 (a) K. P. Kallahan and P. A. Piliero, *Inorg. Chem.*, 19(1980)2619; (b) G. D. Friesen, J. W. McDonald, W. E. Newton, W. B. Euler and B. M. Hoffman, *Inorg. Chem.*, 22(1983)2202; (c) A. Muller, R. Jostes, V. Flemming and R. Potthast, *Inorg. Chim. Acta*, 44(1980)L33.
- 5 (a) J. V. Caspar and T. J. Meyer, *Inorg. Chem.*, 22(1983)2444; (b) B. P. Sullivan, D. J. Salmon, and T. J. Meyer, *Inorg. Chem.*, 17(1978)3334; (c) E. C. Johnson, B. P. Sullivan, D. J. Salmon, S. A. Adeyemi and T. J. Meyer, *Inorg. Chem.*, 17(1978)2211.
- 6 J. M. Calvert and T. J. Meyer, *Inorg. Chem.*, 21(1982)3978.
- 7 B. Durham, J. L. Walsh, C. L. Carter and T. J. Meyer, *Inorg. Chem.*, 19(1980)860.
- 8 D. M. Klassen and G. A. Crosby, *J. Chem. Phys.*, 48(1968)1853.
- 9 N. E. Tokel-Takvoryan, R. E. Heminway and A. J. Bard, *J. Am. Chem. Soc.*, 95(1973)6582.
- 10 (a) J. V. Caspar, T.D. Westmoreland, G. H. Allen, P. G. Bradly, T. J. Meyer and W. H. Woodruff, *J. Am. Chem. Soc.*, 106(1984)3492; (b) S. M. Angel, M. K. DeArmond, R. J. Donohoe, K. W. Hanck and D. W. Wertz, *J. Am. Chem. Soc.*,

106(1984)3688.